

MHD BOUNDARY LAYER FLOW OF NON-NEWTONIAN FLUIDS WITH VARIOUS EFFECTS

A thesis submitted by

ISHWAR MAHARUDRAPPA

(USN: 2BA13PGN01)

Under the guidance of

Dr. Gurunath C Sankad

Professor

Department of mathematics

B.L.D.E. A's V.P. Dr. P. G. Halakatti College of Engineering and
Technology, Vijayapur - 586103

for the award of the degree of

Doctor of Philosophy

in Mathematics



**VISVESVARAYA TECHNOLOGICAL UNIVERSITY
BELAGAVI, KARNATAKA, INDIA**

Research Centre

**Department of Mathematics, B.L.D.E. A's V.P. Dr. P.G. Halakatti College of
Engineering and Technology, Vijayapur -586103, Karnataka, India**

2022



DEPARTMENT OF MATHEMATICS
B.L.D.E.A's V.P.Dr.P.G.Halakatti college of Engineering and Technology,
Vijayapur-586103, Karnataka, India



CERTIFICATE

This is to certify that Mr. **Ishwar Maharudrappa** has worked under my supervision for his doctoral thesis titled "**MHD BOUNDARY LAYER FLOW OF NON-NEWTONIAN FLUIDS WITH VARIOUS EFFECTS**". I also certify that the work is original and has not submitted to any other university wholly or in part for any other degree.

Dr. Gurunath C Sankad

Research supervisor

Professor, Dept. of Mathematics

B.L.D.E. A's V.P. Dr. P. G. Halakatti College of Engineering and Technology,

VIJAYAPUR – 586103

Date: 01-06-2022

Place: VIJAYAPUR

DECLARATION

I hereby declare that the research thesis entitled "MHD BOUNDARY LAYER FLOW OF NON-NEWTONIAN FLUIDS WITH VARIOUS EFFECTS" which is being submitted to the Visvesvaraya Technological University, Belagavi in partial fulfilment of the requirements for the award of degree of Doctor of Philosophy in Mathematics is a bonafide report of the research work carried out by me under the supervision of Dr Gurunath C Sankad and the material contained in this research thesis has not been submitted to any university or institution for the award of any degree.

Ishtar
(Ishtar M)

ISHWAR MAHARUDRAPPA
USN:2BL13PGN01
DEPARTMENT OF MATHEMATICS

Date: 01.06.2022

Place: VIJAYAPUR



Visvesvaraya Technological University

Jnana Sangama, Belagavi – 590 018.

Dr. B. E. Rangaswamy Ph.D
Registrar (Evaluation)

Phone: (0831) 2498136
Fax: (0831) 2405461

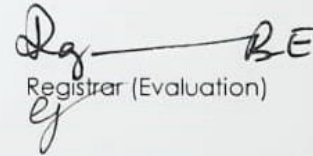
Ref.No. VTU/BGM/Exam /2021-22/ 2339

Date: 15 MAR 2022

Acceptance Letter

Sir/Madam,

The soft copy of Ph.D./M.Sc. (Engineering by research) thesis of **Mr./Mrs. Ishwar Maharudrappa** bearing **USN 2BL13PGN01** has been submitted for Anti-plagiarism check at the office of the undersigned through "Turn-it-in" package. The scan has been carried out and the scanned output reveals a match percentage of **13% which is within the acceptable limit of 25%**. To obtain the comprehensive report of the plagiarism test, research scholar can send a mail to apc@vtu.ac.in along with the USN, Name, Name of the Guide/Co-guide, Research centre and title of the thesis.


Registrar (Evaluation)

To,

Mr. /Mrs. Ishwar Maharudrappa

Research Scholar

Mathematics

B.L.D.E. A's College of Engineering and Technology, Vijayapur -586103

✓ Copy to: Dr. Gurunath C Sankad Professor B.L.D.E. A's College of Engineering and Technology, Vijayapur - 586103

In the memory of my grandfather

Late. Sri Kallappa Policepatil

Dedicated to

My beloved Parents

LATE SMT. PARVATI AND SRI. MAHARUDRAPPA POLICEPATIL

AND

TO ALL MY TEACHERS

ACKNOWLEDGEMENTS

I thank the Visvesvaraya Technological University (VTU), Belagavi and Vachana Pitamaha Dr. P. G. Halakatti College of Engineering and Technology, Vijayapur particularly, the Department of Mathematics, and my working place the Department of Mathematics, Basaveshwar Engineering College (A), Bagalkote for giving me an opportunity to do a Ph.D., and supporting me during my tenure at the Institute. I feel blessed at every step along the way. It has been such a wonderful journey, not just because of great work carried under the roof of the department, but many wonderful people that I got to know and become friends with.

I express my reverential thanks, deep sense of everlasting gratitude and earnest admiration to my esteemed teacher and **research supervisor Dr. Gurnath C Sankad**, Professor, Department of Mathematics, BLDEA's CET Vijayapur, for his intellectual advice, ingenious suggestions, scholarly guidance, invaluable discussions, invariable counsel, unremitting encouragement, meticulous care and perpetual interest shown at different stages of my work, without which, it would have been impossible for me.

I extend my gratitude to the **Chairman, Dr. Veeranna. C. Charantimath** of Basaveshwar Veerashaiva Vidhya vardhak Sangha Bagalkot and honorable members of BVV Sangha Bagalakote, for their kind encouragement and advices during my research work. I extend my gratitude to the **Principal, Dr. S. S. Injagneri** and **Technical Director, Dr. R. N. Herkal** of Basaveshwar Engineering College, Bagalkot for their kind encouragement and advices during my research work.

I would also like to express my gratitude and sincere thanks to Dr P. K. Gonnagar, Dr S. C. Desai, Dr M. Y. Dhange, Dr. A. B. Patil, Dr. Pratima Nagathan and Mr. K. M. Chavan, Mr. Revu Metri, for their kind cooperation and help during my research work.

I express my everlasting debt of gratitude and sincere laurel to my loving parents, Late Smt. Parvati & Sri Maharudrappa Policepatil for their benevolent blessings, without which, it would have been impossible for me to accomplish this work. I express my gratitude to my beloved brothers Chandrakant, Prabhuling and Sharanabasava and my beloved sister Kavita and my beloved Sister-in-laws Sridevi,

Prabhavati, Sunanda and their kids Kishor, Kiran, Chetan, Vaibhav, Annapurna, Aruna, Asharani, Ashwini, Bhavani for their kind co-operation and everlasting encouragement during the course of my work.

I would be failing in my duty, if I don't express the affectionate encouragement given by beloved wife Renuka and my kids Kailashchandra and Bhuvanesh.

I extend my gratitude to the Librarian Dr. Srikant Karkun, Basaveshwar Engineering College Bagalkot for providing the library facilities towards the research work and also for his valuable suggestions. I deeply extend my sincere gratitude to my beloved HOD, Dr. S. S. Benchalli and my colleagues Dr. V. M. Shettar, Dr. S. V. Gurushantanavar, Dr. A. H. Agadi, Smt. V. M. Pudukalkatti, Dr. Mahadev Biradar, Sri. S. S. Bopardekar, Dr. S. K. Patil, Dr. Virupakshaiah DBM, Dr. B. R Hiremath, Dr. P. L. Timmanagoudar, Dr. V. G. Akkimaradi, Sri. B. Veeresh, Dr. Praveen Challagidad, Prof. C. M. Jangin, Prof. M. H. Shirur, Prof. Ramesh, colleagues of other department of Basaveshwar Engineering College (A), Bagalkot, for their kind encouragement in my research work. Special thanks to Dr. G. B. Marali, Dr. Mahabaleshwar, Dr. Jagadish Tawade, Dr. Mahesha N., Dr. Sharangouda Malipatil, Dr. M. B. Malkhed, Dr. S. A. Adaki, Dr. A. G. Hiremath, Dr. Mahantesh. M. N, Sri. Rajkumar Mosali, Dr. Rajesh Singh, and all my Classmates, co-research scholars, and friends for their help and encouragement extended to me during the research work.

I must be thankful to Prof. Srinivas Jangali, Asst. Professor, NIT, Warangal for his kind support and valuable suggestions given to carry out my research work and especially Prof. S.M. Magi who helped me to overcome from the difficulties in the usage of various mathematical tools like MATLAB and Mathematica.

Lastly, I am very much thankful to TEQIP coordinator, BEC (A), Bagalakote for providing financial support to carry out this work.

Ishwar Maharudrappa
VIJAYAPUR, INDIA

2022

Preface

The theoretical analyses of magnetohydrodynamic fluxes and heat transfer in non-Newtonian liquids owing to stretching sheet are provided in this thesis. Fluctuating thermal conductivity, variable wall temperature, and viscous dissipation are among the theoretical considerations. The problems in the nonlinear regimes of free, forced, mixed, or bioconvection involving any liquid are extremely difficult to solve analytically or numerically. The nonlinearity of linked systems of ordinary differential equations is what makes these issues so difficult. The addition of temperature-dependent thermal conductivity, changeable wall temperature, and viscous dissipation to the equation will only make the situation more complicated. Many of these difficult challenges are addressed in the thesis. The thesis is divided into seven chapters.

The **first chapter** serves as an introduction and motivation for the research effort presented in the thesis. A review of relevant literature is provided to demonstrate the importance of the issues under consideration.

The **second chapter** provides a brief overview of non-Newtonian liquids, their characteristics, and applications. Basic equations of mass, linear momentum, and energy conservation, density of nanoparticles and motile microorganisms of non-Newtonian liquids, approximations employed, and dimensionless parameters associated in the issues examined in the thesis are also covered in this chapter.

A theoretical examination of Casson fluid boundary layer flow and heat exchange above a linear stretching sheet under the effect of magnetic fluid is reported in **Chapter 3**. By changing the equations into a system of ordinary differential equations using similarity transformations as a tool, analytical and numerical solutions for the momentum and energy equations may be achieved.

In **chapter 4**, the thermal boundary layer in Casson fluid is subjected to a flow and heat transfer study before being permitted to flow through a pervious linear stretching membrane with variable wall transfer and radiation. The mathematical expressions for flow and heat conduction over a stretched membrane are partial differential equations, which are transformed into ordinary differential equations via similarity transformations. To get the solution to the energy equation, the regular Perturbation approach is used. The effect of Prandtl number, Casson fluid

parameter, suction parameter, and fluid thermal radiation parameter on the flow and heat exchange are described.

In the presence of gyrotactic microorganisms, the combined effects of a magnetic field and a convective boundary state on Casson fluid bioconvection and nanoparticle concentration over a linear stretching sheet with changing wall temperature and thermal radiation impact are discussed in **Chapter 5**. The governing equations for nanoparticles, microorganisms, momentum, temperature, and concentration are simplified using similarity transformations. A growing system of connected nonlinear differential equations is solved using a differential transformation technique and an in-built shooting method (ND Solve).

A study of bioconvection of magnetohydrodynamic boundary layer flow, heat, and mass exchange of Casson fluid containing gyrotactic microorganisms over a linearly extending surface is discussed in **Chapter 6**. The Using Oberbeck-Boussinesq approximations and similarity transformations, physical partial differential equations are turned into a system of linked nonlinear ordinary differential equations. The differential transform approach is used to derive Taylor's series solutions for the momentum, energy, diffusive concentration of nanofluid, and microbe concentration equations, which are compared to numerical solutions. A variety of non-dimensional factors' impacts on bioconvection fluid flow and heat transmission are investigated.

The study of Bioconvection in flow and heat transfer analysis owing to Casson fluid and gyrotactic microorganisms via a porous media in the presence of a magnetic field with viscous dissipation is presented in **Chapter 7**. Using Oberbeck-Boussinesq approximations and similarity transformation, the associated governing equations of the physical situation are deformed into a set of non-linear ordinary differential equations. To get Taylor's series solutions for momentum, energy, nano particle concentration, and microbe density, the derived coupled equations are solved using the Differential transform technique. **Chapter 8** presents the concluding remarks and scope for our future work.

CONTENTS

Acknowledgement	i
Preface	iii
List of figures	ix
Tables	xii
Symbols.....	xiii
Abbreviations	xvi
1 Introduction.....	1
1.1 Objectives	1
1.2 Motives	2
1.3 Scope	3
1.4 Literature Survey	4
1.4.1 Due to the stretching sheet Newtonian fluid flows	4
1.4.2 Non-Newtonian fluid flows due to stretching sheet	8
1.4.3 Casson fluid flow due to stretching sheet	15
1.4.4 Bioconvection in the fluid flow containing nanoparticles and microorganisms	16
2 Classification of fluids governing equations and boundary conditions	22
2.1 Introduction	22
2.2 Fluid state and its physical characteristics	22
2.2.1 Fluid state	23
2.2.2 Ideal fluid or inviscid fluid	24
2.2.3 Viscous fluid or real fluid	24
2.2.4 Newtonian fluids	25
2.2.5 Non-Newtonian fluids	25
2.3 Bioconvection due to nanofluids containing microorganisms	27

2.3.1	Nanofluids	27
2.3.2	Brownian motion.....	28
2.3.3	Thermophoresis.....	28
2.3.4	Viscous dissipation	28
2.3.5	Gyrotactic microorganisms.....	28
2.3.6	Bioconvection	29
2.4	Fundamental equation of fluid dynamics in vectorial form.....	30
2.5	Basic equations of stretching sheet problems	31
2.6	Magnetohydrodynamic (MHD) equations.....	32
2.7	Approximations.....	33
2.7.1	Boundary layer approximations.....	33
2.7.2	Boussinesq Approximations.....	34
2.8	Basic equations after approximations.....	35
2.9	Boundary conditions.....	37
2.10	Dimensionless parameters.....	39
3	Casson fluid flow due to stretching sheet with magnetic effect and variable thermal conductivity	42
3.1	Introduction.....	42
3.2	Mathematical formulation and solution.....	43
3.2.1	Zero th order solution	45
3.2.2	First order solution	45
3.3	Results and discussion.....	46
3.4	Conclusion.....	51

4	Impact of variable wall temperature and radiation on Casson liquid flow across a pervious extending sheet.	52
4.1	Introduction.....	52
4.2	Mathematical formulation and solution.....	52
4.3	Solution of energy equation.....	55
4.3.1	Solution at the zero th order BVP.....	55
4.3.2	Solution at the first order BVP.....	56
4.4	Outcomes and analysis.....	61
4.5	Conclusion	62
5	Casson liquid flow comprising nanofluids and gyrotactic bacteria with varying wall temperature and thermo-radiation	63
5.1	Introduction.....	63
5.2	Mathematical formulation.....	65
5.3	Series solution by DTM.....	67
5.4	Outcomes and analysis.....	69
5.5	Conclusion.....	78
6	Impact of magnetic field on the bioconvection of Casson liquid flow due to microbes and nanoparticles.	80
6.1	Introduction.....	80
6.2	Mathematical formulation.....	82
6.3	DTM Solution.....	84
6.4	Results and Discussion.....	86
6.5	Conclusion.....	97
7	Casson liquid flow comprising microbes across porous stretching sheet with viscous dissipation.	98
7.1	Introduction.....	98
7.2	Mathematical formulation.....	99

7.3	DTM solutions.....	101
7.4	Results and Discussion.....	103
7.5	Conclusion.....	113
8	Conclusion and Scope for the future work	114
8.1	Conclusion.....	114
8.2	Future work.....	115
	Bibliography.....	117
	List of published paper and communicated	136

LIST OF FIGURES

Figure 2.2.1: Rheogram.	26
Figure 3.3.1: Velocity profile for the variations of β .	47
Figure 3.3.2: Velocity profile for the variations of q .	48
Figure 3.3.3: Energy profile for the variations of q .	48
Figure 3.3.4: Energy profile for the variations of temperature constant λ_1 .	49
Figure 3.3.5: Energy profile for the variations of Prandtl number P_r .	49
Figure 3.3.6: Temperature profile for the variations of ϵ .	50
Figure 4.3.1: Velocity of fluid for the variations of s .	58
Figure 4.3.2: Velocity profile for the variations of β .	58
Figure 4.3.3: Velocity of the fluid for the variations of P_r .	59
Figure 4.3.4: Energy profile for the variations of β .	59
Figure 4.3.5: Energy profile for the variations of s .	60
Figure 4.3.6: Energy profile for the variations of P_r .	60
Figure 4.3.7: Energy profile for the variations of T_r .	61
Figure 5.2.1: Bioconvection in the boundary layer flow of nanofluids containing microorganisms.	65
Figure 5.4.1: Velocity of the fluid for the variations of β .	71
Figure 5.4.2: Velocity for the variations of M .	72
Figure 5.4.3: Velocity variation of the liquid for the variations of S .	72
Figure 5.4.4: Temperature profile for the variations of T_r .	73
Figure 5.4.5: Temperature profile for the variations of s .	73
Figure 5.4.6: Temperature profile for the variations of Pr .	74
Figure 5.4.7: Temperature profile for the variations of N_t .	74
Figure 5.4.8: Temperature profile for the variations of N_b .	75

Figure 5.4.9: Concentration profile of nanoparticles for the variations of Le .	75
Figure 5.4.10: Concentration profile of nanoparticles for the variations of M .	76
Figure 5.4.11: Concentration profile of nanoparticles for the variations of s .	76
Figure 5.4.12: Density profile of microbes for the variations of σ .	77
Figure 5.4.13: Density profile of microbes for the variations of Pe .	77
Figure 5.4.14: Density profile of microbes for the variations of s .	78
Figure 6.2.1: Geometrical sketch of the model of bioconvection in the boundary layer flow of nanofluids containing microbes.	82
Figure 6.4.1: Velocity Profile the variations of β .	89
Figure 6.4.2: Velocity profile for the variations of Rb .	90
Figure 6.4.3: Velocity profile for the variations of N_r .	90
Figure 6.4.4: Velocity profile for the variations of Pr .	91
Figure 6.4.5: Temperature profile for the variations of λ .	91
Figure 6.4.6: Temperature profile for the variations of N_t .	92
Figure 6.4.7: Temperature profile for the variations of N_t .	92
Figure 6.4.8: Temperature profile for the variations of Rb .	93
Figure 6.4.9: Concentration profile of the nanoparticles for the variations of λ .	93
Figure 6.4.10: Concentration profile of the nanoparticles for the variations of N_t .	94
Figure 6.4.11: Concentration profile of the nanoparticles for the variations of N_r .	94
Figure 6.4.12: Concentration profile of the nanoparticles for the variations of M .	95
Figure 6.4.13: Concentration profile of microorganisms for the variations of Sc .	95
Figure 6.4.14: Concentration profile of the microbes for the variations of N_t .	96
Figure 6.4.15: Concentration of the microbes for the variations of σ .	96
Figure 6.4.16: Concentration of the microbes for the variations of Pe .	97
Figure 7.4.1: Velocity profile of the fluid for the variations of β .	106

Figure 7.4.2: Velocity profile of the fluid for the variations of Ec .	106
Figure 7.4.3: Velocity profile of the fluid for the variations of M .	107
Figure 7.4.4: Velocity profile of the fluid for the variations of N_b .	107
Figure 7.4.5: Temperature profile of the liquid for the variations of β .	108
Figure 7.4.6: Temperature profile of the liquid for the variations of Ec .	108
Figure 7.4.7: Temperature profile of the liquid for the variations of N_b .	109
Figure 7.4.8: Temperature profile of the liquid for the variations of N_t .	109
Figure 7.4.9: Concentration profile of nanoparticles for the variations of β .	110
Figure 7.4.10: Concentration of nanoparticles for the variations of Ec .	110
Figure 7.4.11: Concentration of nanoparticles for the variations of M .	111
Figure 7.4.12: Concentration of nanoparticles for the variations of N_b .	111
Figure 7.4.13: Concentration of nanoparticles for the variations of Le .	112
Figure 7.4.14: Concentration of microorganisms for the variations of N_t .	112
Figure 7.4.15: Concentration of microorganisms for the variations of Pe .	113

LIST OF TABLES

Table 3.3.1: Nature of local skin coefficient (α) and the temperature gradient ($-\theta'(0)$).	50
Table 4.3.1: Results of $-f''(0)$ for discrete values of the parameters.	57
Table 4.3.2: Results of $-\theta'(0)$ for different values of the parameters.	57

SYMBOLS

- u, v velocity components along x- and y-axes
- α is the volumetric expansion coefficient of the fluid
- β is the Casson fluid parameter
- f dimensionless stream function
- f' non dimensional velocity of the fluid
- ρ is the Casson fluid density
- λ is the slip parameter
- λ_1 is the temperature constant
- ρ_p is the density of nanoparticles
- ρ_m is the microorganism density
- γ is the average volume of microorganisms
- τ heat capacity ratio of the fluid
- τ_w shear stress
- τ_{ij} stress tensor
- a_0 stretching rate
- B_0 Strength of magnetic field
- P_r Prandtl number
- T fluid temperature
- T_n ambient temperature
- T_w fluid temperature at the wall
- k_p Permeability constant.
- C Nanoparticle volume fraction
- C_n ambient nanoparticle volume fraction
- C_w concentration of nanoparticle at the wall
- N volume fraction of motile microorganisms
- N_w volume fraction of microorganisms at the wall
- Dn diffusivity of microorganisms

T_∞ temperature at infinite distance from the wall
 C_∞ concentration of nanofluid at infinite distance from the wall
 N_∞ concentration of microbes at infinite distance from the wall
 k thermal conductivity
 Le traditional Lewis number
 Pe bioconvection Peclet number
 N_b Brownian motion parameter
 Nr is the buoyancy ratio parameter,
 Rb is the bioconvection Rayleigh number
 S mass flux parameter
 N_t thermophoresis parameter
 Sc Schmidt number
 σ bio-convection constant
 M modified magnetic parameter
 ν kinematic viscosity
 μ dynamic viscosity
 q is the Chandrashekar number
 q_r radiative heat flux
 T_r thermal radiation parameter
 ρ_{cp} density of nanoparticles
 ρ_{cf} density of the fluid
 l Characteristic length
 Le traditional Lewis number
 L_b Bioconvection Lewis number
 ρ_m microorganism density
 Tr radiation parameter
 D_B Brownian diffusion coefficient
 D_T thermophoresis diffusion coefficient

R_{ex} Reynold's number
 R_b Bioconvection Rayleigh number
 v_c suction or injection velocity
 ψ stream function
 η similarity variable
 θ dimensionless temperature
 ϕ rescaled nanoparticle volume fraction
 χ dimensionless concentration of microorganisms
 U_w stretching velocity
 C_f skin friction coefficient

ABBREVIATIONS

ODE - Ordinary differential equations.

PDE - Partial differential equations.

MHD -Magnetohydrodynamics.

BVP - Boundary value problems.

DTM - Differential Transform Method

N.sol -Numerical Solutions

Analy. Sol. -Analytical solutions

CHAPTER 1

1. INTRODUCTION

Non-Newtonian fluids in various geometries are briefly discussed in this chapter. The necessity of boundary layer nanofluid flow for a Casson fluid, magnetohydrodynamic fluxes, viscous dissipation and suction and injection effects, stretching sheet and bioconvection are all explored for heat and mass exchange. It also provides a comprehensive literature review based on the topics covered in the following chapters. The study's goals, motivations, and scope of the research are also described.

1.1 OBJECTIVES:

The goal of this thesis is to find a solution to nonlinear boundary value issues that arise in the analysis of fluid and heat flow across an extending sheet. The thesis' research aims are listed below.

1. To be used to create various mathematical models for the influence of various physical characteristics on fluid and heat flow scenarios.
2. To use analytical and numerical approaches to derive information from a theoretical analysis of non-Newtonian fluid flow and heat flow properties without having to undertake experiments.
3. To recognize the impact of various physical parameters on heat exchange process, which helps us in improving the quality of output.
4. To obtain analytical and numerical solutions in order to get qualitative and quantitative information from non-Newtonian flow characteristics by solving the system of coupled non-linear boundary value issues that govern fluid and heat transmission owing to stretched sheet.
5. To provide formulae in terms of mathematical expressions and numerical solutions to analyze energy transmission in the non-Newtonian liquid flow issues.

The main goal of this thesis is to offer a theoretical analysis of flow, heat transfer, nanoparticle concentration, and microbe concentration in non-Newtonian fluid boundary layer flow.

1.2 MOTIVES:

Theoretical investigation of the effects of non-dimensional parameters on energy transmission, nanoparticle density, and motile microbe density in non-Newtonian liquid streams, with or without magnetic influence, will be an important factor in manufacturing, biotechnological production, and other physical engineering applications. The information gathered from the analysis will aid in the comprehension of theoretical scientific foundations, which will help to improve the quality of production or materials in the industries. Our findings would be extremely useful in a variety of technological and biotechnological processes, including aerodynamic extrusion of plastic sheets, biodegradable plastic sheets, continuous stretching in the food industry, manufacturing processes, rolling and extrusion, and boundary layer flow in condensation processes. Its goal is to gather useful data on various cooling parameters related with industrial manufacturing processes.

Boundary layer theory is a crucial subject for mathematicians, physicists, and engineers to understand the importance of boundary value problems in fluid dynamics and aerodynamics. This theory also aids in the comprehension of a variety of physical events that we see on a daily basis. The investigation must also consider the type of the fluid to be studied.

Visco-elastic materials are classified according to their degree of viscosity or elasticity. Essentially, these fluids are complex in nature and may be distinguished from viscous solids, such as rubber, which are more elastic than viscous, and elastic liquids, such as molten polymers and polymer solutions, which are viscous but not elastic. Stress in elastic materials is explicitly dependent on strain. When a force is applied to an elastic material, it deforms, and in the absence of applied force, the material returns to its earlier shape. As a result, it's possible to say that elastic materials have memory, or that they may remember their initial shape. In visco-elastic fluids, on the other hand, the tension is relational to the rate of deformation, and if the applied tension is removed, the strain rate becomes zero. As a result, when fluid

deforms, it forgets to return to its original place. To put it another way, fluids don't remember anything. Soap and polymer solutions are examples of viscoelastic fluids, which have both elastic and viscous properties. To characterize the behaviour of non-Newtonian fluids, we can utilize a variety of fluid models. Various models have different fluid characteristics and importance in various physical situations.

1.3 SCOPE:

The study of fluid properties, heat exchange analysis, concentration of nanoparticles and microorganism's concentration encourages the understanding of useful applications of applied mathematics. The interesting aspects of fluid dynamics have made tremendous advantages in various fields. The work done in this thesis has wide-ranging applications such as:

- i. Analytical and numerical techniques are adapted which would be used as ready-made formulae to find velocity, temperature & concentration distribution in the nanoparticles and the microorganisms.
- ii. The mathematical analysis of different physical models would provide interesting information on various heat controlling parameters associated with the polymer and biotechnological industries.
- iii. Being known the effects of heat controlling parameters, it would be possible to improve the quality of the products in the industries.
- iv. The knowledge on the effects of Casson fluid, magnetic field, porosity to be gained from this study is helpful in understanding improvement of the quality of the products in the industries.
- v. Exact analytical solutions to be obtained in this study would enrich the mathematical foundations in applied mathematics.
- vi. The better approximate solutions to be obtained will have significance in the field of computational fluid dynamics.
- vii. Copper wire drawing, annealing, and tinning.

- viii. Plastic film and artificial fibers are continuously stretched, rolled, and produced.
- ix. Material extrusion and heat-treated materials that move on conveyor belts or between feed and wind-up rollers.
- x. A limitless metallic sheet is cooled.
- xi. In the condensation process, a boundary layer runs along a liquid sheet.

1.4 Literature Survey:

1.4.1 Due to the stretching of the sheet, Newtonian fluid flows

Sakiadis [140]-[142] were the foremost to conduct a conceptual study of boundary-layer stream induced by a stretched surface moving at a persistent velocity. For the laminar flow considered and applied successfully integral approach, accurate as well as approximate solutions are achieved. Blasius [27] and Erickson et al. [55] attempted to expand on Sakiadis [140]-[142] work by exploring heat and mass transport owing to stretched surfaces. The solutions to boundary layer flow owing to a semi-infinite plane surface are clearly distinguishable than those of boundary layer flow due to ambient fluid characteristics (Blasius,[27]) and are significantly unlike those of boundary layer stream due to a semi-infinite plane surface.

Crane [43] was the first to investigate stable boundary layer flows by extending and shrinking a surface linearly. The continuous boundary layer stream of an incompressible viscous liquid was studied using an analytical method. The linear stretching surface travels in its own flat with a linearly increasing velocity as it advances away from a static point.

Gupta and Gupta [65] examined mass and energy exchange in a flow caused by an extending sheet distributing from a thin slit, as well as fluid particle temperature, concentration, and distribution profiles. Chakrabarti and Gupta [1] focused on the hydromagnetic stream and energy exchange near an extending slab and found a comparable shift in speed and heat exchange when unchanging suction was applied to the wall. By converting the energy condition into a differential condition, Anderson et al. [19] were able to find a solution. Carragher [31] used Crane's [43]

problem to examine heat transmission and determined the Nusselt number for the complete range of Prandtl number values.

The power law distinction was used in Grubka and Bobba's [63] heat transfer analysis of surface temperature. Gupta and Sridhar [64] conducted a theoretical investigation of viscoelastic influences in the non-Newtonian liquid stream via absorbent media. It has been demonstrated that in some cases, a fluid experiencing peripheral deformation does not exhibit shear inspissation. The viscoelastic boundary layer stream across an extending sheet with suction and energy transmission was investigated by Siddappa and Abel [151]. They were able to derive analytical estimates for the coefficient of skin friction and the thickness of the boundary layer. The coupled heat exchange owing to extending sheet was explored by Dutta and Gupta [52]. For a variety of Prandtl numbers and stretching speed, a distinction in slip temperature with reserve from the slot was discovered. It was discovered that as the stretching speed increases, the surface temperature drops for a certain Prandtl number.

Dutta [51] found an analytical result to the heat exchange issue of cooling a thin extending slip in a viscous flow involving suction or blowing. The sheet material's local velocity was supposed to be relational to its reserve from the split. The solution's convergence criteria were also created. Chen and Char [36] examined the impact of power law surface temperature and power law heat flux fluctuations on the energy exchange properties of a steady, linearly stretched surface that was suctioned or blown. Rudraiah et al. [133] investigated oscillatory convection in a viscoelastic liquid passing over a pervious sheet heated from below. This issue pertains to the thermal procedures used to produce some heavy crude oils. Soewono et al. [152] looked into the reality of solutions to a nonlinear boundary value issue that occurs in flow and heat exchange over a spreading sheet with adjustable thermal conductivity and temperature reliant on sources of heat or sinks. When a flat surface spreads radially, Karahalios [76] discovered an accurate substitute solution to the time reliant on the Navier-Stokes equation, up to the second order of approximation; the components of velocity were presented in a series.

Vajravelu [159] investigated convective flow and heat exchange at an infinite vertical extending surface in a viscous heat-causing fluid. On the stream and heat exchange, the effects of free convection, suction, and injection were investigated. The

related momentum, energy equations of stream and heat exchange were numerically solved using adjustable step length finite difference approach. Many intriguing behaviors were shown by the numerical outcomes for stream and heat exchange interpretations.

The viscous boundary layer stream above a quadratically extending sheet was initially explored by Kumaran and Ramanaiah [81]. Skin friction and stream line pattern were plotted using stretching constraints. Magyari and Keller [99] studied heat and mass transmission in the boundary layer on an exponentially extended steady sheet involving an exponential temperature distribution both theoretically and numerically. Under Reynolds analogy, Magyari and Keller [97]-[98] investigated the steady boundary layer stream caused by pervious extending surfaces with a changing temperature distribution. Further the authors have investigated classical hydrodynamics free laminar jets, which may be recognized as boundary layer streams provoked by unceasing surfaces submerged in motionless incompressible liquids and expanded at specified values of velocities. By offering an analytic result to the stream issue, it was discovered that in the restrictive scenario of a vanishing adjacent mass flux, this stretching encouraged flow may be transformed into the well-known wall jet using an appropriate scaling transformation. Wang [164] investigated the flow caused by an extending flat boundary with partial slip, and the results are good in agreement with some similarity solutions of Navier-Stokes equations.

Using the rate of stretching parameter at the sheet, Andersson [17] explored slip flow over a linearly expanded surface. The Navier-Stokes equations have an exact analytical solution for all Reynolds numbers that is formally valid. The self-related boundary layer stream of a Newtonian fluid across a porous continuous plane surface stretching with inverse linear velocity was studied by Magyari et al. [100]-[101]. It was demonstrated that in order to generate the right similarity problem from pseudo similarity, a logarithmic expression in the wall coordinate x should be enhanced to the standard definition of the stream function. The inflated-curvature outcomes of this issue fit into single constraint member of numerous results, which may be described in the form of Airy's function, according to innovative analytical results of a recognized boundary value issue.

An exact similarity outcome of the Navier Stokes issue was investigated by Mahapatra and Gupta [103]. The solution depicts a steady asymmetric stagnation point stream approaching a stretched surface. An observed boundary layer arises when the slab extending velocity exceeds the free flow rate, whereas the temperature distribution in the drift is discovered when the sheet is held at a invariable temperature. Energy transmission from the plane to the molten at the stagnation point when the surface temperature exceeds the ambient temperature, whereas heat exchange from the liquid to the extended surface further away from the stagnation point. Using a similarity solution, Partha et al. [119] investigated mixed convection flow and energy exchange near an exponentially extending surface in a static liquid. They discovered that the temperature at the boundary wall and the rate of extending sheet can have a distinct exponential structure. In both helping and opposing flow scenarios, the effects of buoyancy and viscous dissipation on convective transport in the boundary layer region were investigated.

For nonlinear issues emerging in a moving sheet, Xu [166], Liao [85]-[86], Liao and Pop [87], employed the homotopy analysis approach. For the first time, they have obtained an explicit analytic solution with recursive coefficient equations. The impacts of radiation and sources of heat on the MHD stream of a viscoelastic fluid and heat exchange above an extending sheet were investigated by Siddheshwar and Mahabaleswar [116]. With the addition of viscous dissipation, heat occurrence or absorption, and radiation, an exact solution was obtained for the non-linear momentum differential equation and the energy equation. Heat flow in a boundary layer of viscoelastic liquid near an expanding surface with viscous dissipation was examined by Abel et al. [96]. Awad et al. [56] examined the heat and mass exchange characteristics of mixed convection in a fluid saturated pervious medium with radiative heat exchange along a semi-infinite plate. Using a similarity transformation and the Keller box method, the problem was solved. The results were validated by means of the MATLAB package. The radiation impact on the magnetohydrodynamic Newtonian fluid stream near an exponentially extended plate was investigated by Kameswaran et al. [75]. On the heat exchange, the effects of heating generation by friction and viscous dissipation are considered. The impacts of a magnetic field on the radiative stream of a nanofluid across a stretched surface with

heat radiation were explored numerically by Khan et al. [107]. Kumar et al. [117] researched the MHD influence on a Newtonian liquid flow over a super linear stretching sheet and found that the viscous liquid owing to a super linear expanding surface under the sway of MHD has a huge degree of nonlinearity in conducting the solution region with various arrangements.

However, all of the earlier researchers focused on Newtonian fluid flow. In the remaining sections of this chapter, literature survey on the stretching sheet issues with an asymmetrically stressed liquid was carried out.

1.4.2 Non-Newtonian fluid flows due to stretching sheet

The studies of boundary layer flow of heat exchange are relevant to the understanding of the compiling progress in order to improve the quality of goods. A fascinating and important investigation is the liquid with specific qualities across a direct stretching surface and heat transfer marvels; we encounter several manufacturing of mechanical products. The exploration of non-Newtonian boundary layer liquid flow influenced by various considerations and heat exchange study has various usages in manufacturing, for instance, the withdrawal of polymer plates from rinse and wiredrawing, and so on. Further, similar applications of the extending surface include the production of paper, glass fibers, and the freezing of metallic sheets, among others. Several academics have been working on the boundary layer stream and heat exchange examination near the linear extending surface for a few decades.

The study of continuous stream of viscous incompressible liquid near a continuous extending surface is of great interest, and similar flow situations are emerging in several industrial processes, such as desolidifying metallic products in a freezing bath process, ejection of plastic films, and forcing polymer ply through a dye to form polymer ply with a desired cross section. The slit forms the blend during the deposition of such polymer ply, which is then overextended to give the desired thickness, and the plate is solidified when it passages over the freezing system, resulting in a well-graded output. The uniqueness of ply appears to be controlled via heat and mass exchange confined by the ply and fluid. The stretched sheet warms up and mechanically touches the medium fluid during manufacture. Bhatnagar [25]

explored the stream of an Oldroyd-B liquid engaging space across an expandable sheet as a result of the sheet stretching in the presence of a continuous free-stream rate. The governing equations were deformed to a system of coupled non-linear ordinary differential equations by incorporating similarity transformations for the velocity field and the components of the stress tensor. The resulting equations were solved numerically and using a Weissenberg number perturbation. The two solutions were established to be validated when compared. The flow of a power law fluid across an inextensible horizontal sheet moving with steady velocity in its own plane was examined by Fox et al. [60]. Certain non-Newtonian liquid features, such as normal stress difference, are not present in this model.

Rajagopal et al. [128] explored the stream of a 2nd order liquid across an extending surface in the absence of heat transfer and gave a perturbation solution for the velocity distribution. The stream of the Walters' liquid B near an extending slab was explored by Siddappa and Abel [150], and an exact solution to the momentum equation was provided. Walter's liquid B flow past a stretched surface involving suction was also examined by Siddappa and Abel [151]. The boundary-layer stream and the energy equation have both been solved to an exact answer. The coefficient of skin friction and width of the boundary layer were examined. Rajagopal et al. [130] investigated the boundary layer stream of a second order liquid near a stretching surface with a uniform free flow and came up with some intriguing findings. Bujurke et al. [28] examined energy transmission in the drift of a 2nd order liquid above an extending surface using Coleman and Noll's constitutive equation. The temperature distribution in a Walters' liquid B model on a horizontal extending plate was investigated by Chen and Char [35]. The sheet's velocity was thought to be relational to its distance from the split, with the plate exposed to a changing heat flow. Kummer's function was used to express the answer to the heat transfer equation (Abramowitz and Stegun [13]; Andrews [21]). For specifying conditions, several closed-form solutions were investigated. The temperature field's effect on the viscoelastic parameter and the heat flux parameter was also investigated.

Dandapat and Gupta [46] investigated the flow of a second-order liquid as well as the heat exchange caused by an extending sheet. It was investigated how viscoelasticity

affects flow behaviour and heat transmission characteristics. For velocity and temperature distributions, an analytical solution was presented alongside numerical findings. Chang [33] established a closed form solution to the boundary layer issue for a given value of the non-Newtonian constraint. Chen et al. [37] investigated the temperature distribution in Walters' liquid B flowing over a horizontal stretching plate with a constant surface temperature and heat flux. It is revealed that, as the viscoelastic constraint decreases, the temperature at a given point decreases. The dimensionless heat exchange coefficient and temperature distribution in the region around the stretched sheet were determined for various values of the viscoelastic constraints.

The energy exchange in a second order liquid across a steady extending surface with power law surface temperature or power law heat flow was studied by Rollins and Vajravelu [132], which took into report the impacts of internal heat production. The researchers looked at two cases: (i) PST and (ii) PHF. Kummer's function was exercised to determine the solution and energy transfer features. In both the PST and PHF examples, a uniform approximation in terms of a parabolic cylinder function with a boundary layer of width reciprocal of the Prandtl number was presented for large values of Prandtl number. It was also demonstrated that for tiny Prandtl numbers, no boundary layer type solution exists. Pavlov [121] proposed an exact similarity solution for the continual MHD two-dimensional stream of an electrically charged incompressible liquid instigated by the extending plate. Chakrabarti and Gupta [32] built on Pavlov's [121] work to investigate the temperature distribution in an MHD boundary layer stream involving uniform suction. The velocity and energy exchange parameters in the stream involving steady drag near the wall were compared using a similarity solution. Incomplete gamma function was used to solve the equation. The impacts of persuaded magnetic properties and internal heat source or absorbent on stream and energy exchange features through an extending surface were inspected by Kumari et al. [83]. MHD stream of a Walters' liquid B near an extended sheet was studied by Andersson [16] and determined an analytical result for the governing nonlinear boundary layer relations. The topic of heat transport in a second order liquid near a stretching surface was analyzed by Sam and Rao [143]-[144] and for skin friction and heat exchange coefficient, an expression was

found. Further, they found two closed-form solutions to the momentum equation for varying viscoelastic constraints. This raised concerns about the uniqueness of the solution.

MHD convective stream and energy exchange in a viscous heat producing molten across an infinite perpendicular extending sheet were investigated by Vajravelu and Nayfeh [160]. The influence of free convection and heat production or absorption on stream and heat exchange properties was investigated. Numerical solutions are determined for the conservation of momentum, mass, and energy equations. Char [34] investigated heat and mass transmission in an MHD flow of Walters' liquid B across a stretched sheet. Exact as well as approximate results for energy and mass transport features were found for various selections of modified, modified Schmidt number, surface temperature index, magnetic parameter, and Prandtl number.

The study of MHD flow and steadiness of a Walters' liquid B across a stretched surface was carried out by Dandapat et al. [47]. The approach of weighted residuals was used to do a three-dimensional linear stability analysis for disturbances of the type. The magnetic field has been discovered to have a flow-stabilizing effect. Andersson [18] investigated an MHD flow near an extending surface and found a similarity solution for the steady two-dimensional Navier- Stokes equations velocity and pressure. The velocity field solution was found to be identical to Pavlov's [121] solution. MHD boundary layer stream owing to sheet extending with a power law velocity distribution was studied by Chiam [38]. To obtain the similarity equation, a specific form of the magnetic field was chosen. With Crocco's transformation, an analytical result for a large value of magnetic parameters was produced, as well as an accurate expression for the skin coefficient. The resulting boundary value problem was then directly numerically solved using the shooting approach. The presence of suspended nanoparticles in the base fluid was defined by Choi and Eastman [41]. A colloidal mixing of nanoparticles and a base fluid is known as a nanofluid. Chiam [38] obtained the solution for an energy equation of MHD boundary layer stream of an electrically charged fluid across a linearly stretched non-uniform current extending surface. The influence of heat generation, degeneracy, and tension were all taken into account. An exact outcome to the subsequent linear non-homogeneous BVP was

presented in the form of Kummer's expression to the case of PST and PHF, and these are regarded quadratic relations of reserve. Free convection and interior warmth production on stream and energy exchange properties in an electrically charged molten across a uniform extending surface were investigated by Vajravelu and Hadjinicolaou [158]. Ariel [22] investigated the flow of a second order liquid, for a class of singular boundary value problems with a small coefficient of the highest derivative, a fourth-order predictor-corrector method was utilized to get the numerical solution. With frictional heating and internal heat generation or absorption, Abel and Veena [11] investigated the Walters' liquid B stream and heat exchange in a saturated pervious medium across an impervious stretched surface. I PST and (ii) PHF were the two cases that were considered. The velocity field and skin friction have been solved to exact precision. In addition, Kummer's function was used to derive answers for temperature and heat transport characteristics.

Kumari and Nath [82] explored the effect of the magnetic field on the stagnation point stream and heat exchange of a viscous electrically charged fluid above an extending surface, when the sheet and free stream velocity are not identical. Two-dimensional stagnation point flow and flow near a stretched surface in an ambient fluid can be conceived of as a hybrid of two problems. Kelly et al. [77] investigated how a viscoelastic liquid that was incompressible and electrically conducting behaved in terms of heat and mass transmission as it traveled through a plane flexible surface. Takhar et al. [155] investigated Newtonian flow and energy transfer near an extending sheet including magnetic impact and chemical species. The PDEs that govern boundary layer stream and energy transmission were determined utilizing finite-difference approach. Surface skin friction was established to be greatly increased by the magnetic field, whereas surface mass transfer was reduced little. The Schmidt number and the reaction rate were shown to have a big impact on surface mass transfer. A constant stagnation-point stream of an incompressible viscous electrically charged fluid above a flat deformable sheet was presented by Mahapatra and Gupta [104]. The rapidity at a specific location was exhibited to drop or rise including growth in the magnetic impact as soon as the free flow rapidity was fewer or superior than the expanding rate. The energy distribution throughout a stream was computed on a plane assumed at a constant temperature. Thomas algorithm and the finite difference technique were used to generate the findings numerically.

The effects of Hall and ion slip currents on the flow of a magneto micropolar, viscous, incompressible, and electrically charged liquid were studied by Seddeek [148]. He looked at heat exchange from the extending sheet to a micropolar liquid as well. He used the shooting technique to solve the equations by assuming a low magnetic Reynolds number (Hartmann formulation). The Walters' liquid B stream and energy exchange through a non-uniform extending surface imbedded in a pervious medium were studied by Abel et al. [12]. They looked at I PST and (ii) PHF. A similarity transformation was used to translate the non-linear partial differential equations, which are formulated for momentum and energy transfer characteristics, into the system of ordinary differential equations. The nonlinear momentum differential equation that resulted was precisely solved. The energy equation was also solved analytically in the presence of viscous internal heat production or absorption, as well as a first-order chemical process. The continuous laminar stream of a second-grade fluid across a radially stretched sheet was examined by Ariel [23]. The liquid's viscoelasticity was proven to cause a boundary value issue wherein the order of the differential equations beats the number of boundary conditions. For all values of the viscoelastic parameter, the solution was demonstrated to exist. A perturbation solution for a small viscoelastic value was found, as well as an asymptotic solution for a high viscoelastic parameter. Koblinski et al. [115] investigated the mechanisms of heat flow in nanoparticle suspensions.

Liao [87] developed the homotopy analysis approach, a powerful and simple analytic tool for nonlinear problems that provided an exact result of viscous flow of power-law liquid above an extending surface. The explicit analytic outcomes for the pretended second and third order power law fluids are given by recursive equations having coefficient constants. In addition, an analytic equation for skin friction on the moving sheet was provided for actual indices of power law and when the magnetic field value is relatively big. In terms of physics, the magnetic field tends to increase skin friction, indicating that the flow is slowed. Shear-thinning liquids exhibit this effect more than shear thickening liquids. In the presence of radiation, Datti et al. [49] investigated stream of a Walters' B fluid above a non-uniform extended surface involving domestic heat source or sink. Temperature-dependent thermal conductivity was postulated. By applying a similarity transformation for the controlling PDEs,

ODEs were generated. Analytical and numerical techniques were used to solve these equations.

Using a fourth-order Runge-Kutta algorithm and the shooting technique, Afify [14] explored MHD free convective stream and energy transmission across a stretching surface through chemical reaction. For numerous values of chemical reaction rates and liquids with a Prandtl number of 0.71, numerical findings for velocity, temperature, and concentration profiles, as well as the skin friction coefficient, local Nusselt number, and Sherwood number, were reported. Using the quasi-linearization method, Massoudi and Maneschy [105] examined the numerical outcomes to the stream of a second-grade liquid across a stretching surface. Rajagopal and Gupta [127] and Rajagopal et al. [128] investigated this problem using a perturbation approach. Using the similarity transformation proposed by Rajagopal et al. [130], Massoudi and Maneschy [105] utilized the quasi-linearization method to obtain approximate solutions to the relevant equations.

Energy transmission in an MHD stream of a micropolar fluid across an extending sheet involving suction or blowing via permeable surface was examined by Eldabe et al. [54]. Chebyshev's finite difference approach was used to solve the governing equations for linear momentum, rotational momentum, and energy. On the velocities and temperature profiles, the impacts of surface mass transfer, Prandtl number, magnetic field, and porous media were examined. In the presence of a uniform transverse magnetic field, Liu [88] looked at the momentum, heat, and mass transfer of a hydrodynamic liquid past a stretching sheet. Internal heat source or sink is comprised in the mass transmission equation, as are chemically responsive species of order one reactivity. The distance was expected to be a linear function of the concentration and temperature boundary conditions. MHD stream of a power-law liquid across a stretching sheet was recently described by Cortell [42], and the problem was numerically addressed. The literature on the shrinking sheet problem will now be presented.

An oscillatory motion of a viscoelastic liquid via a stretched sheet was examined by Siddheshwar et al. [116]. A power series method was used to get the solution to the equation of motion. Unsteadiness had a significant impact on wall velocity and skin friction, according to the researchers. The unsteady MHD stream of

Maxwellian fluids atop impulsively extending sheets were examined by Alizadeh et al. [15], and the modelled equations were solved using the homotopy analysis method. Nield and Kuznetsov [45] have solved the Cheng–Minkowycz issue for natural convective boundary layer stream in a pervious medium saturated with a nanofluid.

Abel et al. [92] investigated the mathematical study of MHD flow and energy transmission near a horizontal stretched sheet to a laminar liquid film. Using similarity transformation, the flow of a thin fluid film and consequent energy exchange from the stretching surface is examined. Using an effective shooting technique, the numerical solution of the resulting nonlinear differential equations was found. The thickness of the boundary layer is quantitatively investigated for variations in non-dimensional factors. Manjunatha et al. [135] investigated the influence of thermal radiation on stream and energy transmission in the dusty liquid across variable stretched surface. Khidir et al. [79] investigated the thermal-diffusion and viscous dissipation features of natural convection near a vertical plate immersed in a non-Newtonian liquid saturated non-Darcy porous medium. In a vertical channel, Haritha et al. [67] investigated convective energy and mass transmission in the nanoliquids bordered through stretched and immobile fences. From a practical standpoint, controlling the stretching sheet boundary layer flow is critical. Some liquids, such as liquid metals, nuclear fuel slurry, biological liquids, mercury amalgams, paper coating, lubricating oil greases, and plastic extrusions, have applicability in many areas both in the absence and presence of a magnetic field, according to Sarpakaya [147]. The application of a magnetic influence produces a rheostatic impact on the stream because cooling liquids are electrically conducting in most situations. The literature on the Casson fluid flow and magnetohydrodynamic (MHD) stretching sheet problem is briefly reviewed here.

1.4.3 Casson fluid flow due to stretching sheet

Casson fluid has been shown to be useful in a variety of applications where the fluid exhibits non-Newtonian behaviour with an edge shear stress. The model's utility can be shown in fields like medical science, such as blood flow behavior. It also characterizes the behavior of numerous base fluids used as coolants in the food sector, such as sodium alginate, Xianthen gum, and so on. Many heat conduction researchers have studied it extensively due to its use. The magnetohydrodynamic stream of non-

Newtonian liquid across an exponentially pervious flinching surface was examined by Nadeem et al. [136]. In the presence of a uniform transverse magnetic field, Das [74] investigated the impact of partial slip-on continual boundary layer stagnation point flow of an electrically charged micropolar liquid imposed normally near a shrinking surface. Swati et al. [154] investigated the unsteady stream of non-Newtonian liquid across an expanding plate at a fixed temperature. The momentum equation was solved numerically using the shooting method, and the energy equation was subsequently solved numerically using the same way. Pramanik [137] explored the stream of a non-Newtonian liquid near an exponentially extended surface involving suction or blowing near the sheet along with heat transfer. Mahanta and Shaw [61] looked at three-dimensional Casson fluid flow near an extending surface in porous medium. The governing equations were solved with the help of the Spectral Relaxation method. Bhattacharyya et al. [80] studied the thermal boundary layer in Casson fluid flow across a pervious shrinking surface with varying wall temperature and radiation. The influence of magnetohydrodynamic (MHD) on the mixed convection stream of a Casson nanofluid across a nonlinear pervious stretching surface involving viscous dissipation, as well as double stratification and Joule heating was explored by Ramaiah et al. [131]. Ramana Reddy et al. [73] compared Casson and Maxwell's fluid flow near the stretching sheet in the presence of a steady heat source or sink and a magnetic field. Yang et al. [50] studied thermal transport analysis in Casson nanofluid stagnation-point flow across a diminishing surface involving viscous dissipation.

1.4.4 Bioconvection in fluid flow due to nano particles and gyrotactic microorganisms

The term "bioconvection" was coined by Platt [125] to explain the process of pattern formation in shallow suspensions of motile microorganisms. The directed spinning of organisms creates and maintains a macroscopic disparity in the concentration of bacteriological inhabitants, which is known as bioconvection. Bioconvection due to nanoliquids and microbes is an important exploration due to recent bionanomaterials producing needs. In such unstable settings, bioconvection flow occurs at the interface of a liquid comprising microorganisms or bacteria, and the boundary layer including microbes dispersed as bioconvection units, which can be

classified as oxytactic or gravitaxis, gyrotactic microbes. Childress et al. [40] provided a model for collective drive and pattern development in layered suspensions of negatively geotactic bacteria. The findings are compared to patterns formed by the ciliated protozoan *Tetrahymena pyriformis*. Pedley and Kessler [122]-[123] examined bioconvection of hydrodynamic processes in the suspension of swimming microorganisms and pattern development. Bees and Hill [89]-[90], [23] released a series of studies on the methodology for analyzing and measuring the bioconvection patterns created by aqueous cultures of the single-celled alga *Chlamydomonas nivalis* as a function of cell concentration, suspension depth, and time. Andras Czirik et al. [20] looked into the properties of the patterns during the onset of the instability and later during its development into a completely nonlinear convection method. Using the continuum model proposed by Pedley et al. [124], Ghorai and Hill [134] studied the occurrence and stability of periodic arrays of two-dimensional plumes in deep chambers. After that, the outcomes of related equations are determined by applying finite difference approach. Hopkins and Lisa [106] proposed a numerical approach and a computer model for analyzing the group dynamics of geotactic, gyrotactic, and chemotactic microorganisms immersed in a viscous fluid. Kuznetsov and Avramenko [4]-[5] investigated bioconvection in a liquid comprising of motile oxytactic, gyrotactic microorganisms through saturated porous media and established an analytical expression for the porous medium's critical permeability. The influence of tiny particles on the steadiness of bioconvection in a suspension of gyrotactic microbes in a layer of finite depth was explored by Kuznetsov and Avramenko [6]. Avramenko and Kuznetsov [7] looked into the stability of gyrotactic microbe suspension in a stacked fluid and porous layer system. Patterns generation of gravitactic microbe in a vertical cylinder is represented by the Navier–Stokes equation linked with the microorganism conservation equation, according to Alloui et al. [168]. These equations were numerically solved using the control volume approach. Bioconvection patterns suspensions of swimming microorganisms that are slightly denser than water, theoretical and practical advances, comprising nonlinear examination of the patterns, diffusion in shear streams, dimensions of cell swimming behaviour, and innovative efforts to formulate more concentrated suspensions were presented by Hill and Pedley [110]. Kuznetsov [8] investigated bioconvection in a system comprising both gyrotactic microorganisms and nanoparticles, concluding that

these microbes generate or improve nanofluid convection. Croze et al. [114] looked at bioconvection and cell diffusion in horizontal tubes with imposed stream. The patterns caused by suspensions of the gyrotactic and gravitactic green biflagellate algae *Chlamydomonas* in horizontal tubes subjected to an imposed flow are quantified for the first time in this experimental investigation. Kuznetsov [2] investigated a nanofluid including nanoparticles and oxytactic bacteria. The Galerkin solution provides important physical perceptions into the behaviour of this system, as well as confirming that the fluctuating means of volatility is achievable in a rather system. Aziz et al. [3] evaluated the free convection boundary layer stream past a horizontal flat surface embedded in a pervious medium saturated with nanofluid comprising gyrotactic microbes. In the presence of both nanoparticles and motile microbes, Xu and Pop [66] investigated a mixed convection stream of a nanofluid across an extending surface with steady free flow. The implications of essential physical parameters such as velocity, energy, nanoparticle concentration, and density of motile microbes, profiles are addressed, and analytical solutions with high accuracy are derived for the deformed equations with the usage of homotopy analysis method (HAM).

Makinde and Khan [162], Das et.al [48], and Khan et al. [163] evaluated the impact of bioconvection constraints on the dimensionless velocity, energy, concentration of nanoparticle and motile microbes, as well as Sherwood, local Nusselt, and motile microbe counts. MHD nanofluid bioconvection caused by gyrotactic microbes across a convectively heated stretched surface, as well as a vertical sheet involving slip and chemical response via pervious intermediate.

The bioconvection caused by the hydromagnetic stream of a water-based fluid comprising nanoparticles and motile microbes near a porous vertical continual sheet was studied by Mutuku and Makinde [165]. The combined influence of buoyancy forces and magnetic fields on the interface of motile bacteria and nanoparticles produces bioconvection. The boundary value problem is solved using appropriate similarity transformation and shooting quadrature, as well as the Runge Kutta–Fehlberg integration scheme. Hady et al. [59] reported a numerical analysis of an unsteady thermal bioconvection boundary layer stream of a nanofluid comprising motile microbes along an extending surface involving the magnetic and viscous

dissipation properties. An explicit finite difference method is utilized to find the numerical results. The thermophoresis and Brownian movement effects are conveyed for in the nanofluid model. The results show that each bioconvection Rayleigh number and magnetic parameter have a favorable impact on the density of microbes and dimensionless Nusselt number, whereas Eckert number and Grashof number have the opposite effect. Uddin et al. [95] explored the impacts of 2nd order rapidity slip, microorganism species slip, thermal slip, and Stefan blowing on bioconvection physical phenomenon stream of a nanofluid near a horizontal surface surrounded in an exceedingly pervious medium including the presence of an inactively restricted boundary values. The Chebyshev collocation method is utilized to solve the similarity equations numerically. A Nakamura tri-diagonal finite difference method is used to validate the results.

Using an explicit finite difference approach, the numerical solution is achieved. The nanofluid model takes into account the effects of a variety of variables. Tausif et al. [157] investigated the various slip impacts on bioconvection of gyrotactic microbes and nanoparticles in a liquid stream. Graphs and charts are utilized to investigate the impacts of different slip constraints on flow characteristics. Slip constraints are closely associated with numerous physical aspects of the stream, according to the investigation.

The bioconvection stream of nanofluid embedded gyrotactic microbes near a vertical wavy cone was investigated by Siddiqa et al. [139]. The numerical findings obtained utilizing an implicit finite difference iterative technique, show that the amplitude of the wavy cone surface and half cone angle have a significant impact on the heat exchange coefficient, mass transmission constant, and microorganism density constant. The influence of Brownian movement and thermophoresis on radiative Casson liquid in a two-dimensional flow across a moving wedge loaded with gyrotactic microbes with magnetic effects were explored by Raju et al. [30]. Ramzan et al. [109] investigated the stream of a magneto Jeffrey nanofluid past an angled stretched cylinder with heat generation or absorption and thermal radiation. Thermal and concentration stratification effects are taken into consideration as well. Temperature and concentration distributions have been found to be diminishing functions of thermal and solutal stratification factors. Pal and Mondal [118]

demonstrated bioconvection due to nanofluid embedded gyrotactic microbes across an exponentially extended surface comprising heat radiation. Talha et al. [94] explored MHD stable incompressible viscous Williamson's nano fluid including exponential domestic heat production and motile microbes atop the extending surface. In the presence of a magnetic field and a heat source or sink, Aamir Ali et al. [9] explored the stream of Maxwell nanofluid surrounded with motile microbes over a stretched surface. In comparison to the case of a heat sink, the thickness and temperature of the thermal boundary layer in the case of a heat source have been seen to rise. Rehman et al. [78] investigated the interaction of motile microorganisms with nanofluid near a vertical stretching sheet, and also studied the influence of bioconvection Peclet number, Schmidt number, and the microorganism's concentration difference parameter on motile gyrotactic microorganism density. The combined effects of convective boundary conditions and the magnetic field on the bioconvection in nanofluid flow with gyrotactic microbes near an expanding sheet were investigated by Chakraborty et al. [156]. Alzahrani et al. [53] demonstrated third-grade liquid flow with gyrotactic microorganisms on a horizontal porous expanding sheet involving a magnetic effect. Nayak et al. [91] explored the impacts of speed, concentration, motile microbes, and slip on the stream with a chemical consequence, finding that negligible values of Prandtl number intensify the magnetic influence and accelerate microbe distribution. Srinivasacharya and Sreenath [44] investigated the bioconvection of micropolar fluid in an annulus containing microorganisms in which the outer cylinder rotates, as well as the density of motile microbes and their slip parameter.

Hossein Zadeh et al. [70] studied the impacts of mixed liquid stream including motile microbes and nanoparticles on momentum, energy, and concentration profiles on a horizontal cylinder with magnetic field and viscous dissipation. Hosseinzadeh et al. [71] investigated magnetohydrodynamic (MHD) flow on a surface with microorganisms and nanoparticles. Thermophoresis, thermal radiation, Brownian movement, bioconvection Schmidt number, Peclet number, and magnetic field all have an impact on concentration of microbes, skin friction coefficient, Sherwood number, and Nusselt number.

Rahila Naz et al. [126] examined entropy generation dynamics in a magnetohydrodynamic flow of Williamson nanofluid containing gyrotactic

microorganisms. The Brownian motion parameter can be used to increase nanoparticle concentration, while the temperature difference parameter can be used to manage the entropy production process. Yu-Ming Chu et al. [167] looked at the impact of a third-grade fluid model (non-Newtonian) on a stretchy surface containing gyrotactic microorganisms in a steady, incompressible, and two-dimensional laminar flow. Larger thermophoresis parameters and Brownian movement were shown to be more susceptible to the thermal field and associated layer thickness. In the presence of a magnetic field, Fazal Haq et al. [58] investigated the flow behaviour of stratified Williamson nanofluid across the porous surface of a stretching cylinder containing gyrotactic microorganisms. In addition, a growth in the vortex viscosity constraints enhances the penetration of microorganisms from the sheet to the border layer and amplifies the density number of motile microorganisms. Zuhra et al. [145] studied the simultaneous stream and energy transmission of Casson and Williamson nanofluids across a pervious medium in the presence of gyrotactic microorganisms and a cubic autocatalysis chemical reaction under buoyancy forces. The convective heat exchange properties of MHD nanofluid flow in a three-dimensional geometry, comprising oxytactic motile microbes moving through a spinning cone were examined by Mogharrebi et al. [108].

CHAPTER 2

Classification of Fluids, Governing Equations and Boundary Conditions

2.1 INTRODUCTION

The purpose of this chapter is to present the classification of fluids as well as the fundamental principles of fluid dynamics that apply to them. The chapter's goal is to go over the essential equations for the dynamics of Newtonian and Casson liquid due to a stretched sheet. Boussinesq approximations and the boundary layer approximations are thoroughly examined. The momentum and energy boundary conditions for stretching surface issues are also discussed. The dimensionless parameters that arise in the problems under consideration are also grouped together.

2.2 Fluid State and Its Physical Characteristics

Solid and fluid matter are the two most common types of matter. Solids can withstand both marginal internal tension and normal, whereas fluids can only withstand normal tension at rest. The stress at any point occupying in an area is referred to as normal stress, while the tension at any point engaging in a region is $\lim_{A \rightarrow 0} \left(\frac{F}{A} \right)$, referred to as fluid pressure. Only when the medium is continuous does this hold true. As a result, it is critical to explain the continuum theory, which can be described as below.

Continuum Hypothesis

Liquids are aggregations of particles, broadly spread out for the air and densely spread out for the fluids, as is well known. In comparison to the molecular diameter, the distance between molecules is extremely large. The particles are not static in a pattern, but rather, flow around spontaneously. These molecules are constantly colliding and moving at random. When we imagine the liquid to be made up of discrete particles flowing at random, the computing means turn out to be useless, adding to the problem's complexity. To get around this problem, we assume the fluid is unceasingly dispersed in a specific space. A liquid constituent can be split

indeterminately in this way. In a particular space, they are evenly dispersed. A fluid element can be separated indefinitely in this way. The "Continuum Hypothesis" is the name given to this theory of continuity. We assume that the dimensions of a liquid particle are enormously insignificant in comparison to the overall dimensions conquered by the liquid, that the liquid particle is a physical object, and that the fluid density is a continuous function of place and time under the premise. As a result, pressure at a point in a continuum is defined as

$$P = \lim_{A \rightarrow A^*} \left(\frac{F}{A} \right) \quad (2.2.1)$$

In keeping with the continuum method, F is the force normal to the surface A , and A^* is the smallest area surrounding the point. In addition, the density of a continuum is determined by

$$\rho = \lim_{V \rightarrow V^*} \left(\frac{M}{V} \right), \quad (2.2.2)$$

In accordance with the continuum approach, M denotes the mass contained in volume V , and V^* denotes the smallest volume surrounding the point.

Homogeneity

In all sections of the system, the fluid characteristics are considered to be the same. This assumption might be broken in a suspension, for example, if the particles were not evenly distributed.

Isotropy

When a fluid's property (pressure density, for example) is the same in all directions at a place, it is said to be isotropic. If a fluid's property is not the same in all directions, it is said to be anisotropic.

2.2.1 Fluid State

Liquid, gaseous, and plasma are the three different types of fluids. Fluid dynamics is concerned with the first two states, while plasma dynamics is concerned with the third. Hydrodynamics and aerodynamics are the two corresponding branches of fluid dynamics, the former dealing with water and other fluids and the latter

employing an air and other gases. Another common classification is based on the practical significance of fluid friction. All tangential strains induced by friction are ignored in the "perfect fluids." The term "real fluids" refers to situations where friction is taken into consideration appropriately.

2.2.2 Ideal Liquid or Inviscid Liquid

"An ideal liquid has no other properties beyond density." When such a fluid flows, no resistance is encountered". In other words, Inviscid liquids are those where two connecting surfaces do not go through tangential force, but constraint one another using normal force, as soon as the liquids are in movement. This translates to "inviscid liquid has no internal resistance to shape change." Whether the liquid is at rest or in movement, the normal force at every point of a perfect liquid is identical in all directions. Perfect liquids or frictionless liquids are other names for inviscid fluids. Nature does not have such a fluid. The mathematical analysis is made easier by the assumption of perfect fluids. Under some conditions, however, low viscosity fluids like air and water can be classified as ideal liquids.

2.2.3 VISCOUS OR REAL LIQUID

"Viscous liquids or real liquids have surface tension, viscosity, and compressibility in addition to density" or "Viscous fluids or real fluids suffer tangential as well as normal tensions when they are in movement." This is also fact adjacent to a liquid-soaked solid wall. The attribute of a real fluid imposing normal tension and tangential while in movement is known as viscosity. During the motion of a viscous liquid, internal resistance is very essential. Internal resistance to fluid motion is one of the most essential features of viscous fluids. Because viscosity is a property of real fluids, it also demonstrates some resistance to changing their shape. The following two groups of viscous or actual fluids are distinguished.

- i. Newtonian Liquid
- ii. Non-Newtonian Liquid

2.2.4 NEWTONIAN LIQUIDS

Newtonian fluids follow Newton's law of viscosity, which stipulates that "shear tension is proportional to velocity gradient." As a result, we obtain a straight line passing through the origin when plotting shear stress versus rate of strain. This curve is known as the liquid's Rheogram or flow curve. For a Newtonian liquid, the equation of constitutive is

$$\tau_{ij} = \left(\frac{2}{3} \mu q_{k,k}\right) \delta_{ij} + \mu(q_{i,j} + q_{j,i}) \quad , \quad (2.2.4)$$

where τ_{ij} are the components of stress, δ_{ij} are the Kronecker's delta tensor components, q_i are the components of velocity, and μ is the viscosity coefficient.

2.2.5 NON-NEWTONIAN LIQUIDS

The term "non-Newtonian liquid" refers to a liquid that does not satisfy Newton's law or has a non-linear flow curve. This indicates that the viscosity of a non-Newtonian liquid is dependent on other parameters such as shear rate, the apparatus in which the liquid is housed, and even the liquid's historical history, rather than being constant at a particular temperature and pressure. Rheology is the study of non-Newtonian liquids. Based on the non-linearity of the stream curve and the amount of time the liquid has been sheared, non-Newtonian liquids are classified as follows.

Non-Newtonian liquids Classification:

Non-Newtonian liquids with non-linear stream curvatures can be classified into three groups.

- i. Non-Newtonian liquids are ones whose fleece size at any point is the relation of the shearing tension near the place and does not depend on anything else.
- ii. There is a more sophisticated structure where the relationship between shear rate and shear tension is dependent on the length of time the liquid has been sheared or its previous motion history. Non-Newtonian fluids are a class of complex fluid systems that are **time dependent**.

iii. There are several fluid systems that display partial elastic recovery after deformation and have features of both solids and fluids. These fluid systems are referred to as **viscoelastic liquids**.

Time-independent non-Newtonian liquids

The rheological equation of the form governs the behavior of these liquids,

$$e_{ij} = f(\tau_{ij}), \quad (2.2.5)$$

i.e., In such liquids, the rate of strain is independent of the time it takes to shear the liquid. Depending on the nature of the function f , these liquids can be categorized into four types (see Skelland, 1967):

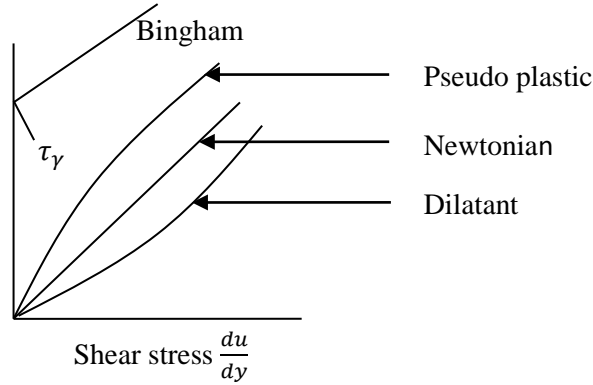


Figure.2.2.1: Rheogram

1 Bingham plastic: The shear stress axis intersects the flow curve, which is a straight line. The equation for these liquids is as follows:

$$\tau_{ij} = \left(\mu + \frac{\tau_y}{(e_{ij}e_{ij})^{1/2}} \right) e_{ij}, \quad (2.2.6)$$

Where μ the coefficient of viscosity is, τ_y is the yield stress, τ_{ij} is shear stress and

$$e_{ij} = \frac{\partial q_i}{\partial x_j} + \frac{\partial q_j}{\partial x_i}.$$

2 Casson fluids have a yield stress. The constitutive equation for these liquids is

$$\tau_{ij} = \left[k_c^2 + \tau_y + \frac{k_c \tau_y^{1/2}}{\left(\frac{1}{2} \sum_c \sum_d e_{cd} e_{cd} \right)^{1/2}} \right] e_{ij}, \quad (2.2.7)$$

where k_c^2 , is the Casson's viscosity constant that applies to a certain liquid and τ_y is the yield stress.

2.3 Bioconvection Due to Nanofluid Containing Gyrotactic Microorganisms

The Thermal characteristics of nanofluids are quite good. When gyrotactic microorganisms are added to a nanofluid, it improves heat transfer, mixing, and the nanofluid's thermal properties. This is due to the turn over impact and the formation of spontaneous patterns caused by the motile microbes' biased migration as they seek better environments. As a result, nanofluid bioconvection has a wide range of direct applications in gas modeling and oil-bearing microbial improved oil revival, as well as the pharmaceutical business. The synthesis of biofuels from microorganisms, particularly hydrogen or biodiesel, has sparked considerable attention. For these alternative fuels to be commercially competitive, existing bioreactors must be refined. Despite the fact that the field of nanofluids has received a lot of attention, the qualities of swimming cell suspension have received little attention. More exploration of heat exchange in the nanofluid bioconvection is needed to understand the factors that improve heat transmission.

2.3.1 Nanofluids

In the recent discoveries of nanofluids, cooling technology had spawned a solution. This is because, when compared to normal liquids, nanofluids exhibit negligible congestion, superior convective and conductive heat exchange capabilities. Nanofluids are useful in a variety of industrial applications due to their cooling properties. Nuclear reactors and computer coolants are two applications where nanofluids are used. The broad range of claims for nanofluids is the primary motivator for the study in this area. The use of nanofluids in some microsystems has sparked a lot of attention recently, according to recent papers. Micro-reactors, micro-heat pipes, and micro-channel heat sinks are only a few of the microsystems available. Nanomaterials have also demonstrated their ability to be used in a variety of bio-microsystems, including enzyme biosensors. The development of chip-size micro-devices for assessing nanoparticle toxicity has also sparked a lot of attention. Nanomachines, nanostructures, nanofibers, nanowires, and nanoparticles are some of

the potential application areas for nanomaterials available in biotechnology. Nanofluids are employed to conserve both material and heat in the exchanger. Biological sensors, pharmaceuticals, and agriculture are just a few of the applications that might be developed by combining biotechnology components with nanofluid.

2.3.2 Brownian Motion

Brownian motion is caused when nanoparticles travel through the molecules of the base fluid and collide with nearby particles. When two particles collide, the heat transfer mode can boost the nanofluid's overall thermal conductivity. A diffusive path is the result of Brownian motion. It is clear that as the temperature rises, the diffusivity rises, resulting in a rise in thermal conductivity.

2.3.3 Thermophoresis

Particle thermophoresis, which is analogous to thermal diffusion, is a non-uniform mixed-stream influence between mass and energy transmission in simple fluid combinations (the Soret effect). The scattered particles exhibit a continuous drift velocity on top of Brownian motion when a colloidal disturbance is to be found in the temperature gradient, with the thermophoretic motion being referred to as the thermal diffusion coefficient. The particles subsequently concentrate on the cold or hot side, resulting in a steady state concentration gradient for low particle concentration, depending on the indication.

2.3.4 Viscous Dissipation

The effects of viscous dissipation are generally only noticeable in high viscous flows or when the velocity distribution has a large gradient. In high-velocity flows, such steep slopes occur at the macroscale. Even with low-velocity flows, such steep gradients can occur due to the small size of microscale devices. As a result, viscous dissipation in microchannels should be taken into account. Viscous dissipation exists as a source term in the liquid stream and creates temperature distribution variance due to the conversion of the fluid's kinetic motion to thermal energy.

2.3.5 Gyrotactic Microorganisms

In recent years, the study of natural pattern development in motile microbe suspensions has gained interest. These organisms have developed millions of years

ago, whether they're in our bellies or changing the global climate through photosynthesis in the sea. The power of microorganisms could be harnessed. Alcohol is produced as an unwanted byproduct by some algae and bacteria, but it is a valuable commodity to humans, not least because it may be utilized as a fuel. Plastics, fertilizers, waste treatment plants, and solid fuels can all benefit from algae and their products. The goal of this thesis is to explain why swimming microbe suspensions have certain patterns.

A living being that can grow, digest food, and reproduce on a regular basis is known as "organism." A single cell or a multicellular creature could be the source of the problem. Microorganisms are tiny organisms that can't be seen with the naked eye. Organisms are classified into five different groups: prokaryotes, protists, fungi, plants, and animals.

2.3.6 Bioconvection

Bioconvection is a phenomenon in which motile microbe suspensions produce spontaneous flow patterns. Nanofluids are connected to this phenomenon. Motile bacteria in a nanofluid can spin dynamically in response to provocations such as chemical(s) attraction, light, and gravity. When motile microbes are added to a deferral, mass transfer and mixing are two of the advantages that are gained. Gas modeling and the pharmaceutical industry, oil-bearing microbial enhanced oil recovery, microfluidic devices, sedimentary basins, and many more direct uses of nanofluid bioconvection are just a few examples. The production of biofuels from microorganisms, particularly hydrogen and biodiesel, has piqued interest. Existing bioreactors must be refined in order for these alternative fuels to be commercially competitive. The field of nanofluids has been widely explored due to their numerous uses. However, in biotechnology applications, the characteristics of swimming cell suspension have been under-utilized or completely neglected. In light of the rising demand for nanofluids and the various prospective applications of bioconvection in nanofluid, this project intends to investigate bioconvection of a non-Newtonian nanofluid across a stretching sheet with gyrotactic microorganisms.

2.4 Fundamental Equations of Fluid Dynamics in Vectorial Form

The fundamental equations of fluid dynamics are a set of nonlinear partial differential equations that must be solved to investigate any liquid motion. The basic equations that control all flow phenomena are listed here:

1. Physical principle (Law of conservation of mass): It is impossible to produce or destroy mass.

Equation of continuity:

$$\frac{\partial \rho}{\partial t} + \nabla \cdot (\rho \vec{q}) = 0, \quad (2.4.1)$$

Where, \vec{q} is the velocity of the fluid and ρ is the fluid density.

2. Physical principle (Law of conservation of momentum): The overall force acting on a liquid mass confined in a control volume in space is same as that of rate of change of linear momentum over time.

Equation of motion:

$$\rho \frac{D\vec{q}}{Dt} = \rho \vec{X} - \nabla p + \nabla \cdot \tau, \quad (2.4.2)$$

where, p and τ denotes viscous stress tensor (Only deviatoric strains are present) and the liquid's pressure. The operator $\frac{D}{Dt} = \frac{\partial}{\partial t} + \vec{q} \cdot \nabla$ is the physical derivative. The equation of motion (2.4.2) is also known as the **Navier-Stokes equation**.

3. Physical principle (Law of conservation of energy): The rate of raise in the internal energy is equal to sum of heat supply through surface, work done by friction and dissipated energy.

Equation of energy:

$$\rho \frac{DU}{Dt} = -\nabla \cdot \vec{Q} - p \nabla \cdot \vec{q} + \phi, \quad (2.4.3)$$

Here, internal energy is denoted as, $\bar{Q} = -k\nabla T$ (Fourier's law) represents direction of energy flow, $\varphi = \nabla \cdot (\tau \vec{q}) - \vec{q} \cdot \nabla \tau$ is the function of dissipation. The fundamental equations of fluid dynamics are the three equations listed above (see Tritton, 1979; Yuan, 1970). In the case of a stretching sheet problem, we may now simplify these equations.

2.5 Basic Equations of Stretching Sheet Problem

Conservation of mass

The differential version of the continuity equation is represented by the equation (2.4.1). In the concerns discussed in this thesis, the concentration of the conserving liquid is assumed to be constant, hence the phase derivative of concentration in equation (2.4.1) disappears, and the continuity equation takes the final form presented below.

$$\nabla \cdot \vec{q} = 0, \quad (2.5.1)$$

Conservation of linear momentum

Before proceeding, we make the following assumptions:

1. The cooling liquid flows because the sheet is stretched, implying that there is no pressure gradient driving the liquid i.e., $\nabla p_{mot} = 0$.
2. It is believed that the flow will be steady i.e., $\frac{\partial}{\partial t} = 0$.

The momentum equation (2.4.2) assumes the following form using the above assumptions.

$$\rho(\vec{q} \cdot \nabla) \vec{q} = \nabla p + \rho \vec{X} + \nabla \cdot \tau, \quad (2.5.2)$$

For Newtonian, equations (2.2.1) provide the stress tensor τ .

Conservation of energy

We don't detect the impacts of viscous dissipation, internal heat production, or radiation on velocity profiles except buoyancy is present since the temperature has no

influence on the velocity profile owing to the hypothesis of a homogenous liquid. These affects are only obvious on the temperature profile if there is a one-way connection between temperature and velocity; if there is a two-way coupling, the impacts are visible on both the velocity and temperature profiles. Furthermore, viscoelasticity manifests itself indirectly rather than explicitly in energy conservation. Using the flow assumptions and equation (2.4.1), the heat transfer equation (2.4.3) with internal energy $U = C_p T$ is produced.

$$\rho C_p (\vec{q} \cdot \nabla) T = k \nabla^2 T + \varphi, \quad (2.5.3)$$

Both Newtonian and non-Newtonian models use the aforementioned type of energy conservation. Similarly, for incompressible fluids, the energy equation will be as follows

$$\rho C_p \left(\frac{\partial T}{\partial t} + (v \cdot \nabla) T \right) = \tau_{ij} \cdot L + k \nabla^2 T + \rho r_h \quad (2.5.4)$$

Here, T stands for temperature, and , $\tau_{ij} \cdot L$ stands for viscous dissipation, k for thermal conductivity, r_h for radiative heating, and the above equation assumes the form in the absence of radiative heating,

$$\rho C_p \left(\frac{\partial T}{\partial t} + (v \cdot \nabla) T \right) = \tau_{ij} \cdot L + k \nabla^2 T, \quad (2.5.5)$$

2.6 Magnetohydrodynamic (MHD) Equations

When the displacement currents and free charges are ignored, the basic equations of MHD are as follows,

$$\begin{aligned} \nabla \cdot \vec{E} &= 0, \\ \nabla \cdot \vec{H} &= 0, \\ \nabla \times \vec{E} &= -\mu_m \frac{\partial H}{\partial t}, \\ \nabla \times \vec{H} &= \vec{j}, \\ \nabla \cdot \vec{j} &= 0, \end{aligned} \quad (2.6.1)$$

here, \vec{E} denotes electric field, \vec{H} denotes magnetic field, \vec{J} is denotes moment density and μ_m is the magnetic viscosity. The Maxwell equations are the MHD equations listed above. The density at the moment \vec{J} is given by, Ohm's law, in the following form:

$$\vec{J} = \sigma(\vec{E} + \mu_m \vec{q} \times \vec{H}), \quad (2.6.2)$$

When the conduction current $\sigma\vec{E}$ is negligible compared to $\sigma\mu_m\vec{q} \times \vec{H}$ Ohm's law gives

$$\vec{J} = \sigma\mu_m\vec{q} \times \vec{H}, \quad (2.6.3)$$

When the magnetic Reynolds number R_m is of less magnitude, the Lorentz force takes the form

$$\mu_m\vec{J} \times \vec{H} = \sigma\mu_m^2 H_0^2 \vec{q}, \quad (2.6.4)$$

Where H_0 is the applied magnetic field, we now go over two key approximations utilized in the theoretical analysis of stretching sheet problems.

2.7 Approximations

The following approximations were used to get the fundamental equations:

2.7.1 Boundary layer approximation

Ludwig Prandtl, a German scientist, proposed the concept of laminar boundary layers in 1904. Prandtl proposed in his study that the flow around a solid mass may be divided into two sections for liquids with extremely low viscosity: "liquid motion with very small friction."

- i. The boundary layer is a very thin layer in the immediate vicinity of the body that is thought to be dominated by viscous effects.
- ii. Outside of this layer, the viscous effects may be deemed minimal, and the liquid is called inviscid. The Navier-Stokes equations are streamlined to a

theoretically flexible model using this hypothesis, and these equations are referred to as boundary layer equations.

2.7.2 Boussinesq Approximation

If the flow is impacted by gravity, the Boussinesq approximation is utilized. The liquid is acted upon by gravity as a body force i.e., $\vec{X} = \rho \vec{g}$. Consider the most fundamental version of the Navier-Stokes equation for a Newtonian liquid, which is required for the Boussinesq approximation explanation.

$$\rho \frac{D\vec{q}}{Dt} = -\nabla p + \rho \vec{g} + \mu \nabla^2 \vec{q}, \quad (2.7.1)$$

If p and ρ are now perturbed about the values of p_{stat} and ρ_{stat} in a reference condition of hydrostatic equilibrium where $\nabla p_{stat} = \rho_{stat} \vec{g}$ (i.e., one sets $p = p_{stat} + p'$ and $\rho = \rho_{stat} + \rho'$ the above equation becomes

$$(\rho_{stat} + \rho') \frac{D\vec{q}}{Dt} = -\nabla p' + \rho' \vec{g} + \mu \nabla^2 \vec{q}, \quad (2.7.2)$$

This equation means that in determining the gravitational effect, only changes in density ρ' from some standard values matter. The density variation ρ' is assumed to be minimal in comparison to ρ_{stat} in the approximation being considered currently. We get the following when we rewrite the previous equation.

$$\left(1 + \frac{\rho'}{\rho_{stat}}\right) \frac{D\vec{q}}{Dt} = -\frac{1}{\rho_{stat}} \nabla p' + \frac{\rho'}{\rho_{stat}} \vec{g} + \nu \nabla^2 \vec{q}, \quad (2.7.3)$$

When ρ' is insignificant in comparison to ρ_{stat} , the density ratio $\frac{\rho'}{\rho_{stat}}$, compared to a liquid density ρ_{stat} , it functions as a tiny adjustment to inertia. However, in the context of buoyancy, this ratio is crucial.

Boussinesq [27a] approach entails ignoring density change in the inertia term while keeping it in the buoyancy term. Variations in liquid characteristics are also ignored in this approximation when viscosity and diffusion are factored in. Other constraints are required in compressible fluids, and the term 'Boussinesq approximation' is frequently used to describe these. Spiegel and Veronis [152a] go into great length on these topics, and only the conclusions will be quoted here. To

begin, potential density must be substituted for density. Small density deviations from a standard ρ_{stat} are limited by two factors: the vertical scale of the average movement should be significantly lower than the scale height, and varying density deviation owing to local pressure discrepancies should be minimal. The last of the extra criteria is the most essential; it means that the liquid can be viewed as incompressible, which means that sound and shock waves are excluded. Finally, in an unstable flow, the ratio of length to duration of any variation ought to be significantly smaller than the sound velocity, to confirm that evidence regarding pressure variations is delivered efficiently and instantly, as it would be in an incompressible viscous fluid.

2.8 Basic Equations after Approximations

Equation of Continuity

For a two-dimensional stream we have $\vec{q} = (u, v, 0)$, and therefore the equation of continuity equation (2.4.1) takes the following form:

$$\frac{\partial u}{\partial x} + \frac{\partial v}{\partial y} = 0, \quad (2.8.1)$$

Equation of motion

In the case of a linear stretching sheet problem, we get the equation of motion, which recovers the other two horizontal and vertical problems. We must employ both of the previously mentioned approximations. It is worth noting that, the velocity along the x -axis in the linear stretching sheet problem is considered to be $u = bx$. In component form, we express the equation (2.4.2) as follows:

$$\rho \left(u \frac{\partial u}{\partial x} + v \frac{\partial u}{\partial y} \right) = [\nabla p + \rho \vec{g}]_x + \left(\frac{\partial \tau_{xx}}{\partial x} + \frac{\partial \tau_{xy}}{\partial y} \right), \quad (2.8.2)$$

$$\rho \left(u \frac{\partial v}{\partial x} + v \frac{\partial v}{\partial y} \right) = [\nabla p + \rho \vec{g}]_y + \left(\frac{\partial \tau_{yx}}{\partial x} + \frac{\partial \tau_{yy}}{\partial y} \right), \quad (2.8.3)$$

By considering the stress-rate-of-strain relationship for Newtonian and non-Newtonian cooling liquids, we can now particularize the equation of motion.

Equation of momentum for stretching surface issue including a Newtonian and non-Newtonian fluids:

Equation of motion can be recast in the form by means of the definition of stress tensor for a Newtonian liquid from equation (2.2.1).

$$u \frac{\partial u}{\partial x} + v \frac{\partial u}{\partial y} = \nu \left(\frac{\partial^2 u}{\partial x^2} + \frac{\partial^2 u}{\partial y^2} \right) + \nu \frac{\partial}{\partial x} \left(\frac{\partial u}{\partial x} + \frac{\partial v}{\partial y} \right), \quad (2.8.4)$$

$$u \frac{\partial v}{\partial x} + v \frac{\partial v}{\partial y} = \nu \left(\frac{\partial^2 v}{\partial x^2} + \frac{\partial^2 v}{\partial y^2} \right) + \nu \frac{\partial}{\partial y} \left(\frac{\partial u}{\partial x} + \frac{\partial v}{\partial y} \right), \quad (2.8.5)$$

where the pressure gradient ∇p is assumed to be zero. Thus the equation can also be simplified for two-dimensional Newtonian fluid flow as

$$u \frac{\partial u}{\partial x} + v \frac{\partial u}{\partial y} = \nu \left(\frac{\partial^2 u}{\partial y^2} \right), \quad (2.8.6).$$

For the non-Newtonian fluid Casson fluid model is used in our study and the equation of motion can be taken in simplified form as

$$u \frac{\partial u}{\partial x} + v \frac{\partial u}{\partial y} = \nu \left(\beta + \frac{1}{\beta} \right) \left(\frac{\partial^2 u}{\partial y^2} \right), \quad (2.8.7)$$

where β is the Casson fluid parameter

Equation of energy

$$\rho c_p \left(\frac{\partial T}{\partial t} + u \frac{\partial T}{\partial x} + v \frac{\partial T}{\partial y} \right) = k \left(\frac{\partial^2 T}{\partial y^2} \right) + \mu \phi, \quad (2.8.8)$$

For two-dimensional steady incompressible fluid flow, the boundary layer energy equation is as follows:

$$\rho c_p \left(u \frac{\partial T}{\partial x} + v \frac{\partial T}{\partial y} \right) = k \left(\frac{\partial^2 T}{\partial y^2} \right) + \mu \phi, \quad (2.8.9)$$

Concentration of Nanofluids

It states that the entire species concentration of the framework beneath thought is always consistent. The mass flux based on the thermophoretic dissemination as well as the Brownian movement is given by.

$$j = j_T + j_B = \rho D_B \nabla C - \rho D_T \frac{\nabla T}{T_\infty}, \quad (2.8.10)$$

The condition for mass exchange within the absence of chemical response is generally presented as below

$$\frac{dC}{dt} = -\frac{1}{\rho} \nabla \cdot j \quad , \quad (2.8.11)$$

Therefore, equation of mass exchange takes the form

$$\frac{\partial C}{\partial t} + v \cdot \nabla C = \nabla \cdot \left(D_B \nabla C + D_T \frac{\nabla T}{T_\infty} \right) \quad , \quad (2.8.12)$$

Concentration of Microorganisms

There exist three major components of microorganism exchange that is plainly visible convection, irregular movement of microorganisms and self-moved swimming. The flux j_1 of microorganisms is characterized as

$$j_1 = nV + nW_c \hat{p} - D_m \nabla n \quad , \quad (2.8.13)$$

where nV is the flux due to advection, $W_c \hat{p}$ is the average relative swimming velocity and D_m is the diffusivity of microorganisms. The governing microorganism equation can be expressed as follows

$$\frac{\partial n}{\partial t} = -\nabla \cdot j_1 \quad , \quad (2.8.14)$$

Where j_1 is the microorganisms flux.

2.9 Boundary Conditions

The fluids mostly interact with their surroundings via shared limits. Boundary conditions are the outcome of mathematically expressing these boundary interactions. As a result, boundary conditions are limitations insisted on the conservation relations to define how the field under investigation imitates to its surroundings. As a result, boundary conditions are mathematical explanation of the interactions at the boundary that come from nature. These criteria are automatically applied once a system or a stream field is selected. Indeed, if boundary conditions aren't evident, the system's borders may not be natural, resulting in an ill-posed mathematics issue. The boundary surroundings may include movement, boundary values of field variables, rate of mass,

external stress, momentum flux, and relationships between them. In addition to boundary requirements, starting conditions are required when solving problems involving the time evolution of flow fields.

The number of boundary conditions required is determined by the type of the presiding partial differential equations. In general, elliptic equations need boundary requirements on all sides of the boundary, hyperbolic equations require boundary conditions upstream but not downstream, and parabolic equations require initial conditions and boundary conditions everywhere except downstream.

Boundary Conditions on Velocity

The type of the liquid stream and the geometry of the boundary wall affect the boundary conditions on velocity. We explore a constant, incompressible Casson fluid passing across a flat elastic sheet in this thesis. The surface is extended with a speed proportional to the distance from the origin $x = 0$ by applying two equal and opposite forces along the x -axis. The following are the mathematical representations of velocity boundary conditions:

$$\begin{aligned} u &= bx, & v &= 0 \quad \text{at } y = 0 \\ u &\rightarrow 0, & \frac{\partial u}{\partial y} &\rightarrow 0 \quad \text{as } y \rightarrow \infty, \end{aligned} \tag{2.9.1}$$

THERMAL BOUNDARY CONDITIONS

The thermal boundary conditions are influenced by the type of heating process used. The prescribed surface temperature was taken into account in our research (PST Case). The following is a mathematical depiction of such temperature boundary conditions:

$$\begin{aligned} T &= T_w = T_\infty + A \left(\frac{x}{l} \right)^{\lambda_1} \quad \text{at } y = 0, \\ T &\rightarrow T_\infty \quad \text{as } y \rightarrow \infty, \end{aligned} \tag{2.9.2}$$

2.10 Dimensionless Parameters

Every physical problem entails the measurement of physical quantities in various units. The physical problem, on the other hand, should not be affected by the unit of measurement. The dimensions of each physical quantity are written down in terms of fundamental units in dimensional analysis of any problem. We may then generate non-dimensional numbers by dividing and rearranging the various units.

A dimensional analysis of any issue provides data on the qualitative behaviour of the physical problem. We may use the dimensionless parameter to understand the physical significance of a problem-related phenomena. When it comes to obtaining dimensionless parameters, there are usually two options (i) The inspectional analysis (ii) The dimensionless analysis.

The latter approach was adopted in this thesis. Using certain dependent and independent characteristic values, the basic relations are constructed dimensionless in this manner. Certain dimensionless numbers occur as coefficients of various terms in these equations as a result of this procedure. The following sections discuss some of the dimensionless parameters that were employed in this thesis.

PRANDTL NUMBER

Non-linear convection is the method of thermal energy release that is related with a wide range of events in the convection problem. The motion is based on the Prandtl number, which is defined as

$$P_r = \frac{\text{viscous force}}{\text{thermal force}} = \frac{\mu c_p}{K}.$$

Chandrasekhar Number

Chandrasekhar number is represented by q and is defined as the square of the Hartmann number

$$q = Mn^2 = \frac{\sigma \mu_m^2 H_0^2}{\rho c}.$$

Eckert Number

The immeasurable quantity Eckert number is termed as E_c and is defined as

$$E_c = \frac{b^2 l^2}{c_p A}.$$

Where b, l, C_p are some velocity, characteristic length, and specific heat at constant pressure reference values, respectively.

Radiation Parameter

$$N = \frac{KK^*}{4\sigma T_\infty^3}.$$

Here, the Stefan-Boltzmann constant is represented by σ and the absorption coefficient is denoted by K^* , T_∞ is the temperature far away from the wall and the thermal conductivity of the fluid is denoted by K .

Skin Friction

We may compute the viscous drag, commonly known as skin friction, by integrating the boundary layer equations and obtaining the velocity distribution and the position of the point of separation. The shearing tension on the wall is determined by

$$\tau_0 = \mu \left(\frac{\partial u}{\partial y} \right) \text{ at } y = 0.$$

In the case of two-dimensional flow, the viscous drag is

$$D_\rho = b \int_0^l \tau_0 \cos \varphi \, ds.$$

The height of the cylindrical body is denoted by b . s is the co-ordinate measured along the surface, and φ is the angle between the tangent to the surface and the free stream velocity U .

Nusselt Number

The Nusselt number is the most essential dimensionless parameter in heat exchange issues, and it is defined as

$$N_u = \frac{-h}{(T_w - T_\infty)} \left(\frac{\partial T}{\partial y} \right)_{y=0}.$$

Where, $(T_w - T_\infty)$ is the temperature differential between the fluid and the wall and h is a characteristic length. This dimensionless quantity is defined as the ratio of actual heat exchange rate to the rate at which heat would be transmitted by conduction alone for a given temperature differential between the plates.

Lewis Number

The Lewis number is named after Warren Lewis, who proposed the concept in 1939. It refers to the relationship between the Prandtl and Schmidt numbers. When heat and mass transmission occur at the same time, the Lewis number is critical. It can be stated as follows

$$L_e = \frac{\alpha}{D}.$$

Where α and D are the thermal and mass diffusivity, respectively.

CHAPTER 3

Casson Fluid Flow Due to Stretching Sheet with Magnetic Effect and Variable Thermal Conductivity

3.1 INTRODUCTION

Theoretical study of Casson fluid flow across a linear stretching surface under the sway of magnetic effect is carried out in this chapter. The study of a continual stream of viscous incompressible liquids across a steady stretching surface is fascinating, and similar flow situations are emerging in a number of manufacturing processes, including desolidifying metallic products in a freezing bath process, ejection of plastic films, and forcing polymer ply through a dye to form polymer ply with a desired cross section. During the deposition of such polymer ply, the slit creates the mix, which is then stretched to the proper thickness, and the sheet solidifies as it travels through the cooling system, resulting in a well-graded output. The idiosyncrasies of ply appear to be controlled by heat and mass transmission contained by the ply and fluid. The stretching sheet develops a thermal and mechanical bond with the medium fluid during manufacture. Sakiadis [141] was the first to introduce a boundary layer flow across a continuous solid slab that was moving at a steady velocity. Crane [43] developed a solution for the two-dimensional incompressible boundary layer flow of adhesive fluid created by a stretching plate. This flow problem had already been employed in a variety of physical situations.

Magyari and Keller [99] used both exact and approximating techniques to attempt the boundary layer stream issue on an exponentially extending surface with ascending temperature diffusion. MHD Casson liquid near a pervious linearly flexible plate was explored by Nadeem et al. [136]. The impacts of MHD boundary layer stream of Casson fluid over stretching and shrinking surface with wall mass transmission were explored by Bhattacharya et al. [26] using an analytical solution. Mahanta and Shaw [102] explored three-dimensional Casson fluid streams via a pervious linearly stretched surface with a convective boundary requirement using the Spectral Relaxation Method. The analytical solution of convective energy and mass transport of a nanoliquids confined by stretched and immobile borders in a perpendicular channel was proposed by Haritha et al. [67]. The influence of wall

characteristics on the diffusion of a solute in the peristaltic movement of a Newtonian liquid was studied by Sankad and Dhange [146]. The fluid conditions of boundary layer Casson fluid stream across a nonlinearly extending slab including viscous dissipation are invented by Gangadhar et al. [62]. MHD convective flows of Casson fluid across a nonlinear elastic sheet with temperature-dependent viscosity and thermal conductivity were examined by Abderrahim [10] using a novel mathematical technique. Krishna et al. [93] studied the MHD flow of Casson nanofluid across an infinite exponential porous surface in a rotating frame with slip velocity.

After performing similarity transformations, we have determined the analytical solutions for the momentum and energy equations. Additionally, an attempt was made to numerically solve nonlinear-coupled equations in order to obtain the solutions and behaviours of each of the parameters.

3.2 Mathematical Formulation

A stretching sheet is used to simulate the two-dimensional flow of an incompressible, steady non-Newtonian fluid. The flow region refers to $y > 0$ and corresponds at $y = 0$. The accompanying dimensional form of equations represent the flow and heat transport with radiation impacts.

$$\frac{\partial u}{\partial x} + \frac{\partial v}{\partial y} = 0, \quad (3.2.1)$$

$$u \frac{\partial u}{\partial x} + v \frac{\partial u}{\partial y} = v \left(1 + \frac{1}{\beta} \right) \frac{\partial^2 u}{\partial y^2} - \frac{\sigma B_0^2 u}{\rho}, \quad (3.2.2)$$

$$u \frac{\partial T}{\partial x} + v \frac{\partial T}{\partial y} = \frac{K}{c_p} \frac{\partial^2 T}{\partial y^2}. \quad (3.2.3)$$

The following are the associated boundary conditions for this issue:

$$u = a_0 x, \quad v = 0, \quad T = T_w = T_\infty + A \left(\frac{x}{l} \right)^{\lambda_1}, \quad \text{when } y = 0, \left. \begin{array}{l} u \rightarrow 0, \quad T \rightarrow T_\infty \quad \text{as } y \rightarrow \infty. \end{array} \right\} \quad (3.2.4)$$

Where A is a constant, a_0 is the stretching rate, l is the sheet's characteristic length, T_w is the wall temperature, and T_∞ is the fluid's temperature at an infinite distance from the membrane.

Assume that the magnetic inclusion is negligibly small, and that the charge gained along the course is expanded upon ejection. We use the following similarity transformation to solve Equations (3.2.1) through (3.2.3).

$$u = a_0 x f'(\eta), \quad v = -\sqrt{a_0 \nu} f(\eta), \quad \eta = \sqrt{\frac{a_0}{\nu}} y, \quad \theta = \frac{T - T_\infty}{T_w - T_\infty}, \quad (3.2.5)$$

As per the relation (2.2.7) for the Casson fluid model, relations (3.2.1) through (3.2.3), as well as the boundary conditions (3.2.4), are written as follows.

$$\left(1 + \frac{1}{\beta}\right) f'''(\eta) = [f'(\eta)]^2 + q f'(\eta) - f(\eta) f''(\eta), \quad (3.2.6)$$

$$(1 + \epsilon \theta) \theta'' + P_r f(\eta) \theta' - \lambda_1 P_r \theta f'(\eta) + \epsilon (\theta')^2 = 0, \quad (3.2.7)$$

$$\left. \begin{aligned} f(\eta) = 0, \quad f'(\eta) = 1, \quad \theta(\eta) = 1 \quad \text{at} \quad \eta = 0 \\ f'(\eta) \rightarrow 0, \quad \theta(\eta) \rightarrow \infty \quad \text{as} \quad \eta \rightarrow \infty \end{aligned} \right\} \quad (3.2.8)$$

Where, β is the Casson fluid parameter, $q = \frac{\sigma B_0^2}{\rho a_0}$ is Chandrasekhar number,

$$P_r = \frac{\mu C_p}{k_\infty}, \quad k = k_\infty (1 + \epsilon \theta) \quad \text{and} \quad \epsilon = \frac{k_w - k_\infty}{k_w} \quad \text{and} \quad \lambda_1 \quad \text{is the temperature constant.}$$

We get a closed-form solution for the equation of momentum by solving equations (3.2.6) and (3.2.7) using conditions (3.2.8).

$$f(\eta) = \frac{1 - e^{-\alpha \eta}}{\alpha},$$

$$\text{where } \alpha = \frac{\sqrt{\beta(1+q)}}{\sqrt{\beta+1}}. \quad (3.2.9)$$

The local skin friction coefficient is $f''(0) = -\alpha$, and it is calculated for various penetration parameter values.

Equations (3.2.7) and (3.2.8) have been solved using the usual Perturbation approach. Let's pretend that the exact solution of equation (3.2.7) is in the form

$$\theta(\eta) = \theta_0(\eta) + \epsilon \theta_1(\eta) + \epsilon^2 \theta_2(\eta) + \epsilon^3 \theta_3(\eta) + \dots, \quad (3.2.10)$$

where $\theta_0(\eta)$, $\theta_1(\eta)$, $\theta_2(\eta)$, $\theta_3(\eta)$, ... are obtained as first, second, third, and so on order boundary value problems. The above sequence of BVP will be generated by using equations (10) in equations (7) and (8) and then equating like powers of ϵ on both sides.

3.2.1 Zeroth order solution

The zeroth-order differential equation is

$$\varepsilon \theta_o'' + \left\{ 1 - \frac{P_r}{\alpha^2} - \varepsilon \right\} \theta_o' + 2\theta_o = 0, \quad (3.2.11)$$

The boundary conditions are

$$\left. \begin{aligned} \theta_o(\varepsilon) &= 1 \text{ as } \varepsilon_o = -\frac{P_r}{\alpha^2} \\ \theta_o(\varepsilon) &\rightarrow 0 \text{ as } \eta \rightarrow \infty. \end{aligned} \right\} \quad (3.2.12)$$

Equation (3.2.11) is transformed into a feeder hypergeometric relation by appropriate substitution, and the result is given in the form of Kummer's function.

$$\theta_o(\eta) = b_o(\varepsilon)^{\frac{P_r}{\alpha^2}} M \left\{ \frac{P_r}{\alpha^2} - 2, \frac{P_r}{\alpha^2} + 1, \varepsilon \right\}, \quad (3.2.13)$$

where M is Kummer's function, with the usual notation in the standard form,

$$\varepsilon = -\left(\frac{P_r}{\alpha^2}\right) e^{-\alpha\eta}, \quad \text{and} \quad b_o = \frac{1}{(\varepsilon)^{\frac{P_r}{\alpha^2}} M \left[\frac{P_r}{\alpha^2} - 2, \frac{P_r}{\alpha^2} + 1, \frac{-P_r}{\alpha^2} \right]}$$

3.2.2 First-order solution

The first-order differential equation is

$$\varepsilon \theta_1'' + \left\{ 1 - \frac{P_r}{\alpha^2} - \varepsilon \right\} \theta_1' + 2\theta_1 = -\{\varepsilon \theta_o \theta_o'' + \theta_o \theta_o' + \varepsilon (\theta_o')^2\}, \quad (3.2.14)$$

The boundary conditions are

$$\left. \begin{aligned} \theta_1(\varepsilon) &= 0 \text{ as } \varepsilon_1 = -\frac{P_r}{\alpha^2} \\ \theta_1(\varepsilon) &\rightarrow 0 \text{ as } \varepsilon_1 \rightarrow \infty \end{aligned} \right\} \quad (3.2.15)$$

The solution of equation (3.2.14) with aid of equation (3.2.15) is

$$\theta_1 = \theta_{11} + \theta_{12}, \quad (3.2.16)$$

where

$$\theta_{11} = c_o(\varepsilon)^{\frac{P_r}{\alpha^2}} M \left\{ \frac{P_r}{\alpha^2} - 2, \frac{P_r}{\alpha^2} + 1, \varepsilon \right\}, \quad c_o = \frac{-\sum d_r(\varepsilon)^{r+2}}{(\varepsilon)^{\frac{P_r}{\alpha^2}} M \left[\frac{P_r}{\alpha^2} - 2, \frac{P_r}{\alpha^2} + 1, \frac{-P_r}{\alpha^2} \right]}, \quad (3.2.17)$$

$$\theta_{12} = \sum d_r \varepsilon^{r+2}. \quad (3.2.18)$$

After ignoring phrases containing second and higher powers in, ε is a relatively small amount. The energy equation's answer is in the form

$$\theta(\eta) = \theta_o(\eta) + \varepsilon \theta_1(\eta). \quad (3.2.19)$$

The numerical solutions for the present study have also been completed by using MATHEMATICA software. The analytical and numerical solutions are presented in Table 1.

3.3 Results and Discussion

A collection of numerical results for several parameters such as Casson fluid parameter (β), Chandrasekhar number (q), Prandtl number (P_r), temperature constant (λ_1) and temperature variable coefficient (ε) on the flow, variables are presented in Figures 3.3.1–3.3.6.

The decrease in the velocity profile for numerous rising values of the Casson fluid parameter and the Chandrasekhar number is depicted in Figures 3.3.1 and 3.3.2. Because the Laurent force has an effect on fluid velocity, when the Casson fluid parameter and Chandrasekhar number increase, the fluid velocity drops.

Figures 3.3.3–3.3.6 demonstrate the temperature profile for different values of Chandrasekhar number, Prandtl number, temperature constant, and temperature variable coefficient. The relationship between temperature and Chandrasekhar number is shown in Figure 3.3.3 If the emergent values of q are in the range (0.5,1), the temperature will be reduced less. There is a rise in temperature when q grows from 1 to 2. The reason for this is because when $q < 1$ is little, the magnetic intensity is low, and when $q > 1$ is large, the magnetic intensity is great.

Because of the heat exchange between the sheet and the fluid, Figure 3.3.4 indicates a loss in temperature growth for larger values of the temperature constant. The temperature drops as the Prandtl number rises, resulting in an increase in the speed of the fluid model's boundary layer thickness and heat loss (Figure 3.3.5). The temperature profile for changing the values of the thermal conductivity variable coefficient constant is depicted in Figure 3.3.6. Because the constant coefficient of the

thermal variable increases the magnitude of the temperature, the temperature profile is improved, resulting in an increase in heat flow.

Furthermore, we attempted to extract (see Table 3.3.1) the impact of the Casson liquid parameter on the local skin friction coefficient ($-f''(0)$) and heat gradient ($-\theta'(0)$). According to the table, as the Casson liquid parameter and Chandrasekhar number (Modified Magnetic parameter) grow, the skin friction coefficient on the wall increases and the temperature differential at the wall decreases. This is due to an induced magnetic field, which reduces the heat flux at the stream wall and retards force on it. In addition, under the sway of the magnetic domain, the Casson liquid parameter is more reactive.

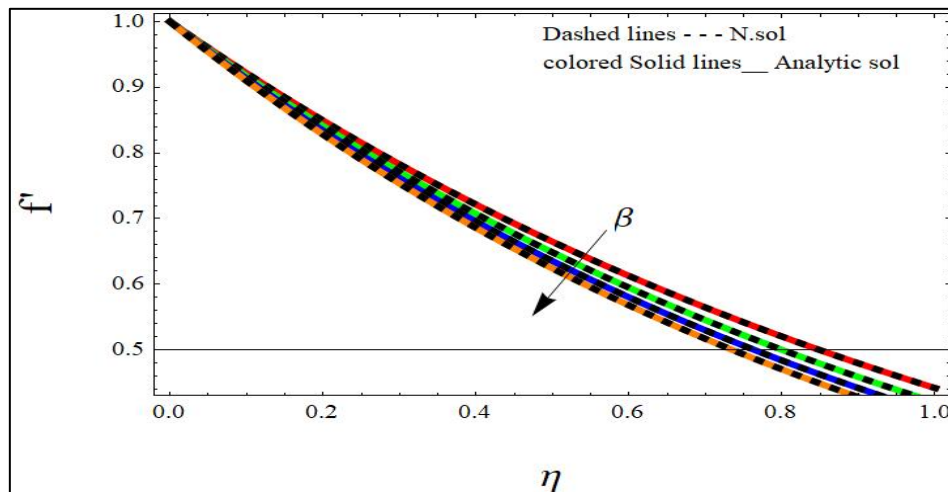


Figure 3.3.1 Velocity profile for distinct values of Casson fluid parameter $\beta=0.5, 0.6, 0.7, 0.8$ with $q=1$.

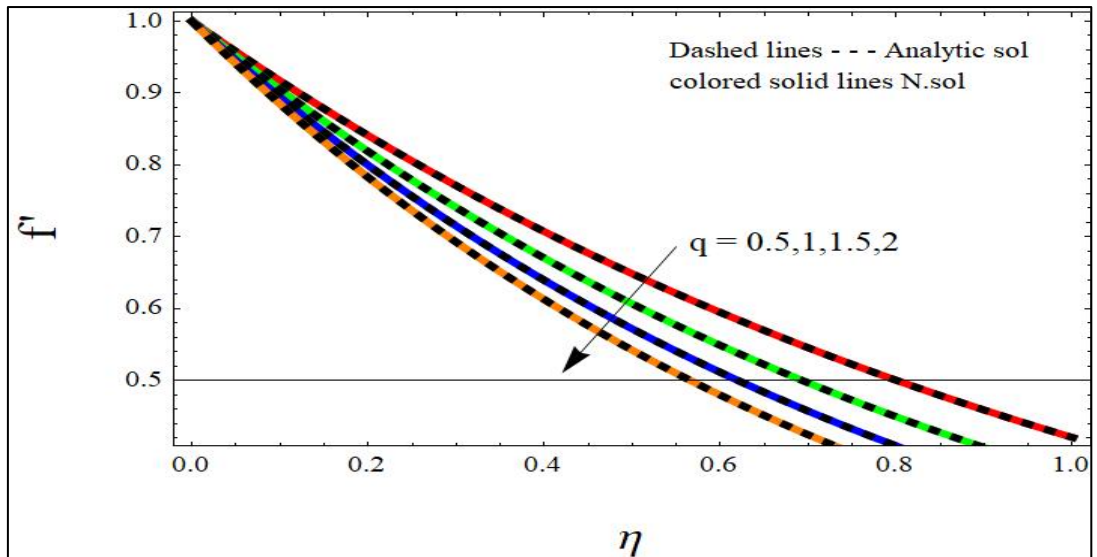


Figure 3.3.2 Velocity profile for distinct values of Chandrasekhar number $q = 0.5, 1, 1.5, 2$ with $\beta = 1$.

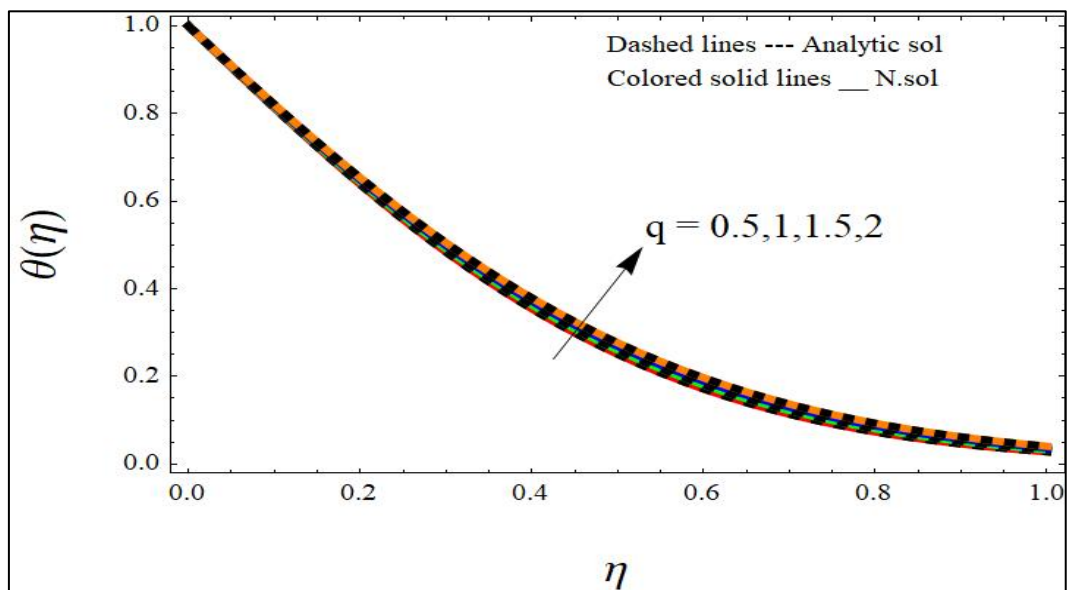


Figure 3.3.3 Energy profile for unlike values of Chandrasekhar number q with $\beta = 1, P_r = 6.2, \epsilon = 0.1,$ and $\lambda_1 = 2$.

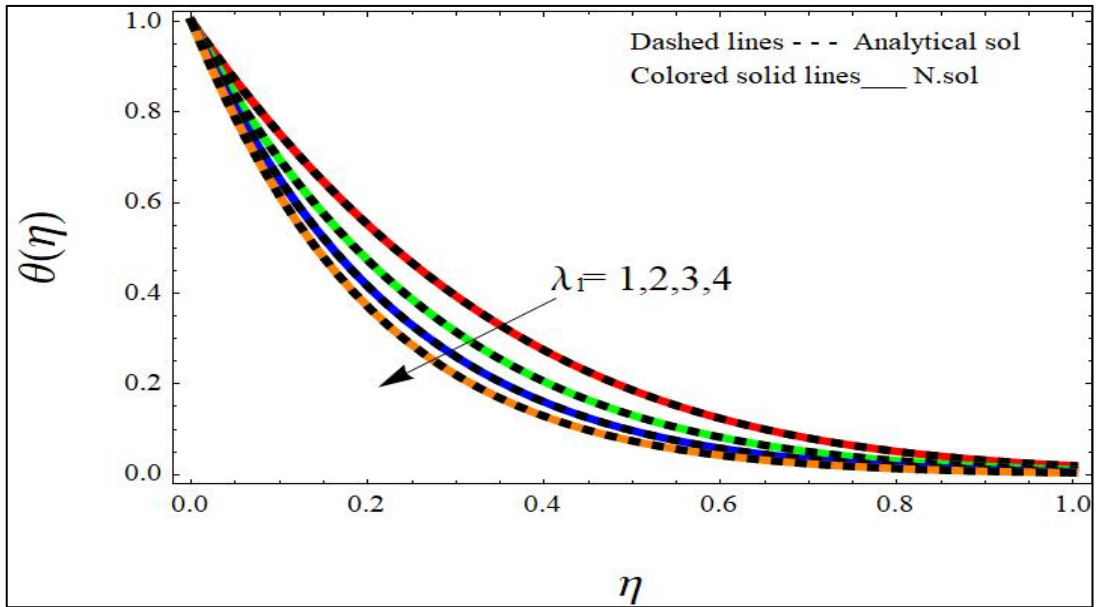


Figure 3.3.4 Energy profile for different values temperature constant $\lambda_1 = 1, 2, 3, 4$ with $P_r = 6.2, q = 0.5, \beta = 1$.

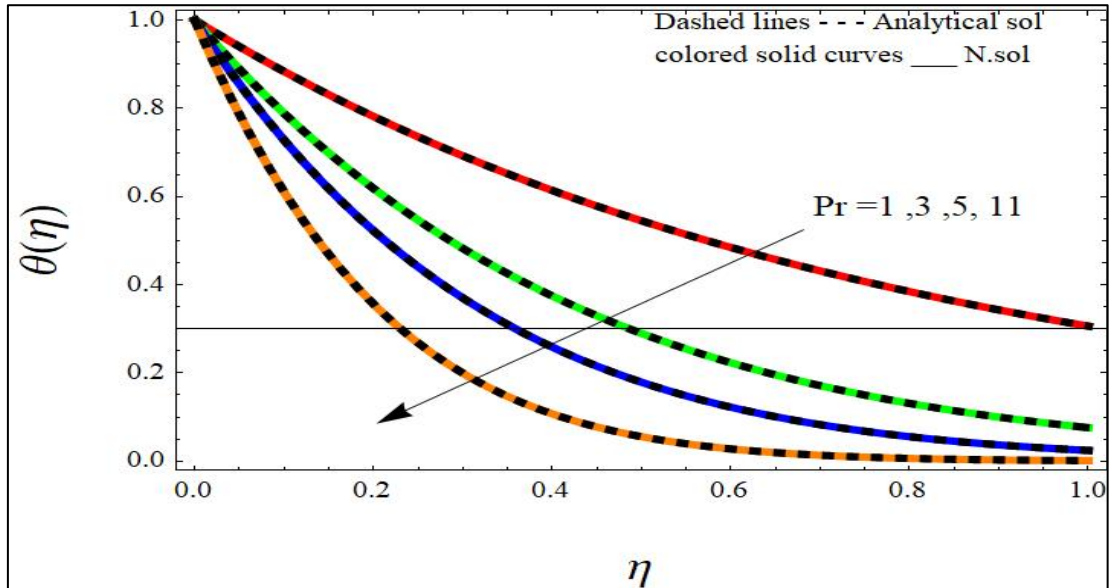


Figure 3.3. 5 Energy profile for different values of Prandtl number $P_r = 1, 3, 5, 11$ with $q = 1, \beta = 1$ and $\lambda_1 = 2$.

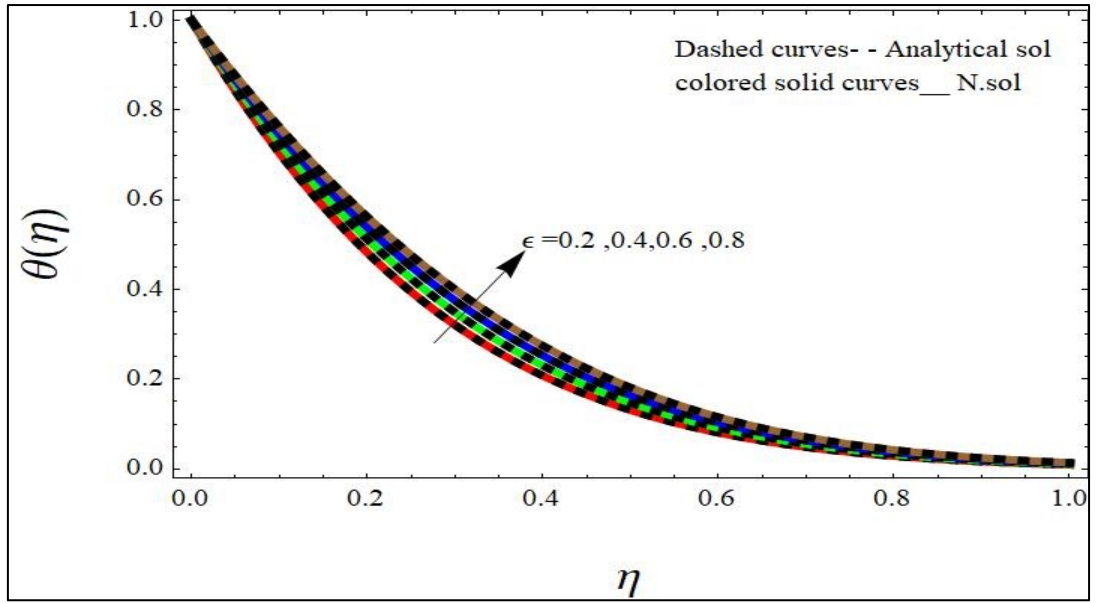


Figure 3.3.6 Temperature profile for different values thermal variable coefficient $\epsilon = 0.2, 0.4, 0.6, 0.8$ with $P_r = 6.2, q = 0.5, \beta = 1$ and $\lambda_1 = 2$.

Table 3.3.1 Nature of local skin coefficient (α) and the temperature gradient ($-\theta'(0)$) for distinct values of Casson parameter (β) and Chandrasekhar number (q) with ($P_r = 1, \epsilon = 0.1, \lambda_1 = 2$)

q	β	$\alpha = -f''(0)$	$\alpha = -f''(0)$	$-\theta'(0)$	$-\theta'(0)$
		Analytical sol	N.sol	Analytical sol	N.sol
1	0.1	0.42640143	0.42640214	1.39450881	1.39450842
	0.2	0.57735025	0.57735027	1.35348185	1.35648105
	0.3	0.67936622	0.67936619	1.33023889	1.33023872
	0.4	0.75592894	0.75592892	1.31027914	1.31027911
	0.5	0.81649658	0.81649656	1.29432803	1.29432845
	0.6	0.86602540	0.86602540	1.28118347	1.28118363
	0.7	0.90748521	0.90748521	1.27011492	1.27011481
	0.8	0.94280904	0.94280904	1.26064049	1.26064056
	0.9	0.97332852	0.97332853	1.25242430	1.25242444
	1.0	1.00000000	1.00000000	1.24522263	1.24522290

q	β	Analy. sol $-f''(0)$	Numerical sol $-f''(0)$	Analy. sol $-\theta'(0)$	Numerical sol $-\theta'(0)$
2	0.1	0.52223296	0.52223298	1.39450881	1.39450842
	0.2	0.70710678	0.70710677	1.35348185	1.35648105
	0.3	0.83205029	0.83205029	1.33023889	1.33023872
	0.4	0.92582009	0.92582009	1.31027914	1.31027911
	0.5	1.00000000	1.00000001	1.29432803	1.29432845
	0.6	1.06066017	1.06066017	1.28118347	1.28118363
	0.7	1.11143786	1.11143786	1.27011492	1.27011481
	0.8	1.15470053	1.15470053	1.26064049	1.26064056
	0.9	1.19207912	1.19207911	1.25242430	1.25242444
	1.0	1.22474487	1.22474487	1.24522263	1.24522290

3.4 CONCLUSION

Analytical and computational approaches are used to explore the stream of Casson liquid across an impermeable linear extending surface involving magnetic impact. Following are the most important conclusions:

- As the Casson fluid parameter and Chandrasekhar number increase, the boundary layer thickness falls due to the applied magnetic force.
- As the Casson fluid parameter rises, the local skin friction coefficient and temperature gradient rise with it.
- With increasing Prandtl number values, the thickness of the boundary layer decreases.

CHAPTER 4

Impact of Variable Wall Temperature and Radiation on Casson Liquid Flow across a Pervious Extending Sheet.

(Part of the chapter is published in springer 2019)

4.1 INTRODUCTION

The sway of a magnetic field on a Casson liquid stream near a stretched surface was discussed in the preceding chapter. The effect of varying wall temperature and radiation on Casson fluid flow across extending sheets via porous medium is examined in this chapter. Because of their widespread use in the manufacturing industries, research on boundary layer flow of diverse non-Newtonian fluids is regarded as one of the most significant in physical science and engineering concerns. According to the literature review, several researchers used analytical or numerical approaches to study boundary layer stream with non-Newtonian liquids in diverse conditions. We have attempted to investigate the stream and energy transmission analysis of a non-Newtonian Casson liquid in a thermal boundary layer above a pervious linear extending slab with variable wall temperature and radiation in this chapter. By converting partial differential equations into ordinary differential equations with similarity transformation, the governing equations are then solved using the regular perturbation method. The exact outcomes are validated with approximate outcomes and are presented through graphs. For the numerical solutions we have used Mathematica software built in functions NDSolve and are plotted using the same package.

4.2 Mathematical Formulation and the Solution

Consider a non-Newtonian Casson fluid moving down the x -axis through a porous linear stretching surface with liquid flow restricted above $y > 0$. Impact of the mass suction velocity, the Casson liquid parameter, the Prandtl number, and thermal radiation are used to analyze flow and heat conduction.

$$u_x + v_y = 0 \quad , \quad (4.2.1)$$

$$uu_x + vu_y = v \left(1 + \frac{1}{\beta}\right) u_{yy} - \frac{v}{k'} u \quad , \quad (4.2.2)$$

$$uT_x + vT_y = \frac{k}{\rho c_p} T_{yy} - \frac{1}{\rho c_p} (q_r)_y \quad , \quad (4.2.3)$$

Where ρ the density of the fluid, T is the temperature of the liquid, q_r is the radiative heat flux and, c_p is the specific heat at constant pressure. u and v are the components of velocity in the x and y directions, respectively. The bounding criteria are as follows:

$$\left. \begin{array}{l} u = a_0 x, \quad v = v_c \quad , \text{when} \quad y = 0 \\ u \rightarrow 0 \quad \quad \quad \text{as} \quad y \rightarrow \infty \end{array} \right\} \quad , \quad (4.2.4)$$

where v_c denotes the mass suction velocity and $a_0 > 0$ denotes the stretching rate.

Using the transformations for similarity,

$$u = bxf'(\eta), v = -\sqrt{bv}f(\eta) \quad \text{and} \quad \eta = \sqrt{\frac{b}{v}}y, \quad (4.2.5)$$

In the Equations (4.2.1) and (4.2.2), we obtain

$$\left(1 + \frac{1}{\beta}\right) f'''(\eta) - [f'(\eta)]^2 + f(\eta)f''(\eta) - P_r k_1 f''[\eta] = 0, \quad (4.2.6)$$

$$\text{Where; } v = \frac{\mu}{\rho} \quad ; \quad P_r = \frac{\chi}{k'b} \quad ; \quad k_1 = \frac{v}{\chi} \quad ,$$

Similarly, the associated boundary conditions are obtained as

$$\left. \begin{array}{l} f(\eta) = -\frac{v_c}{\sqrt{bv}}, \quad f'(\eta) = 1 \quad \text{at} \quad \eta = 0 \\ f'(\eta) \rightarrow 0, \quad \text{as} \quad \eta \rightarrow \infty \end{array} \right\} \quad , \quad (4.2.7)$$

Assuming $f(0) = s$, $s > 0$ corresponds to mass suction, whereas $s = 0$ corresponds to impermeable surface. We obtain when we solve Eqs. (4.2.6) and (4.2.7),

$$f(\eta) = s + \frac{1-e^{-\alpha\eta}}{\alpha}, \quad \text{where } = \frac{s \pm \sqrt{s^2 + 4\left(\frac{\beta+1}{\beta}\right)(P_r k_1 + 1)}}{2\left(\frac{\beta+1}{\beta}\right)}, \quad (4.2.8)$$

Theoretically, thermal conductivity varies linearly with temperature, and it is given by

$$k = k_{\infty}\{1 + \epsilon \theta(\eta)\}, \quad (4.2.9)$$

We have taken $\epsilon = 0.1$, to find the solution in this study since is believed to be a modest parameter. The radiative heat flux is created as follows, as stated in the Rosseland approximation,

$$q_r = -\frac{4\sigma^*}{3k^*} \frac{\partial(T^4)}{\partial y}, \quad (4.2.10)$$

The mean absorption coefficient is k^* , whereas the Stefan-Boltzmann constant is σ^* , We use Taylor's series in the increasing powers of the difference of the temperature distribution in the flow to expand T^4 about T_{∞} and is given by

$$T^4 = T_{\infty}^4 + 4T_{\infty}^3(T - T_{\infty}) + 6T_{\infty}^2(T - T_{\infty})^2 + \dots, \quad (4.2.11)$$

Higher order terms above the first degree were disregarded in the expansion, and the result was approximated as

$$T^4 \cong -3T_{\infty}^4 + 4T_{\infty}^3 T, \quad (4.2.12)$$

Using equations (4.2.10) and (4.2.12), we get

$$\frac{\partial q_r}{\partial y} = \frac{-16\sigma^* T_{\infty}^3}{3k^*} \frac{\partial^2 T}{\partial y^2}, \quad (4.2.13)$$

Therefore, energy equation (4.2.3) can be rewritten as

$$uT_x + vT_y = \frac{1}{\rho c_p} \frac{\partial}{\partial y} \left\{ \left(k + \frac{16\sigma^* T_{\infty}^3}{3k^*} \right) T_y \right\}, \quad (4.2.14)$$

The type of heating procedure determines the thermal boundary conditions to be applied. We address the scenario of a prescribed power law surface temperature in our study, which is given by

$$\begin{aligned} T = T_w = T_{\infty} + A \left(\frac{x}{l} \right)^{\lambda_1}, & \text{ at } y = 0 \\ T \rightarrow \infty, & \text{ as } y \rightarrow \infty \end{aligned} \quad (4.2.15)$$

Where, T_w is the wall temperature, l is the sheet's characteristic length, A is a constant, and T_{∞} is the fluid's temperature at an infinite distance from the membrane. For our convenience the temperature constant λ_1 is set at 2 in this case.

Set up non dimensional temperature $\theta(\eta)$ as

$$\theta(\eta) = \frac{T-T_\infty}{T_w-T_\infty} , \quad (4.2.16)$$

Utilizing the equations, (4.2.14) and (4.2.16), we get

$$(1+\epsilon \theta + T_r)\theta''(\eta) + P_r f(\eta)\theta'(\eta) - 2P_r\theta(\eta)f'(\eta) + \epsilon (\theta'(\eta))^2 = 0, \quad (4.2.17)$$

$$\text{Where } P_r = \frac{\mu C_p}{k_\infty} , T_r = \frac{16\sigma^* T_\infty^4}{3k_\infty k^*} ,$$

and the associated boundary condition takes the form

$$\left. \begin{aligned} \theta(\eta) &= 1, & \text{at } \eta &= 0 \\ \theta(\eta) &\rightarrow 0, & \text{as } \eta &\rightarrow \infty \end{aligned} \right\} , \quad (4.2.18)$$

4.3 Solution of the Energy Equation

We use the regular Perturbation approach to solve the above nonlinear thermal boundary layer equation. The exact solution to equation (4.2.17) is assumed as

$$\theta(\eta) = \theta_0(\eta) + \epsilon \theta_1(\eta) + \epsilon^2 \theta_2(\eta) + \epsilon^3 \theta_3(\eta) + \dots , \quad (4.3.1)$$

Where $\theta_0(\eta), \theta_1(\eta), \theta_2(\eta), \theta_3(\eta), \dots$ are the zeroth order, first order, second order, third order...solution and these are to be determined. For that the sequence of BVP will be generated by using equation (4.3.1) in equation (4.2.17) and (4.2.18) and equating like powers of ϵ on both the sides.

4.3.1. Solution at the zero-th order BVP:

$$(1 + T_r)\epsilon\theta_0'' + \left\{1 + T_r - \frac{P_r v_c}{\alpha} - \frac{P_r}{\alpha^2} - \epsilon\right\}\theta_0' + 2\theta_0 = 0 , \quad (4.3.2)$$

The boundary conditions are:

$$\left. \begin{aligned} \theta_0(\epsilon) &= 1, & \text{at } \epsilon_0 &= -\frac{P_r}{\alpha^2} \\ \theta_0(\epsilon) &\rightarrow 0, & \text{as } \epsilon_0 &\rightarrow \infty \end{aligned} \right\} , \quad (4.3.3)$$

The above zeroth order differential equation can be turned into a confluent hypergeometric equation by making appropriate substitutions, and the answer can be written in terms of Kummer's function as follows,

$$\theta_0(\eta) = C_0 e^{-\alpha\left(\frac{B}{A}\right)\eta} M\left[B + (n-3)A, B + nA, \left(\frac{\epsilon}{A}\right)\right] - a_1 \left(\frac{P_r}{\alpha^2}\right) e^{-\alpha\eta} + a_2 \left(\frac{P_r}{\alpha^2}\right)^2 \quad (4.3.4)$$

Where, M is Kummer's function with its usual notation, $\varepsilon = -\left(\frac{Pr}{\alpha^2}\right) e^{-\alpha\eta}$,

$$A = (1 + T_r), \quad B = \frac{Prv_c}{\alpha} + \frac{Pr}{\alpha^2},$$

$$C_o = \frac{1 + a_1\left(\frac{Pr}{\alpha^2}\right) - a_2\left(\frac{Pr}{\alpha^2}\right)^2}{M\left[B + (n-3)A, B + nA, \left(\frac{-Pr}{\alpha^2 A}\right)\right]},$$

$$a_1 = \frac{(B-2A)}{A(A+B)},$$

$$a_2 = \frac{(B-2A)(B-A)}{A^2(A+B)(2A+B)(2!)}.$$

4.3.2. Solution at the first order BVP:

$$(1 + T_r)\varepsilon\theta_1'' + \left\{1 + T_r - \frac{Prv_c}{\alpha} - \frac{Pr}{\alpha^2} - \varepsilon\right\}\theta_1' + 2\theta_1 = -\{\varepsilon\theta_o\theta_o'' + \theta_o\theta_o' + \varepsilon(\theta_o')^2\}, \quad (4.3.5)$$

The boundary conditions are:

$$\left. \begin{aligned} \theta_1(\varepsilon) &= 1, & \text{at } \varepsilon_1 &= -\frac{Pr}{\alpha^2} \\ \theta_1(\varepsilon) &\rightarrow 0, & \text{as } \varepsilon_1 &\rightarrow \infty \end{aligned} \right\}, \quad (4.3.6)$$

For the homogeneous part of the equation, the solution of the first order equation will be achieved as in the zeroth order.

$$\theta_{11} = d_o e^{-\alpha(B/A)\eta} M\left[B + (n-3)A, B + nA, \left(\frac{\varepsilon}{A}\right)\right] - a_1\left(\frac{Pr}{\alpha^2}\right) e^{-\alpha\eta} + a_2\left(\frac{Pr}{\alpha^2}\right)^2 e^{-2\alpha\eta}, \quad (4.3.7)$$

$$\text{Where } d_o = \frac{-\sum d_r(\varepsilon)^{2+r}}{M\left[B + (n-3)A, B + nA, \left(\frac{-Pr}{\alpha^2 A}\right)\right]},$$

The particular integral part of the equation can be found by associating numerous powers of ε on both parts and solution will be of the form.

$$\theta_{12} = \sum d_r \varepsilon^{r+2}, \quad (4.3.8)$$

Therefore, the solution of first order is

$$\theta_1 = \theta_{11} + \theta_{12}, \quad (4.3.9)$$

Due to small magnitude values, the findings of the higher solution are ignored, and we search for the ultimate outcome for the energy equation in the form

$$\theta(\eta) = \theta_o(\eta) + \varepsilon \theta_1(\eta), \quad (4.3.10)$$

Tables and Figures:

Table 4.3.1 Results of $-f''(0)$ for discrete values of the parameters.

β	P_r	k_1	s	2	4	6	8	10
0.5	3	1		1.53518	2.0	2.52753	3.09717	3.069425
1				2.0	2.73205	3.56155	4.44949	5.37228
2				2.4305	3.44152	4.58199	5.79361	7.04518
3				2.63746	3.79129	5.08945	6.4641	7.88068
5				2.84027	4.13873	5.5957	7.13392	8.71578
7				2.94034	4.31174	5.84845	7.46863	9.13322
2	1	1		2.0	3.09717	4.3094	5.5726	6.861
	2			2.23014	3.27698	4.44949	5.68513	6.95426
	3			2.4305	3.44152	4.58199	5.79361	7.04518
	4			2.61032	3.59411	4.70801	5.89845	7.13392
	3			2.77485	3.73703	4.82843	6.0	7.22063
		1		1.53518	2	2.52753	3.09717	3.69425
				1.19087	1.48676	1.82137	2.18466	2.56832
				1	1.21525	1.45743	1.72076	2
		2		2.92744	3.87192	4.94392	6.09854	7.30546
		3		3.33333	4.23927	5.26599	6.37851	7.5497
		4		3.68513	4.56512	5.55903	6.63879	7.78055

Table 4.3.2 Results of $-\theta'(0)$ for different values of the parameters, where we have taken $\varepsilon = 0.1, k_1 = 1$

β	P_r	T_r	α	s	$-\theta'(0)$	β	P_r	T_r	α	s	$-\theta'(0)$
2	3	1	2.25733	2.5	4.40418	2	1	1	2.25733	2.5	1.69161
			2.36401	2.7	4.68432		2				3.03087
			2.52753	3	5.0937		3				4.47455
			3.09717	4	6.4581		4				6.09476
0.5			0.816497	0	1.49854		5				7.84656
1			1		1.36302		2	1			1.69161
1.5			1.09545		0.825758			2			3.03087
2			1.1547		1.39406			3			4.47455

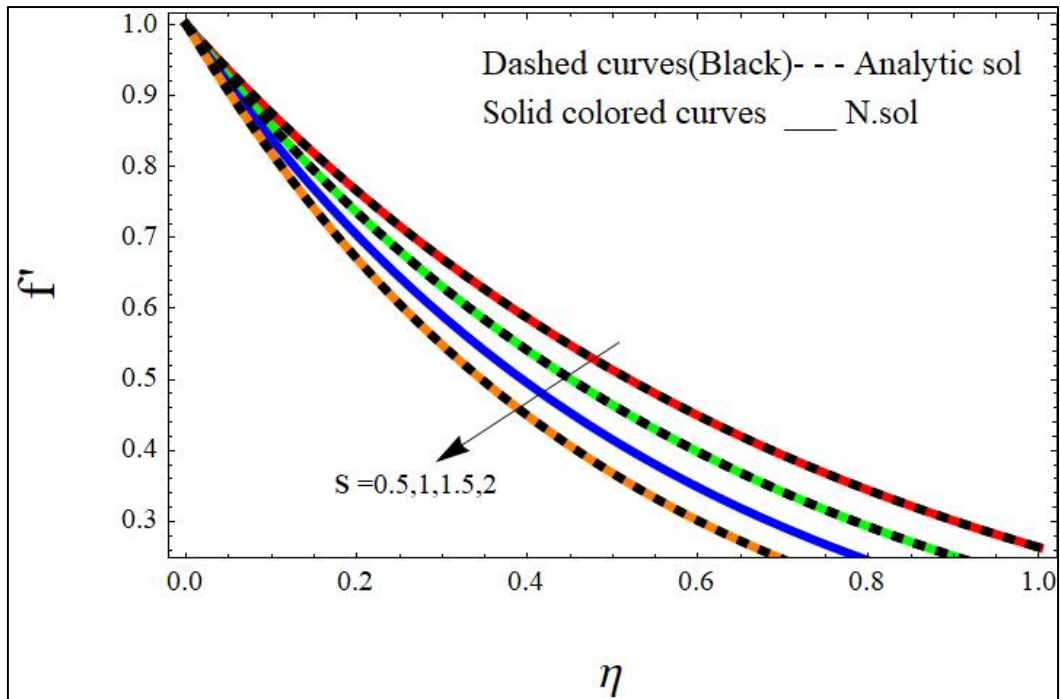


Figure 4.3.1 Velocity profile for distinct values of S , taking $\beta = 2, k_1 = 1, P_r = 1$

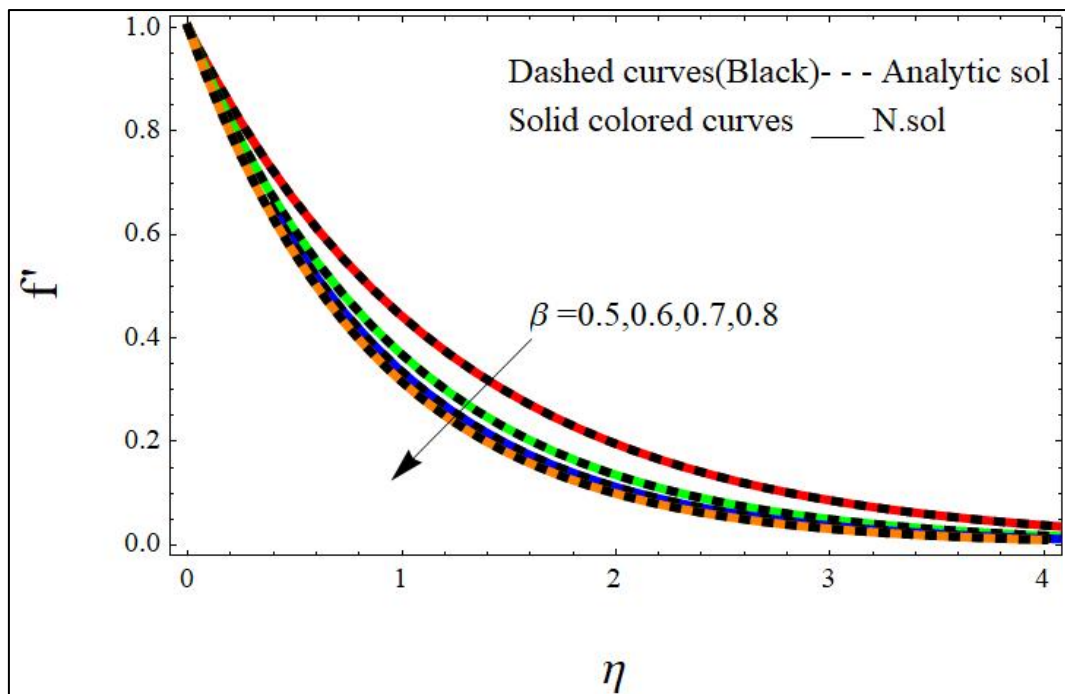


Figure 4.3.2 Velocity profile for the fluid for distinct values of β , taking $v_c = 0, k_1 = 1, P_r = 1$

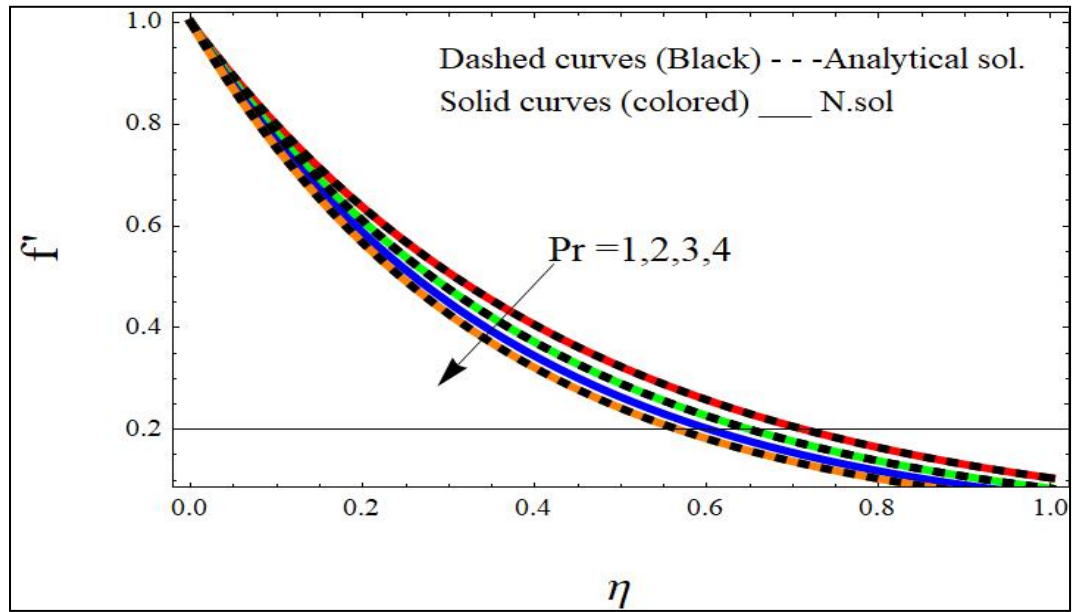


Figure 4.3.3 Velocity profile for the variations of P_r with $\beta = 2$, $k_1 = 1$, $s = 2.5$, $T_r = 1$

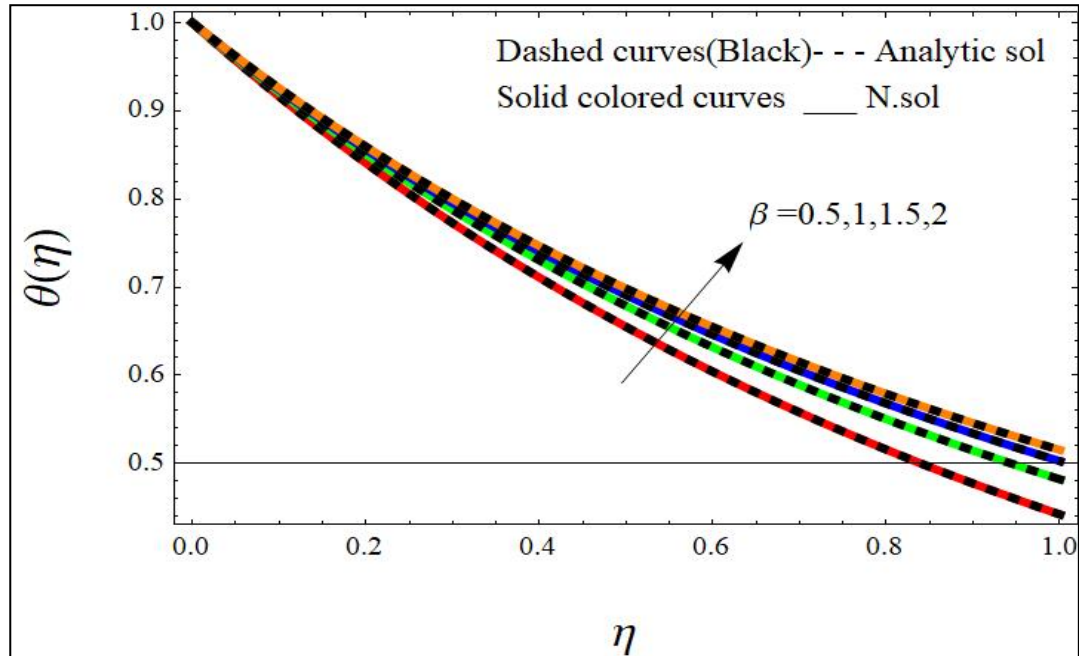


Figure 4.3.4 Energy profile for different values of β with $s = 2.5$, $k_1 = 1$, $P_r = 1$.

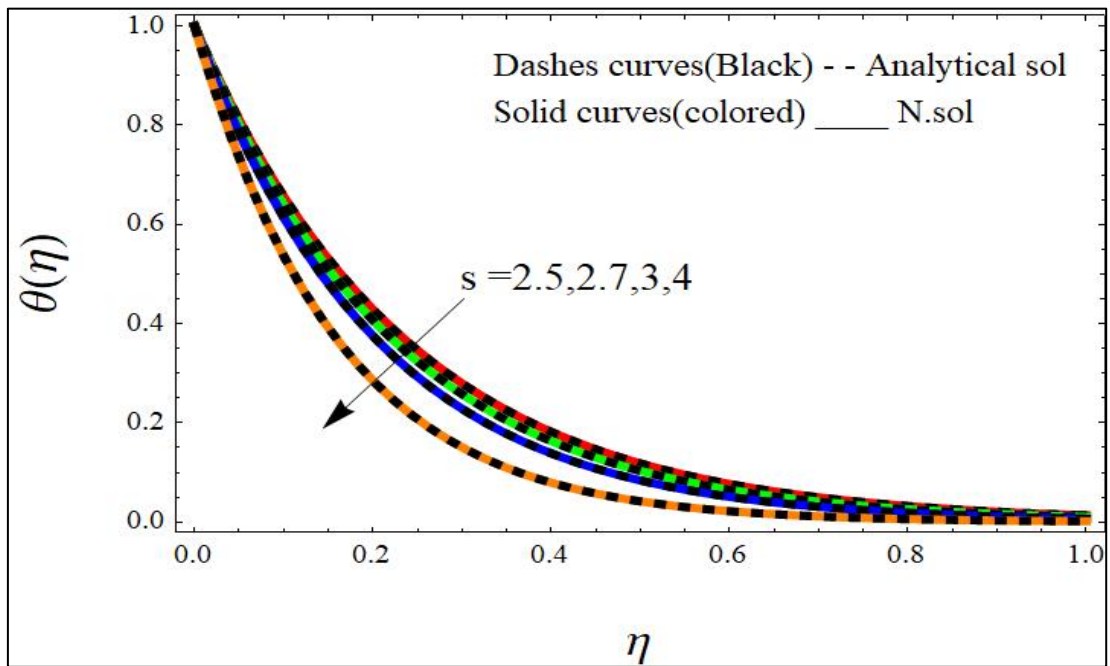


Figure 4.3.5 Energy profile for different values of s with $P_r = 3, T_r = 1, k_1 = 1$

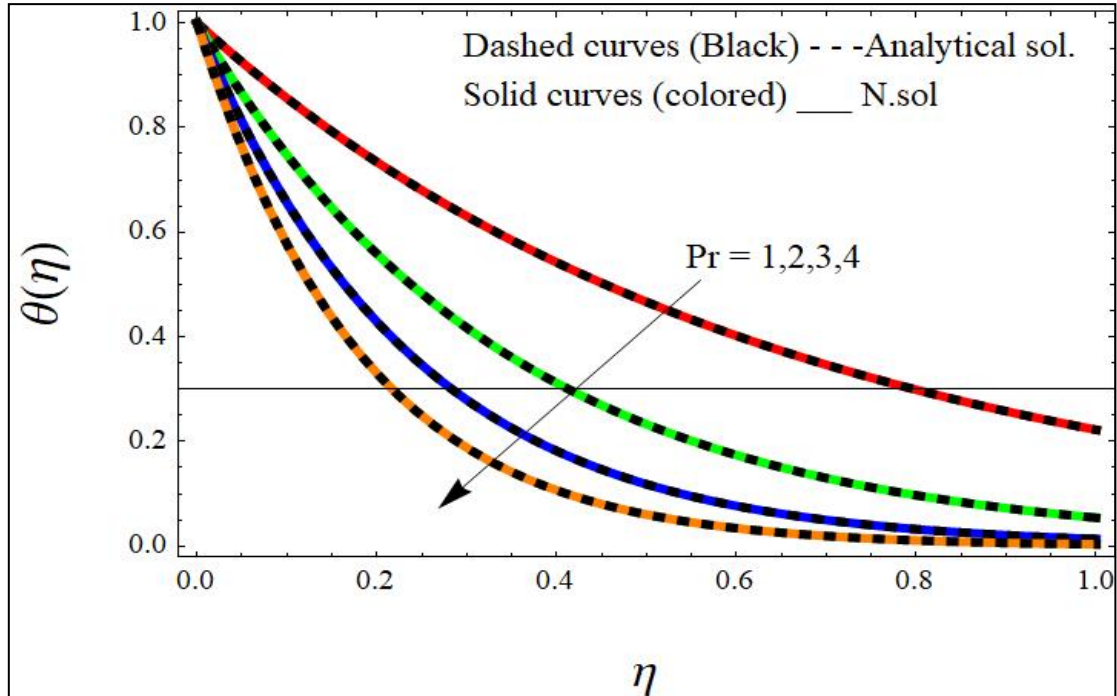


Figure 4.3.6 Energy profile for different values of P_r with $\beta = 2, k_1 = 1, s = 2.5, T_r = 1$

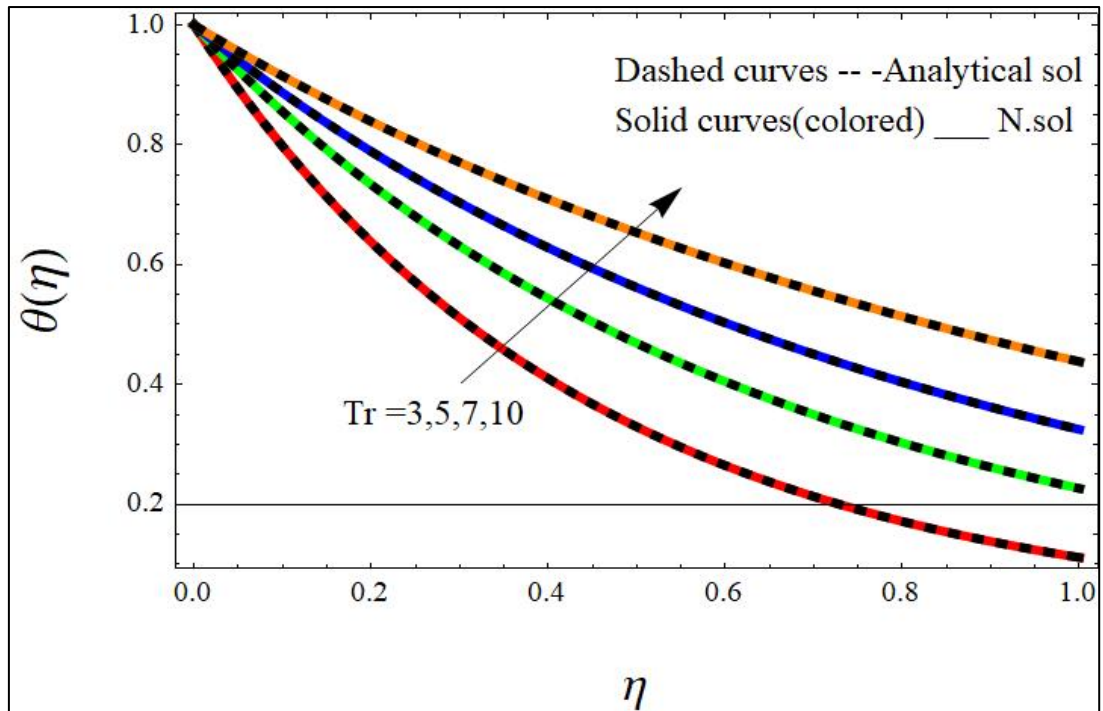


Figure 4.3.7 Energy profile for different values of T_r with $\beta = 2, k_1 = 1, P_r = 3$

4.4 OUTCOMES AND ANALYSIS

The solutions of BVPs encountered in the research of Casson fluid boundary layer stream and energy transmission involving varying wall temperature and thermal radiation through extending surface were analyzed using the regular perturbation method. Graphs are displayed in Figures 4.3.1- 4.3.7 to visualize the influence of distinct constraints on the momentum and energy distribution. The velocity of the boundary layer near the wall falls as the suction parameter s , the Casson fluid parameter, and the Prandtl number P_r for impermeable surfaces increase, as seen in Figures 4.3.1 to 4.3.3. Figures 4.3.4 to 4.3.7 demonstrate the temperature profile with different parameter adjustments. Temperature drops as the mass suction parameter and Prandtl number grow, but temperature rises as the Casson liquid parameter and radiation parameter increase.

In addition, Tables 1 and 2 illustrate the values of the local skin coefficient and temperature gradient for various values of relevant factors. According to the tables, as the Casson liquid parameter, mass suction velocity, and Prandtl number P_r grow, the skin friction coefficient and temperature gradient increase. In the absence of the Prandtl number, the results are consistent with Bhattacharya [80].

4.5 CONCLUSION

In this paper, the flow and heat exchange of Casson liquid over a stretching surface are investigated, as well as wall mass transmission and thermal radiation effects. The boundary layer thickness falls as the Casson fluid parameter, Prandtl number, and radiation increase, and radiation can be minimized by keeping the system at a constant temperature. In order to improve the cooling effect, small values of thermal conductivity coefficient (ϵ) must be chosen.

CHAPTER 5

Casson Liquid Flow Comprising Nanofluids and Gyrotactic Bacteria with Varying wall Temperature and Thermo-Radiation

(The part of the article is published in Elsevier)

5.1 INTRODUCTION

The consequences of variable wall temperature and radiation on the bioconvection of Casson nanofluid flow including gyrotactic microorganisms under the sway of a magnetic properties are conferred in this chapter. The studies of boundary layer flow and heat flow are relevant to the knowledge of the assembly cycle in order to enhance the nature of items. A fascinating and important inquiry is the liquid with specified characteristics across a direct expanding surface and heat exchange marvels; we meet several mechanical assembly units. The exploration of the boundary layer of a non-Newtonian liquid impacted by various considerations, as well as heat transfer analysis, has a wide range of applications in industry, wiredrawing and including the extraction of polymer sheets from color, among others. Cooling metallic plates, glass filaments, producing paper, and so on are all examples of similar uses for the extending sheet. In recent years, a number of experts have carried out substantial study on the boundary layer theory and heat transmission above the linear extending surface. Several scholars have tried to provide exact or approximate outcomes for streams of Newtonian and non-Newtonian liquids near stretching or narrowing surfaces including various consequences and considerations in the boundary layer theory.

A "nanofluid" is a fluid solution with ultrafine particles (diameter 50 nm) (Choi [41]). Traditional heat transfer fluids (mineral oils, water, motor oil, ethylene glycol, and so on) have limited heat transmission capabilities. Nanofluids are colloidal suspensions in base fluids containing nanometer-sized metal and metal oxide particles such as iron, titanium or their oxides, copper, gold, and aluminium. Water, bio-liquids, oil, toluene, and ethylene glycol are all examples of base fluids. Thermal conductivities of base liquids containing nanoparticle suspensions are substantially

greater than those of base fluids, according to tests. Buongiorno [29] developed a revolutionary concept of nanofluid convection energy transmission because of the Brownian motion and thermophoresis. They also argued that turbulence indication has an effect on thermophoresis and Brownian motion, which in turn has an impact on other critical sliding processes.

In the last several years, microorganisms have piqued people's curiosity. Fertilizers, medicine delivery systems, and biofuels are all created with microorganisms (prepared from waste). Microbes have an intense density than water. In general, microbes swim upward, increasing the denseness of the source liquid and causing a variable concentration on the superior surface. Oxytactic, chemo-tactic, gravitaxis, and gyrotactic microorganisms are among the several kinds of microorganisms. There are some substantial differences between microbes and nanoparticles. Self-propelled, the microbes may spin in the liquid in response to provocations for example: chemical attraction, gravity, and light. In contrast, nanoparticles are not automotive; the thermophoresis and Brownian movement influences are responsible for their movement. To increase the rate of mass transmission and microscale combination, as well as the nanofluid's flow stability, the microbes are mixed with a dilute solution of nanoparticles. Bioconvection caused by ultrafine particles and microbes in the fluid stream is an important research topic for improving the nature of bioproducts and biotechnology companies. Through an extending or shrinking slab, Shahid et al. [149] investigated nanofluid stream including gyrotactic microbes and MHD. They looked at how a chemical reaction and thermal radiation affected the flow properties. The impact of motile microorganisms on nanofluid flow, heat, and mass transfer through a vertical stretched sheet was studied by Zadeh et al. [70].

The differential transform method (DTM) is one of the fundamental strategies for dealing with a family of coupled and de-coupled linear or nonlinear boundary value issues and the solutions can be expressed in terms of Taylor's or Maclaurin's series. Zhou [72] proposed this method for studying electrical circuits. DTM is a useful approach for quickly convergent series solutions for a class of nonlinear differential equations that is difficult to solve using known exact techniques. Many

research publications utilizing DTM can be found, few of them are Vedat [161], Hossein et al. [71], Patra et al. [120], Hatami et al. [68] and many more.

The investigation of bioconvection of nanoliquids containing gyrotactic microbes under the sway of magnetic properties, across a linear expanding surface elongated horizontally, and energy transmission examination comprising variable temperature at the wall and thermo-radiation impact are the main intension of this effort. We also looked at exciting aspects of Brownian movement and thermophoresis, as well as the influence of penetrating factors on nanofluid particle flow, heat transfer, and convergence, as well as microbe clustering. The Casson liquid with motile microbes, as well as the thermal radiation parameter and the wall temperature impact, are examined in this chapter. Both Differential Transform and numerical approaches are used to solve the relevant equations. Figures are used to assess the results of the current investigation.

5.2 MATHEMATICAL FORMULATION

Liquid containing gyrotactic microorganisms can flow over the linear extending surface and the liquid is diluted in order for the microbes to survive on the nanoparticles. Under the sway of magnetic field, the surface of the sheet is expanded along the x -axis and the liquid stream is confined uniformly in xy -plane. The induced magnetic field is not taken into account. Consider the effects of the Brownian and Thermophoresis diffusion coefficients (D_B, D_T) on heat conduction. Let T_w, C_w and n_w be the temperature, nanoparticle volume fraction, and microorganism diffusive convergence near the wall, and let $T_\infty, C_\infty, n_\infty$ be the temperature, nanoliquids concentration, and dispersive coefficient of the microbes far away from the surface, respectively.

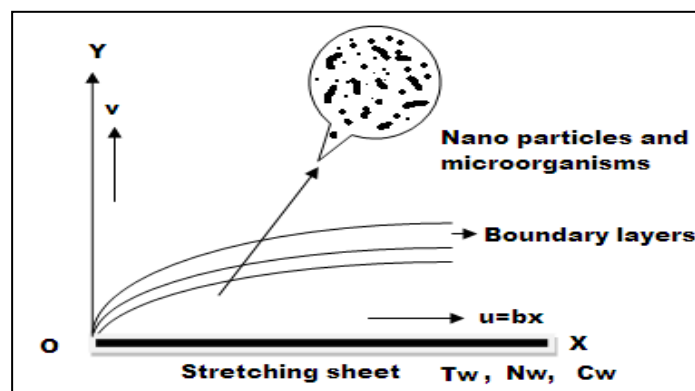


Figure 5. 2. 1 Bioconvection in the boundary layer flow of nanofluids containing microorganisms.

The equations that govern the current problem are as follows:

$$\frac{\partial u}{\partial x} + \frac{\partial v}{\partial y} = 0, \quad (5.2.1)$$

$$u \frac{\partial u}{\partial x} + v \frac{\partial u}{\partial y} = \nu \left(1 + \frac{1}{\beta} \right) \frac{\partial^2 u}{\partial y^2} - \frac{\sigma B_0^2}{\rho} u, \quad (5.2.2)$$

$$u \frac{\partial T}{\partial x} + v \frac{\partial T}{\partial y} = \left(\frac{K}{\rho C_p} \right) \frac{\partial^2 T}{\partial y^2} - \frac{1}{\rho C_p} \frac{\partial q_r}{\partial y} + \tau \left[D_B \frac{\partial C}{\partial y} \frac{\partial T}{\partial y} + \frac{D_T}{T_\infty} \left(\frac{\partial T}{\partial y} \right)^2 \right], \quad (5.2.3)$$

$$u \frac{\partial C}{\partial x} + v \frac{\partial C}{\partial y} = D_B \frac{\partial^2 C}{\partial y^2} + \left(\frac{D_T}{T_\infty} \right) \frac{\partial^2 T}{\partial y^2}, \quad (5.2.4)$$

$$u \frac{\partial N}{\partial x} + v \frac{\partial N}{\partial y} + \frac{bW_c}{c_w - c_\infty} \left(\frac{\partial}{\partial y} (NC_y) \right) = D_m \frac{\partial^2 N}{\partial y^2} \quad (5.2.5)$$

The pertinent boundary conditions for this problem are as follows:

$$\begin{aligned} v = v_c, \quad u = a_0 x, \quad T = T_w = T_\infty + A \left(\frac{x}{l} \right)^{\lambda_1}, \quad C = C_w, \quad N = N_w, \quad \text{as } y \rightarrow 0, \\ u \rightarrow 0, T \rightarrow T_\infty, C \rightarrow C_\infty, N \rightarrow N_\infty \quad \text{as } y \rightarrow \infty, \end{aligned} \quad (5.2.6)$$

The similarity transformations employed in the governing equations are listed below,

$$\begin{aligned} \eta = \sqrt{\frac{c}{g}} y; u = a_0 x f'(\eta); v = -\sqrt{c\vartheta} f(\eta); \theta(\eta) = \frac{T - T_\infty}{T_w - T_\infty}, \phi(\eta) = \frac{C - C_\infty}{C_w - C_\infty}, \\ \chi(\eta) = \frac{N - N_\infty}{N_w - N_\infty}, \quad k = k_\infty (1 + \epsilon \theta) \end{aligned} \quad (5.2.7)$$

The coupled nonlinear ordinary differential equations are

$$\left(1 + \frac{1}{\beta} \right) \frac{\partial^3 f}{\partial \eta^3} - \frac{\partial^2 f}{\partial \eta^2} + f(\eta) \frac{\partial^2 f}{\partial \eta^2} - M \frac{\partial f}{\partial \eta} = 0, \quad (5.2.8)$$

$$(1 + \epsilon \theta + T_r) \frac{\partial^2 \theta}{\partial \eta^2} + (\epsilon + P_r N_t) \left(\frac{\partial \theta}{\partial \eta} \right)^2 + P_r \left\{ f(\eta) \frac{\partial \theta}{\partial \eta} + N_b \left(\frac{\partial \theta}{\partial \eta} \right) \left(\frac{\partial \phi}{\partial \eta} \right) - 2 \frac{\partial f}{\partial \eta} \theta(\eta) \right\} = 0, \quad (5.2.9)$$

$$\frac{\partial^2 \phi}{\partial \eta^2} + \frac{N_t}{N_b} \left(\frac{\partial^2 \theta}{\partial \eta^2} \right) + L_e f(\eta) \frac{\partial \phi}{\partial \eta} = 0, \quad (5.2.10)$$

$$\frac{\partial^2 \chi}{\partial \eta^2} + S_c f(\eta) \frac{\partial \chi}{\partial \eta} - P_e \left\{ \frac{\partial \chi}{\partial \eta} \frac{\partial \phi}{\partial \eta} + \frac{\partial^2 \phi}{\partial \eta^2} (\chi(\eta) + \sigma) \right\} = 0, \quad (5.2.11)$$

The reduced periphery conditions are

$$\begin{aligned} f(0) = v_c, \quad f'(0) = 1, \quad \theta(0) = 1, \quad \phi(0) = 1, \quad \chi(0) = 1, \quad \text{as } \eta \rightarrow 0 \}, \\ f_n(\infty) = 0, \quad \theta(\infty) = 0, \quad \phi(\infty) = 0, \quad \chi(\infty) = 0, \quad \text{as } \eta \rightarrow \infty \}, \end{aligned} \quad (5.2.12)$$

By scaling variables, the system of equations becomes dimensionless:

$$P_r = \frac{v}{m}, M = \frac{\sigma B_0^2}{\rho c}, N_b = \frac{\tau D_B (C_w - C_\infty)}{v}, N_t = \frac{\tau D_B (T_w - T_\infty)}{v T_\infty},$$

$$L_e = \frac{v}{D_B (C_w - C_\infty)}, S_c = \frac{v}{D_n}, P_e = \frac{b W_c}{D_n}, \sigma = \frac{N_\infty}{(N_w - N_\infty)}, \quad (5.2.13)$$

5.3 Series Solution by DTM

The equations with boundary conditions (5.2.8) -(5.2.12) may be translated into the following differential forms, according to Zhou [72]:

$$\left(1 + \frac{1}{\beta}\right) (k+1)(k+2)(k+3)F[k+3] = M(k+1)F[k+1] +$$

$$+ \sum_{m=0}^k (k-m+1)F[k-m+1](m+1)F[m+1] -$$

$$- \sum_{m=0}^k F[k-m](m+1)(m+2)F[m+2]$$

$$\text{Where } F[0] = s, F[1] = 1, F[2] = a_1, \quad (5.3.1)$$

$$(k+1)(k+2)\theta[k+2] = P_r * 2 * \sum_{m=0}^k \theta[k-m](m+1)F[m+1] -$$

$$- P_r \sum_{m=0}^k F[k-m](m+1)\theta[m+1] -$$

$$- N_b P_r \sum_{m=0}^k (k-m+1)\theta[k-m+1](m+1)\phi[m+1] -$$

$$- (\epsilon + P_r N_t) \sum_{m=0}^k (k-m+1)\theta[k-m+1](m+1)\theta[m+1]$$

$$\text{Here, } \theta[0] = 1, \theta[1] = a_2, \quad (5.3.2)$$

$$(k+1)(k+2)\phi[k+2] =$$

$$= L_e \sum_{m=0}^k F[k-m](m+1)\phi[m+1] - \frac{N_t}{N_b} \sum_{m=0}^k (k+1)(k+2)\theta[k+2]$$

$$\text{Where } \phi[0] = 1, \phi[1] = a_3, \quad (5.3.3)$$

$$(k+1)(k+2)\chi[k+2] = P_e \sigma (k+1)(k+2)\phi[k+2] +$$

$$+ P_e \sum_{m=0}^k (k-m+1)\phi[k-m+1](m+1)\chi[m+1] +$$

$$+ P_e \sum_{m=0}^k \chi[k-m](m+1)(m+2)\phi[m+2] -$$

$$- S_c \sum_{m=0}^k F[k-m](m+1)\chi[m+1],$$

$$\text{Where } \chi[0] = 1, \chi[1] = a_4, \quad (5.3.4)$$

The differential transformations of $f(\eta)$, $\theta(\eta)$, $\phi(\eta)$, and $\chi(\eta)$ are denoted as $F[k]$, $\theta[k]$, $\phi[k]$, and $\chi[k]$. Utilizing the above modified equations and the boundary requisites, the supposed constants a_1 , a_2 , a_3 , and a_4 may be derived. Taking $k = 0, 1, 2, 3, \dots$, and $s = 0$, we obtain

$$F[3] = \frac{\beta(1+M)}{6(1+\beta)} ; \quad F[4] = \frac{a_1(1+M)\beta}{24(1+\beta)} ;$$

$$\theta[2] = \frac{P_r}{1+T_r+\epsilon} - \frac{a_2 a_3 N_b P_r}{2(1+T_r+\epsilon)} - \frac{a_2^2 (N_t P_r + \epsilon)}{2(1+T_r+\epsilon)} ;$$

$$\phi[2] = - \frac{N_t \left(\frac{P_r}{1+T_r+\epsilon} - \frac{a_2 a_3 N_b P_r}{2(1+T_r+\epsilon)} - \frac{a_2^2 (N_t P_r + \epsilon)}{2(1+T_r+\epsilon)} \right)}{N_b} ;$$

$$\chi[2] = \frac{a_3 a_4 P_e}{2} - \frac{N_t P_e \left(\frac{P_r}{1+T_r+\epsilon} - \frac{a_2 a_3 N_b P_r}{2(1+T_r+\epsilon)} - \frac{a_2^2 (N_t P_r + \epsilon)}{2(1+T_r+\epsilon)} \right) (1-\sigma)}{N_b} ,$$

similarly, computing $\theta[3]$, $\phi[3]$, $\chi[3]$, $F[5]$... and replacing the above results in the differential Transformed equations and utilizing the Pade approximation with $\lim_{\eta \rightarrow \infty} f'(\eta) = 0$, and by taking $P_r = 6.8, \beta = 0.5, \epsilon = 0.1, T_r = 1, M = 5, N_b = 0.1, N_t = 0.1, L_e = 10, S_c = 1, P_e = 1, \sigma = 0.2$, we can get $a_1 = -1.41421, a_2 = -2.29631, a_3 = -0.761353, a_4 = -1.21743$ and thus the Taylor's series solution for $f(\eta), \theta(\eta), \phi(\eta), \chi(\eta)$ are obtained as follows.

$$f(\eta) = \eta - 0.70710678 \eta^2 + 0.333333 \eta^3 - 0.11785113 \eta^4 + 0.333333 \eta^5 -$$

$$-0.00785674 \eta^6 - 0.0015873 \eta^7 - 0.00028059 \eta^8 + 0.00004409 \eta^9 -$$

$$-0.0000062355 \eta^{10} + 8.01667467 \times 10^{-7} \eta^{11} - \dots \quad (5.3.5)$$

$$\theta(\eta) = 1 - 2.29631088 \eta + 1.975757237 \eta^2 - 2.33636843 \eta^3 + 1.26330833 \eta^4$$

$$- 0.27303305 \eta^5 - 0.781049234 \eta^6 + 1.32714368 \eta^7 - 0.567156644 \eta^8$$

$$- 0.937622474 \eta^9 + 1.956197893 \eta^{10} - 1.4128657111 \eta^{11} + \dots , \quad (5.3.6)$$

$$\phi(\eta) = -0.76135259 \eta - 1.97575723 \eta^2 + 3.60528942 \eta^3 + 1.58098907 \eta^4 -$$

$$- 6.4050803 \eta^5 + 1.631536804 \eta^6 + 6.39940692 \eta^7 - 5.35109107 \eta^8 -$$

$$- 2.79067908 \eta^9 + 5.524592211 \eta^{10} - 0.20836641 \eta^{11} - \dots , \quad (5.3.7)$$

$$\begin{aligned}
\chi(\eta) = & 1 - 1.21743302 \eta - 0.5722382 \eta^2 - 0.5722382 \eta^3 - 0.3408438 \eta^4 - \\
& - 3.92775865 \eta^5 + 3.86466401 \eta^6 + 3.902623735 \eta^7 - \\
& 9.612664149 \eta^8 + 1.13224397 \eta^9 + 14.10829523 \eta^{10} - \\
& - 11.9391550003 \eta^{11} - \dots,
\end{aligned} \tag{5.3.8}$$

5.4 Outcomes and Analysis

This investigation into the current boundary layer stream of the liquid loaded with motile microbes across an extended surface subjected to a magnetic field is carried out. We sought to analyze the influence of thermal radiation with varying wall temperatures, taking into account the thermophoresis parameter and the Brownian movement constraints. The underlying comparisons are solved exactly as well as approximately. The numerical and the DTM outcomes are compared through graphs. Here we have also attempted to represent the outcome as a Taylor's series using the DTM.

Velocity Variation

The velocity profiles for the variations of the parameters of Casson liquid (β), mass transmission (s), and the modified magnetic (M) are shown in Figures 5.4.1 - 5.4.3. The speed of the liquid resists when the Casson liquid parameter is increased, as seen in Figure 5.4.1. The rationale is that when the Casson liquid parameter is increased, the thickness of the boundary layer decreases. The effect of the magnetic field on the liquid flow is shown in Figure 5.4.2. When a magnetic influence is functional regularly to the exterior of a molten, the generated magnetic effect produces a repellent intensity on the molten passage, and hence the rapidity of the liquid decreases. The link between the suction parameter and the fluid velocity is seen in Figure 5.4.3. With rising levels of the mass flux parameter, the liquid flow speed decreases. These findings are quite similar to those of Raju et al. [30] and Nayak et al. [91].

Temperature variation

Figures 5.4.4 - 5.4.8 show temperature profiles for various parameter values. We discovered that rising values of the radiation parameter, Brownian movement

parameter, and thermophoresis parameter result in higher temperatures, while variation in ascending order of the suction parameter and Prandtl number result in lower temperatures. The energy profile of the liquid is shown versus the radiation parameter (T_r) in Figure 5.4.4. The temperature of the molten raises for varied values T_r . This is due to the manner that ascending values of T_r produce a decrease in the viscosity of the molten, which raises the temperature. Figure 5.4.5 illustrates that as soon as the suction constraints rises, the temperature of the molten declines; this is due to an increase in the thickness of the thermal boundary layer at the wall. Because of the nonlinearity of the fluctuating wall temperature. The influence of P_r on the temperature of the molten is depicted in Figure 5.4.6, where growth in the P_r values instigate the energy of the liquid to drop. It is for this reason that as the Prandtl number increases, the thickness of the thermal boundary layer decreases, resulting in a decrease in heat flow. The increase in temperature for the growth of the thermophoresis parameter (N_t) is depicted in Figure 5.4.7. This is due to the fact that each nano molecule has different thermophoresis parameter values, which causes the thickness of the thermal boundary layer at the wall to decrease, and thus temperature increases. Figure 5.4.8 shows how the temperature profile improves when the Brownian movement parameter (N_b) is increased. As the value of (N_b) grows, the collision rate between nanoparticles increases, assisting in the growth of heat generation. These findings support those of Chakraborty [156] and Nayak et al. [91].

Concentration profiles of nanoliquids

Figure 5.4.9 - 5.4.11 illustrates the volume concentration of nanoparticles. The concentration of nanoparticles is found to decrease as non-dimensional parameters such as the Lewis number (Le), mass suction (s), and thermal radiation parameter (T_r) are changed. The concentration nanoparticles profile for the variation of Le is shown in the Figure 5.4.9. When Le varied in ascending order, the concentration of nanoparticles volume falls. Nanoparticles with lower mass diffusivity have lower concentrations. The relationship between the density of nanoparticles and the magnetic number is seen in Figure 5.4.10. As the magnetic parameter is increased, the particle concentration increases. When a magnetic field is applied to nanoparticles, dipoles occur, which are allied in the direction of same magnetic field, growing the density of nanoliquids. Figure 5.4.11 shows how the density of nanoliquids changes

with the mass suction parameter. As the suction parameter is increased, the concentration of nanoparticles drops. The suction parameter causes the nanoliquids to disperse and segregate, lowering the nanoparticle concentration. These outcomes are in accord with the findings of Chakraborty [156], Shahid [149], Nayak et al. [91], Zadeh et al. [71].

Concentration profiles of microbes

The Figure 5.4.12 - 5.4.14 shows the microorganism concentration profile. The density of microbes decreases as the bio-convection constant increases (see Figure 5.4.12). Because microorganisms have a higher density than nanoparticles, bio-convection occurs as the density of microorganisms decreases. The density of microbes against the Peclet number for bioconvection is shown in Figure 5.4.13. With increasing Peclet number, the density of microbes falls. The density of motile microbes is shown in Figure 5.4.14 as a function of the mass flux parameter. As the suction parameter is increased, the density of motile microorganisms drops. These findings are reliable with those of Nayak et.al [91] and Zadeh et.al [71].

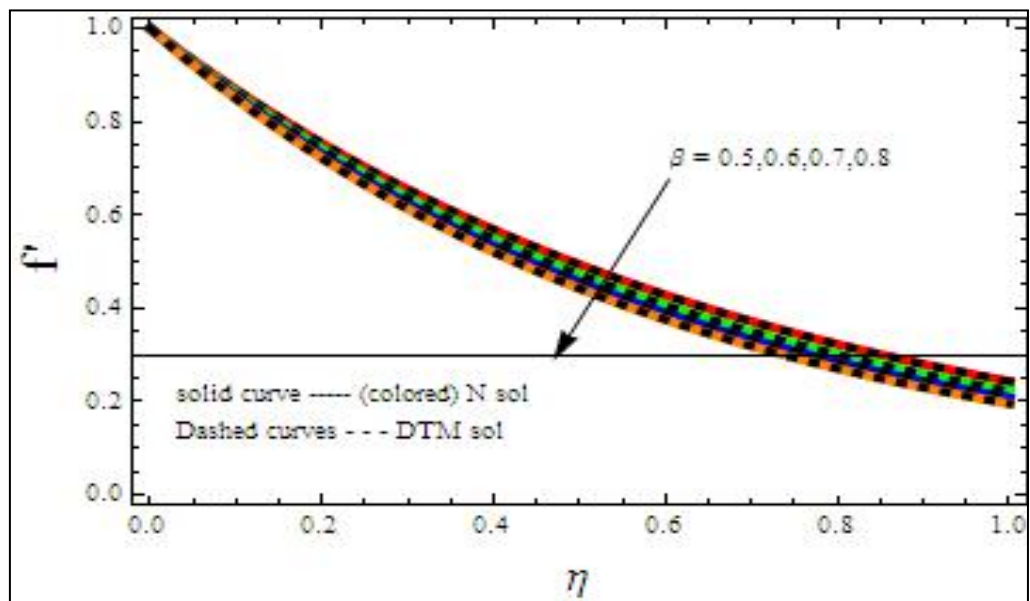


Figure 5.4.1 Velocity of the fluid for $\beta = 0.5, 0.6, 0.7, 0.8$.

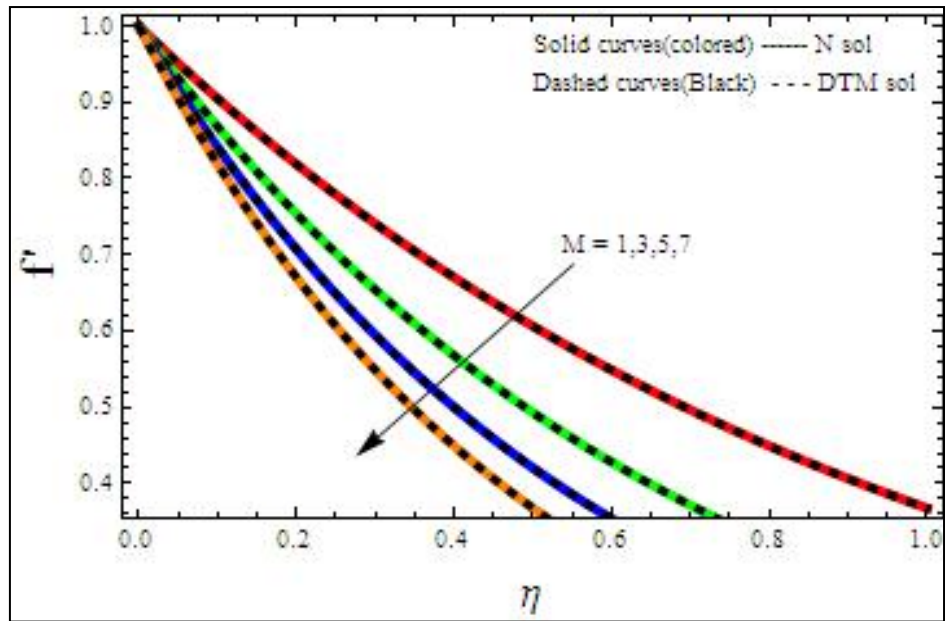


Figure 5.4.2 Velocity of the fluid for the variations of M .

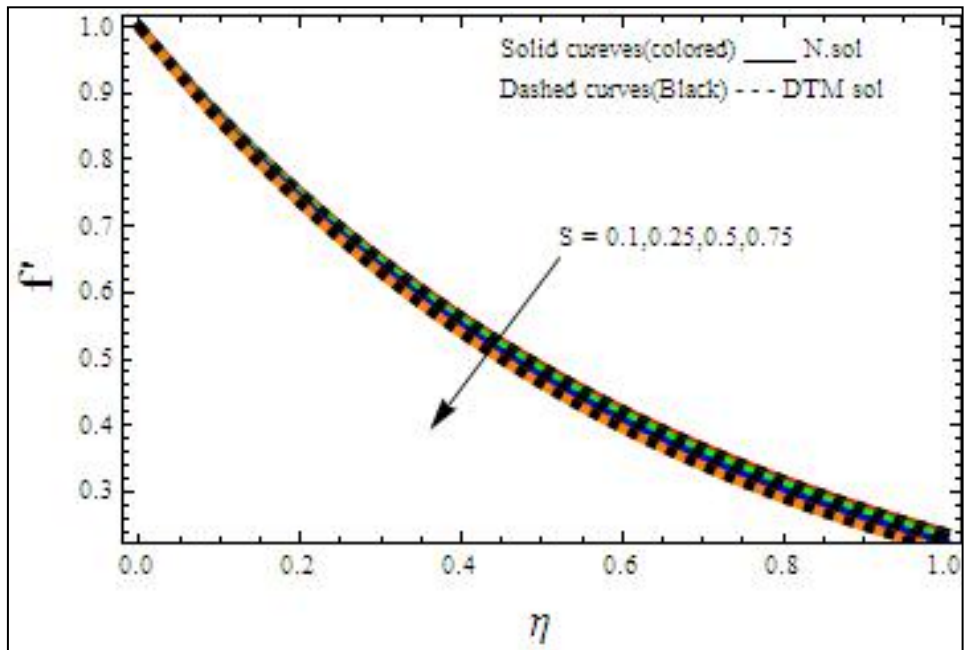


Figure 5.4.3 Velocity of the fluid for the variation of $S = 0.1, 0.25, 0.5, 0.75$.

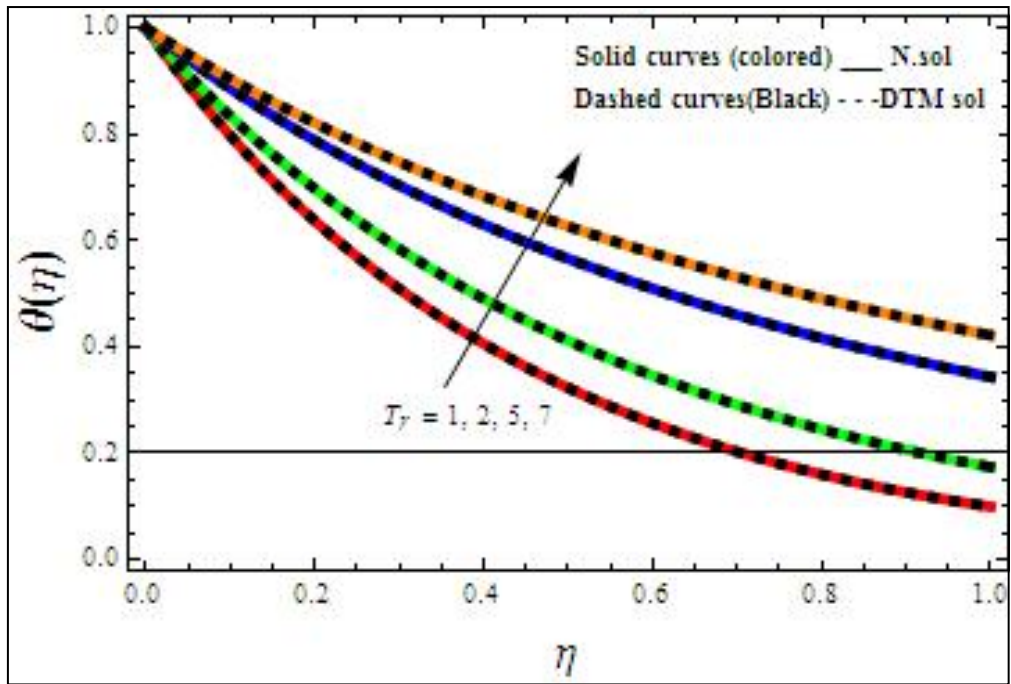


Figure 5.4.4 Temperature profile for distinct values of radiation parameter $T_r = 1, 2, 5, 7$.

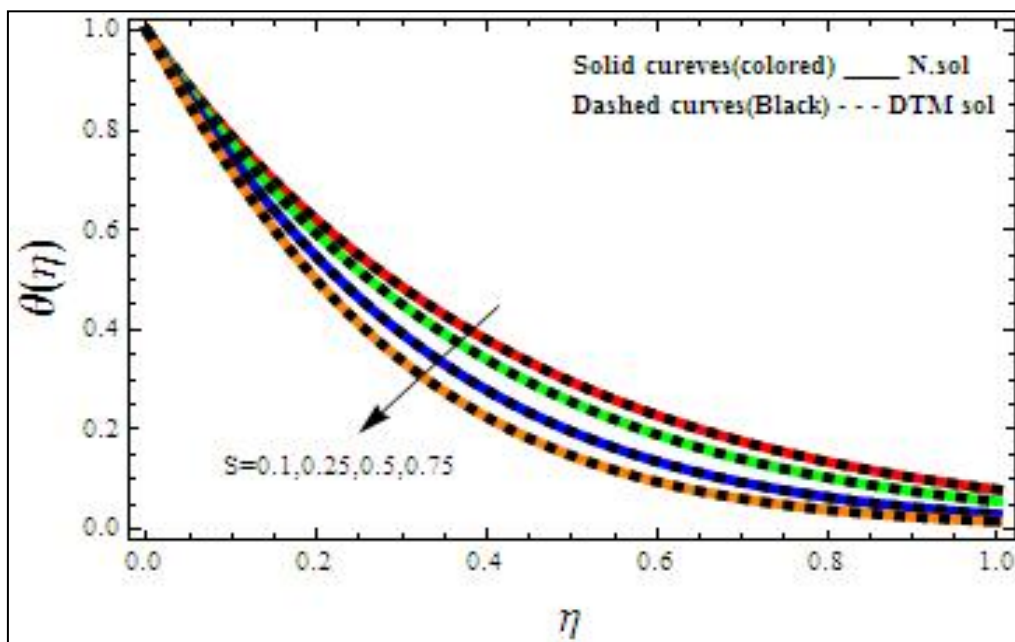


Figure 5.4.5 Energy profile for the variations mass flux parameter $s = 0.1, 0.25, 0.5, 0.75$.

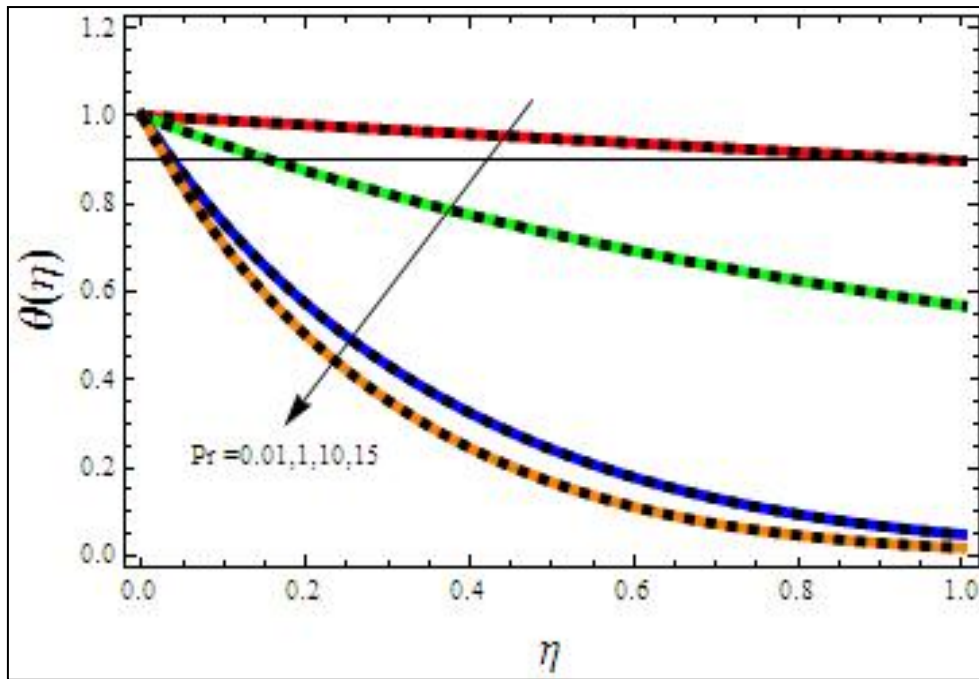


Figure 5.4.6 Temperature profile for different values of $Pr = 0.01, 1, 1.2, 1.5$

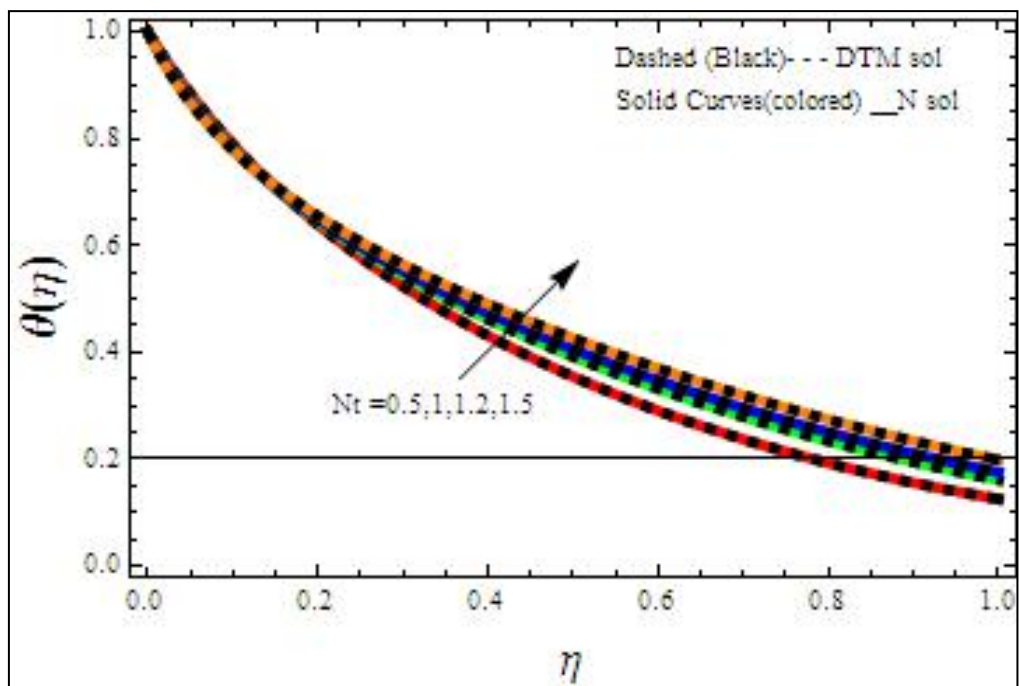


Figure 5.4.7 Energy profile for the variations of $N_t = 0.5, 1, 1.2, 1.5$

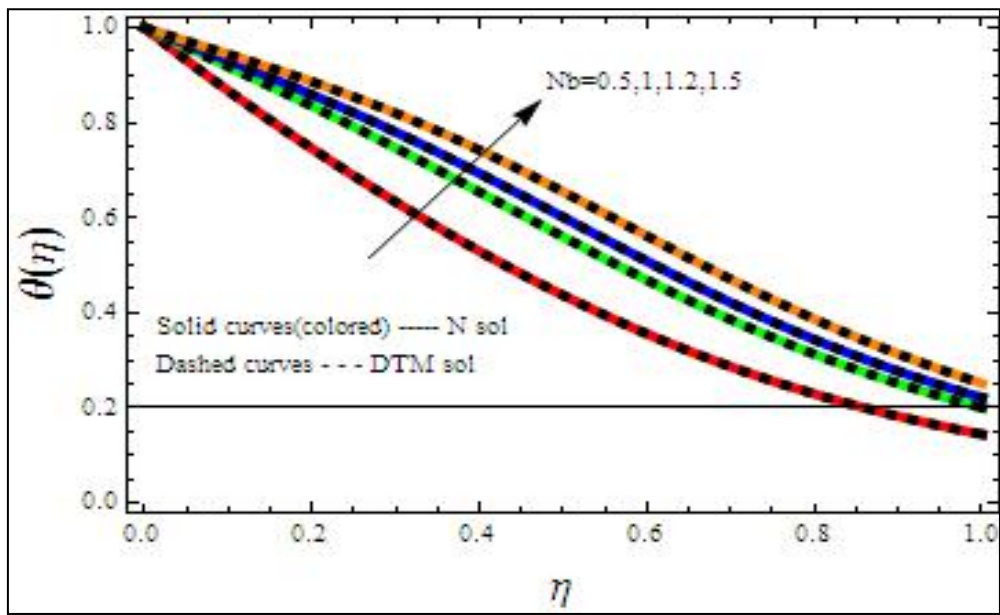


Figure 5.4.8 Energy profile for the variations of $N_b = 0.5, 1, 1.2, 1.5$

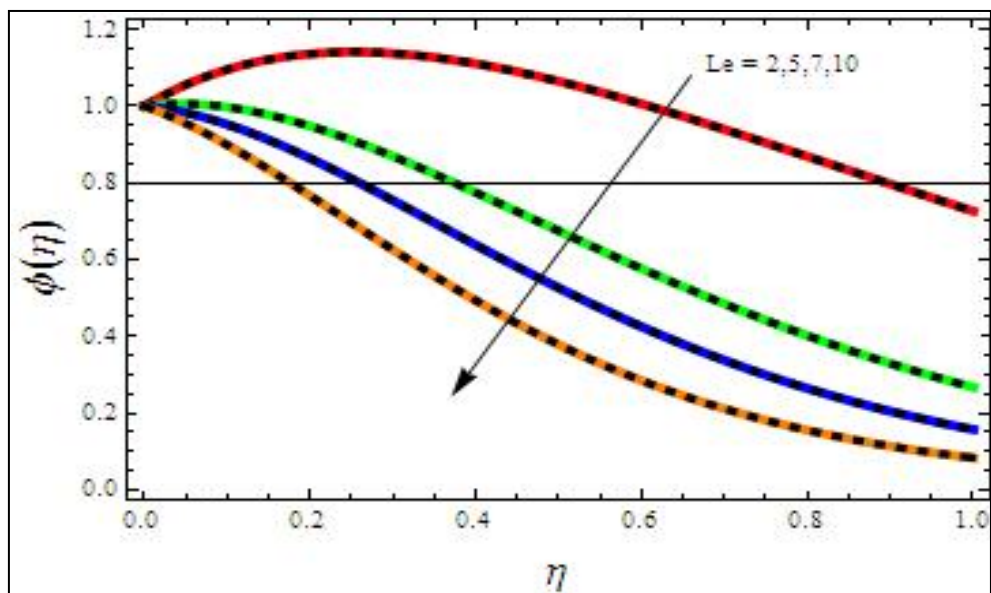


Figure 5.4.9 Concentration profile of nanoparticles for the variations of $Le = 2, 5, 7, 10$

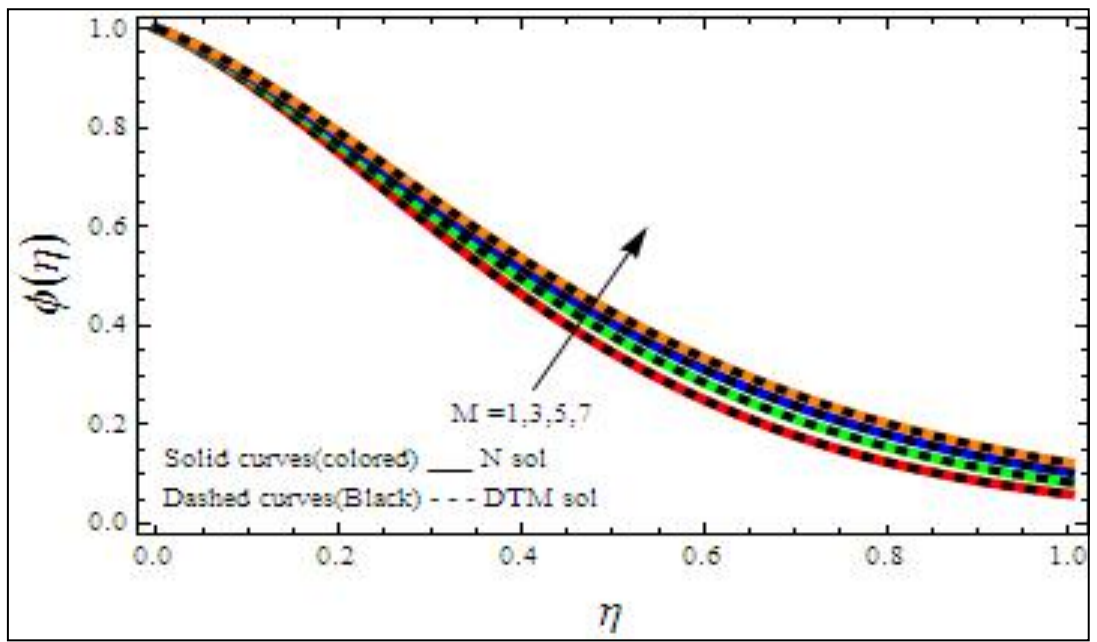


Figure 5.4.10 Concentration profile of nanoparticles for the variations of $M = 1, 3, 5, 7$

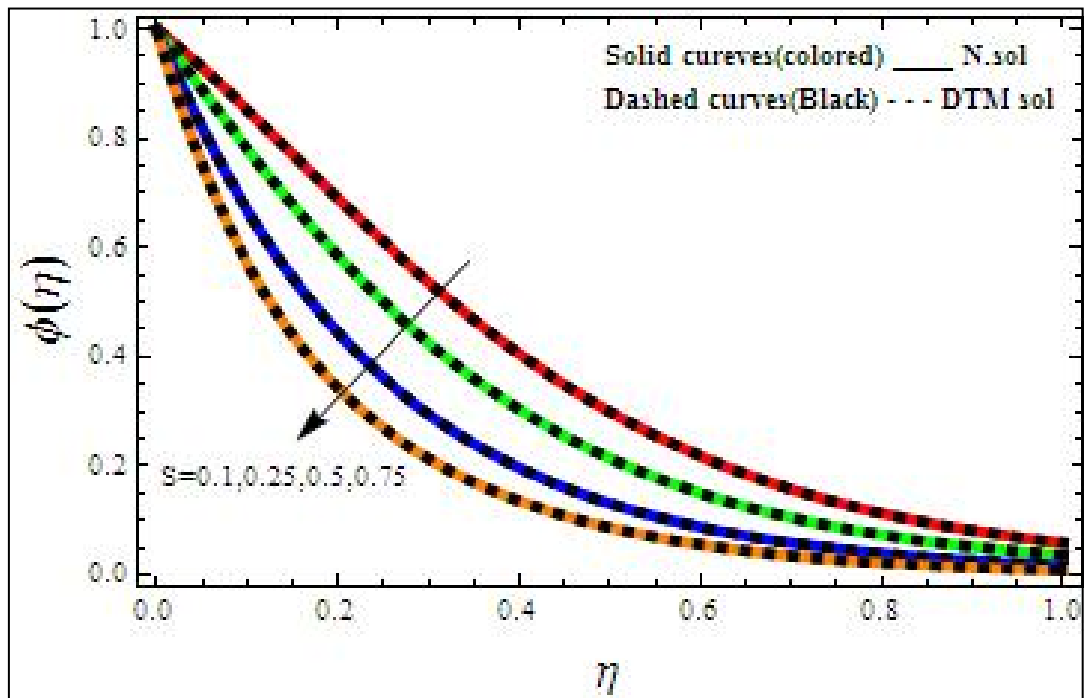


Figure 5.4.11 Concentration profile of nanoparticles for the variations of $s = 0.1, 0.25, 0.5, 0.75$.

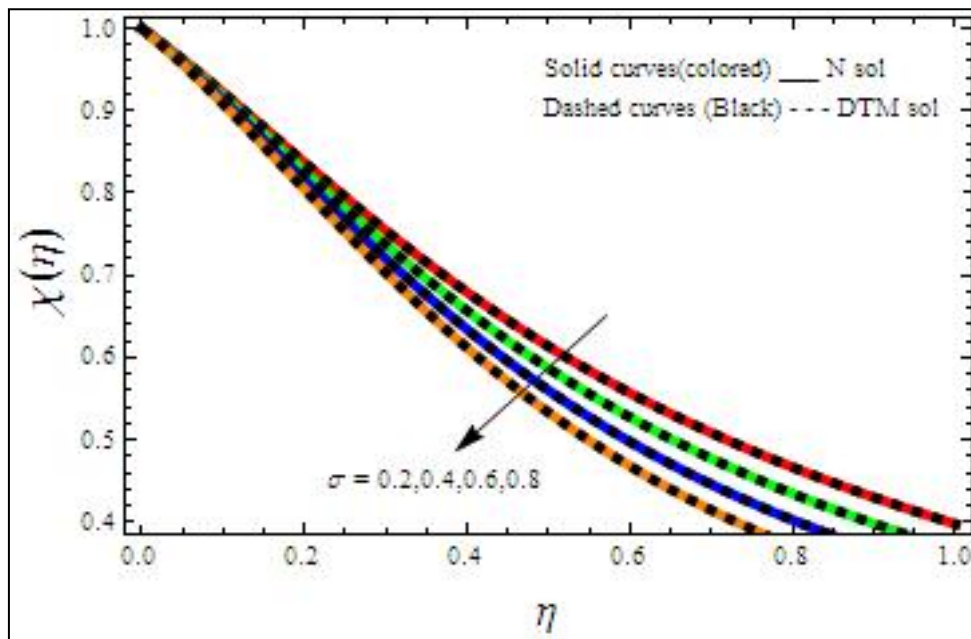


Figure 5.4.12 density profile of microbes for the variations of $\sigma = 0.2, 0.4, 0.6, 0.8$.

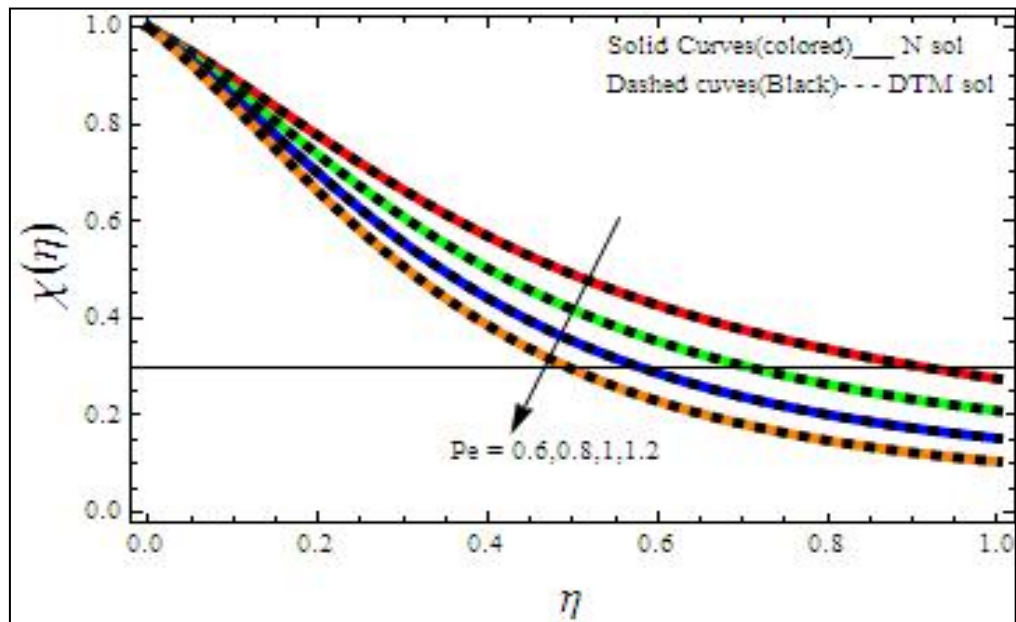


Figure 5.4.13 Density profile of microbes for the variations of $Pe = 0.6, 0.8, 1, 1.2$.

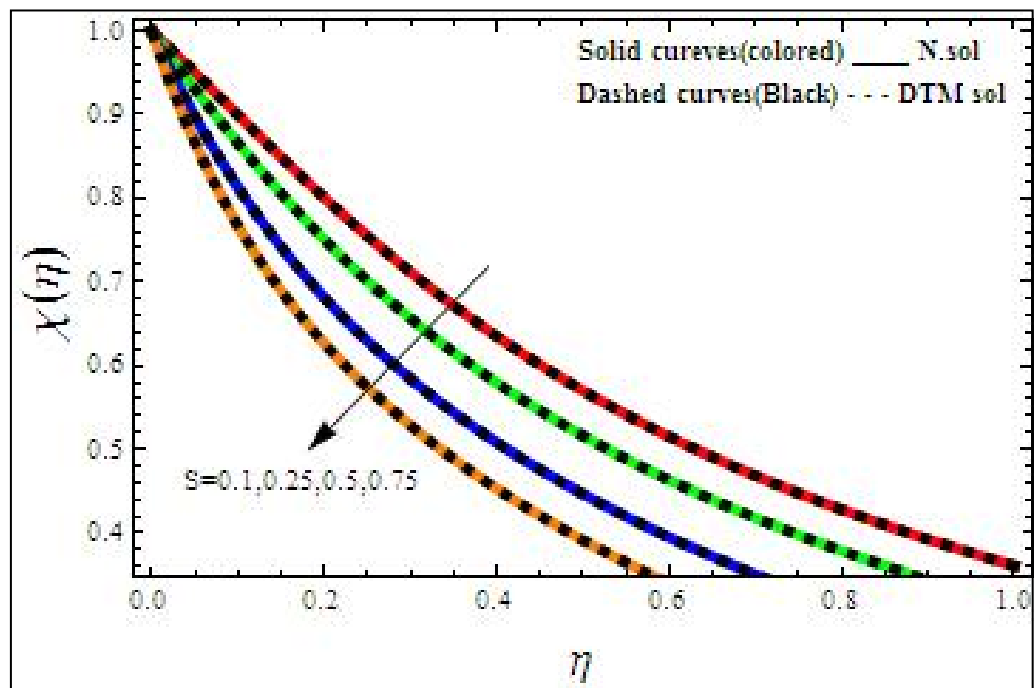


Figure 5.4.14 Density profile of microbes for the variations of $s = 0.1, 0.25, 0.5, 0.75$.

5.5 CONCLUSION

We wanted to find a semi-intuitive and approximate solution for a set of coupled nonlinear equations involving MHD non-Newtonian liquid stream incorporating motile microbes on a linearly extended surface in the current work. Molten stream, energy transmission comprising the thermal radiation effect, and changeable temperature at the walls are all being researched. The concentrations of nanoparticles and microorganisms are also examined and graphed utilizing a variety of non-dimensional properties. The important points of the current investigation are summarized below.

- The thermophoresis parameter (N_t), Brownian movement parameter (N_b), and the thermal radiation parameter (T_r) all have increasing values, resulting in an increase in fluid temperature.
- The temperature of the fluid is lowered by Prandtl number (P_r) and suction parameter (s).
- The magnetic field parameter (M) raises the density of the nanoparticles in the flow while the Lewis number (Le) and suction parameter (s) decrease.
- For increasing Peclet number (P_e), suction parameter (s), and bio-convection constant (σ), the density of microbes drops.

CHAPTER 6

Impact of Magnetic Field on the Bioconvection of Casson Liquid Flow Due to Microbes and Nanoparticles.

(Part of the chapter is published in *Advanced Mathematics scientific Journal (AMSJ)*)

6.1 INTRODUCTION

The major purpose of this chapter is to use Oberbeck-Boussinesq approximations to explore the influence of Brownian motion and thermophoresis parameters on bioconvection in a Casson nanofluid stream containing gyrotactic microorganisms with magnetic impact. The physical scenario encountered in many industrial and technical applications is the stream and energy transmission of nanofluids with diverse characteristics in the boundary layer near a steady flat extended surface. The analysis of the Newtonian and non-Newtonian liquid streams, as well as energy exchange with diverse impacts, has found widespread use in industries such as wire drawing and polymer evulsion from dyes among others. Tinning, cooling metallic plates, polymer sheet ejection, paper, and making glass fibers are some of the other engineering implementations of the stretched sheet. A lot of study on flow and energy exchange across the extending surface has been done by notable scientists in the boundary layer theory for the last several decades.

Alloui et al. [168] published a computational solution for thermo-bioconvection that had become blocked due to gyrotactic microorganisms. Khan et al. [112] examined the consequences of a magnetic field and Navier slip on boundary layer stream with energy and mass transmission in water-based nanoliquids surrounding motile microbes. The numerical findings are generated using the similarity transformation and Oberbeck-Boussinesq approximation. Mehmood et al. [169] demonstrated the influence of stagnation point stream on an expanding slab containing microbes under the sway of an induced magnetic field. In addition, Akbar et.al [111] quantitatively investigated bioconvection, Brownian motion, and thermophoresis of motile microbes and nanoliquids across a stretched plate involving

magnetic effect. The properties of thermophoresis and Brownian movement on the radiative stream of Casson liquid across a moving wedge including motile microbes and magnetic impact were recently published by Raju et al. [30]. Khan et al. [113] examined mixed convection of non-Newtonian fluid sheets due to nanoparticles and motile microbes using the homotopy analysis approach. Khan [114] used inactively controlled nanoliquids model boundary conditions to investigate bioconvection in stable second-grade liquids thin stream comprising nanoliquids and motile microbes. The governing equations were solved analytically using HAM.

Zhou's [72] approach, often known as the differential transform method (DTM), is a time-saving technique frequently utilized by scientists. DTM, a fundamental method of solving differential equations given beginning or boundary conditions, may be used to get the Taylor's series as the outcomes. This technique is extremely adaptable and easy to understand, it can easily be automated. In contrast to HAM, no additional settings are required. Many researchers have lately been successful in achieving convergence of series solutions to their issues. DTM is discovered to be an alternate method for obtaining quick convergence series solutions for nonlinear ODEs as well as PDEs that cannot be solved exactly. DTM was used to solve linear and nonlinear set of ODEs by Mirzaee [57]. Hatami et al. [68] employed DTM to analyze Newtonian and non-Newtonian nanoliquids stream, with good agreement between numerical and experimental outcomes. Sepasgozar et.al [138] used DTM to find the series solution for non-Newtonian liquid stream in an axisymmetric channel with a porous wall's momentum and heat exchange equations.

The goal of this chapter is to look into a bioconvection investigation of Casson nanofluid flow above the stretched sheet, which includes gyrotactic microbes, under the sway of magnetic field. We also used the Oberbeck-Boussinesq approximations to investigate intriguing elements of Brownian motion, thermophoresis, and energy transmission analyses of the studied fluid. Using the differential transform approach and the numerical method, we attempted to solve the governing equations.

6.2 Mathematical Formulation

Consider adding gyrotactic microorganisms to an incompressible water-based Casson nanofluid. The bacteria are thought to be alive since the combined fluid is

dilute. The stretching sheet is stretched along the x – axis and the liquid is allowed to stream above the stretched surface under the sway of an induced magnetic field normal to the stretched surface. An induced magnetic field isn't taken into account. The stretched sheet surface is supposed to be moving at a linear speed. Let D_b represent Brownian diffusion coefficient and D_t represent the influence of the thermophoresis diffusion coefficient on heat conduction. Let T_w , C_w , and N_w signify temperature, nanoparticle volume fraction, and microbe diffusive concentration near the wall, respectively, while T_∞ , C_∞ , N_∞ denote energy, coefficient of nanoliquids, and microbes diffusive concentration far away from the surface respectively, as shown in the Figure 6.2.1.

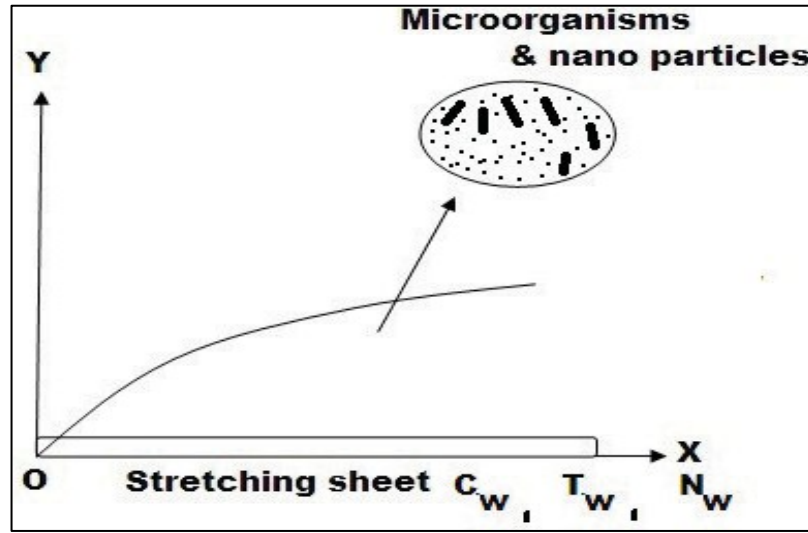


Figure 6.2.1 Geometrical sketch of the model of bioconvection in the stream of nanofluids containing microbes

Mathematically formulated equations are:

$$\frac{\partial u}{\partial x} + \frac{\partial v}{\partial y} = 0, \quad (6.2.1)$$

$$u \frac{\partial u}{\partial x} + v \frac{\partial u}{\partial y} = \nu \left(1 + \frac{1}{\beta} \right) \frac{\partial^2 u}{\partial y^2} - \frac{\sigma B_0^2}{\rho} u + \left(\frac{1 - C_\infty}{\rho_f} \right) \rho_\infty g \alpha (T - T_\infty) - \left(\frac{\rho_p - \rho_\infty}{\rho_f} \right) g (C - C_\infty) - \left(\frac{\rho_m - \rho_f}{\rho_f} \right) g \gamma (N - N_\infty), \quad (6.2.2)$$

$$u \frac{\partial T}{\partial x} + v \frac{\partial T}{\partial y} = \left(\frac{K}{\rho C_p} \right) \frac{\partial^2 T}{\partial y^2} + \tau \left(D_B \frac{\partial C}{\partial y} \frac{\partial T}{\partial y} + \frac{D_T}{T_\infty} \left(\frac{\partial T}{\partial y} \right)^2 \right), \quad (6.2.3)$$

$$u \frac{\partial C}{\partial x} + v \frac{\partial C}{\partial y} = D_B \frac{\partial^2 C}{\partial y^2} + \left(\frac{D_T}{T_\infty} \right) \frac{\partial^2 T}{\partial y^2} , \quad (6.2.4)$$

$$u \frac{\partial N}{\partial x} + v \frac{\partial N}{\partial y} + \frac{bW_c}{c_w - c_\infty} \left(\frac{\partial}{\partial y} (NC_y) \right) = D_m \frac{\partial^2 N}{\partial y^2} , \quad (6.2.5)$$

The Casson model's flow and heat transfer boundary conditions are as follows

$$\begin{aligned} v = 0, u = a_0 x, T = T_w, C = C_w, N = N_w \quad \text{as } y \rightarrow 0, \\ u \rightarrow 0, T \rightarrow T_\infty, C = C_\infty, N \rightarrow N_\infty \quad \text{as } y \rightarrow \infty, \end{aligned} \quad (6.2.6)$$

Incorporating the similarity transformation into the governing equations is as follows:

$$\begin{aligned} \eta = \frac{y}{x} Ra_x^{1/4} f(\eta), \psi = m Ra_x^{1/4} f(\eta), \theta(\eta) = \frac{T - T_\infty}{T_w - T_\infty}, \varphi(\eta) = \frac{C - C_\infty}{C_w - C_\infty}, \\ \chi(\eta) = \frac{N - N_\infty}{N_w - N_\infty}, Ra_x = \frac{(1 - C_\infty) \alpha g \Delta T_f}{m \nu} x^3, \end{aligned} \quad (6.2.7)$$

The following nonlinear ordinary differential equations are linked nonlinearly:

$$(1 + 1/\beta) f_{\eta^3} - (1/2 P_r) f_{\eta^2} + (3/4 P_r) f f_{\eta^2} - M f_{\eta} + \theta - N_r \phi - R b \chi = 0, \quad (6.2.8)$$

$$\theta_{\eta^2} + (3/4) f \theta_{\eta} + N_b \theta_{\eta} \phi_{\eta} + N_t \theta_{\eta}^2 = 0, \quad (6.2.9)$$

$$\phi_{\eta^2} + \left(\frac{3}{4} \right) L_e f \phi_{\eta} + (N_t/N_b) \theta_{\eta^2} = 0, \quad (6.2.10)$$

$$\chi_{\eta^2} + (3/4) S_c f \chi_{\eta} - P_e \{ \phi_{\eta} \chi_{\eta} + \phi_{\eta^2} (\chi + \sigma) \} = 0, \quad (6.2.11)$$

The dimensionless boundary conditions that go with it are

$$\left. \begin{aligned} f(0) = 0, f_{\eta}(0) = \lambda, \theta(0) = 1, \phi(0) = 1, \chi(0) = 1 \quad \text{as } \eta \rightarrow 0 \\ f_{\eta}(\infty) = 0, \theta(\infty) = 0, \phi(\infty) = 0, \chi(\infty) = 0 \quad \text{as } \eta \rightarrow \infty \end{aligned} \right\}, \quad (6.2.12)$$

the dimensionless parameters that are utilized in (6.2.8) to (6.2.11) are:

$$M = \frac{\sigma B_0^2 x^2}{\rho \nu Ra_x^{1/2}}, N_r = \frac{(\rho_p - \rho_\infty) \Delta C_w}{\rho_f (1 - c_\infty) \alpha \Delta T_f}, R_b = \frac{\gamma \Delta N_w \Delta \rho}{\rho_f \alpha (1 - C_\infty) \Delta T_w}, N_t = \frac{\tau D_T (T_w - T_\infty)}{m T_\infty},$$

$$N_b = \frac{\tau D_B (C_w - C_\infty)}{m}, L_e = \frac{m}{D_B}, S_c = \frac{m}{D_m}, P_e = \frac{b W_c}{(C_w - C_\infty)}, \sigma = \frac{N_\infty}{(N_w - N_\infty)}$$

$$\lambda = \frac{a x^2}{m Ra_x^{1/2}}, P_r = \nu / m .$$

6.3 DTM Solution

The equations (6.2.8) - (6.2.12) may be translated into the following Differential forms [Hatami [167]]:

$$\begin{aligned} \left(1 + \frac{1}{\beta}\right)(r+1)(r+2)(r+3)F[r+3] &= M(r+1)F[r+1] - \theta[r] + N_r\phi[r] \\ &+ R_b\chi[r] + \frac{1}{2P_r}\sum_{m=0}^r(r-m+1)F[r-m+1](m+1)F[m+1] - \\ &-(3/4P_r)\sum_{m=0}^rF[r-m](m+1)(m+2)F[m+2], \end{aligned}$$

$$\text{where } F[0] = 0, F[1] = 0, F[2] = a_1, \quad (6.3.1)$$

$$\begin{aligned} (r+1)(r+2)\theta[r+2] &= \left(-\frac{3}{4}\right)\sum_{m=0}^rF[r-m](m+1)\theta[m+1] - \\ &-N_b\sum_{m=0}^r(r-m+1)\theta[r-m+1](m+1)\phi[m+1] - \\ &-N_t\sum_{m=0}^r(r-m+1)\theta[r-m+1](m+1)\theta[m+1] \end{aligned}$$

$$\text{where } \theta[0] = 1, \theta[1] = a_2, \quad (6.3.2)$$

$$\begin{aligned} (r+1)(r+2)\phi[r+2] &= \\ &= \left(-\frac{3}{4}\right)L_e\sum_{m=0}^rF[r-m](m+1)\phi[m+1] - \frac{N_t}{N_b}\sum_{m=0}^r(r+1)(r+2)\theta[r+2], \end{aligned}$$

$$\text{where } \phi[0] = 1, \phi[1] = a_3, \quad (6.3.3)$$

$$\begin{aligned} (r+1)(r+2)\chi[r+2] &= P_e\sum_{m=0}^r(r-m+1)\phi[r-m+1](m+1)\chi[m+1] + \\ &+ P_e\sum_{m=0}^r\chi[r-m](m+1)(m+2)\phi[m+2] \\ &+ P_e\sigma(r+1)(r+2)\phi[r+2] - (3/4)S_c\sum_{m=0}^rF[r-m](m+1)\chi[m+1], \end{aligned}$$

$$\chi[0] = 1, \chi[1] = a_4, \quad (6.3.4)$$

$F[r]$, $\theta[r]$, $\phi[r]$ and $\chi[r]$ are the differential transforms of $f(\eta)$, $\theta(\eta)$, $\phi(\eta)$ and $\chi(\eta)$, while a_1, a_2, a_3 and a_4 are the assumed constants, which may be found using

equations (6.3.1) - (6.3.4) and the boundary conditions. We get the following results for $r = 0, 1, 2, 3, \dots$

$$F[3] = \frac{-1 + N_r + R_b}{6(1 + \frac{1}{\beta})},$$

$$\theta[2] = -\frac{1}{2} a_2 a_3 N_b - \frac{a_2^2 N_t}{2},$$

$$\phi[2] = -\frac{N_t \left(-\frac{1}{2} a_2 a_3 N_b - \frac{a_2^2 N_t}{2} \right)}{N_b},$$

$$\chi[2] = \frac{a_3 a_4 P_e}{2} + P_e \left(\frac{1}{2} a_2 a_3 N_b + \frac{a_2^2 N_t}{2} \right) \frac{N_t}{N_b} (1 + \sigma),$$

$$F[4] = \frac{a_1 M}{12(1 + \frac{1}{\beta})} + \frac{-a_2 + a_3 N_r + a_4 R_b}{24(1 + \frac{1}{\beta})},$$

$$\begin{aligned} \theta[3] = & -\frac{2}{3} a_2 N_t \left(-\frac{1}{2} a_2 a_3 N_b - \frac{a_2^2 N_t}{2} \right) - \\ & -\frac{1}{6} N_b \left(2a_3 \left(-\frac{1}{2} a_2 a_3 N_b - \frac{a_2^2 N_t}{2} \right) - \frac{2a_2 N_t \left(-\frac{1}{2} a_2 a_3 N_b - \frac{a_2^2 N_t}{2} \right)}{N_b} \right), \end{aligned}$$

Similarly, we can obtain, $\phi[3], \chi[3]$, and so on. Using all of the above in the differential inverse transforms, and assuming $P_r = 6.2$, $\beta = 1$, $M = 5$, $N_r = 0.5$, $R_b = 0.1$, $N_t = 0.1$, $N_b = 0.1$, $Le = 10$, $S_c = 0.1$, $P_e = 1$, $\sigma = 0.2$ and solving for a_1, a_2, a_3, a_4 , utilizing the boundary requisites and the Pade approximation with $\text{Lim } f'(\eta) = 0$ as $\eta \rightarrow \infty$, we get $a_1 = 0.144761$, $a_2 = -0.159598$, $a_3 = -0.4891398$,

$a_4 = -0.619069$, and then the series solutions for $f(\eta), \theta(\eta), \phi(\eta), \chi(\eta)$ are obtained as follows.

$$\begin{aligned} f(\eta) = & 0.0723803575\eta^2 - 0.0333333333\eta^3 + 0.0120192699\eta^4 - \\ & -0.0038352688\eta^5 + 0.0009907633\eta^6 - 0.00022955075\eta^7 + \\ & +0.0000587013\eta^8 - 0.0000160486\eta^9 + 0.0000042669\eta^{10} - \\ & -0.00000116244\eta^{11} + 3.2298296 \times 10^{-7}\eta^{12} - + - \end{aligned}$$

$$\begin{aligned}\theta(\eta) = & 1 - 0.159598\eta - 0.00517687\eta^2 - 0.000111948\eta^3 + 0.00072017\eta^4 \\ & - 0.0000914205\eta^5 + 0.0000249909\eta^6 - 9.58335 \times 10^{-6}\eta^7 + \\ & + 7.22131 \times 10^{-8}\eta^8 + 4.64485 \times 10^{-7}\eta^9 - 1.8687 \times 10^{-7}\eta^{10} + \\ & + 1.57907 \times 10^{-7}\eta^{11} - 9.19743 \times 10^{-8}\eta^{12} - ,\end{aligned}$$

$$\begin{aligned}\phi(\eta) = & 1 - 0.48914\eta + 0.00517687\eta^2 + 0.000111948\eta^3 + 0.0214074\eta^4 \\ & - 0.00630385\eta^5 + 0.00152499\eta^6 - 0.0014524\eta^7 + 0.000757427\eta^8 - \\ & - 0.000298733\eta^9 + 0.000148427\eta^{10} - 0.000075264\eta^{11} + 0.0000345801\eta^{12} -\end{aligned}$$

$$\begin{aligned}\chi(\eta) = & 1 - 0.619069\eta + 0.157618\eta^2 - 0.0277013\eta^3 + 0.0297124\eta^4 \\ & - 0.0212832\eta^5 + 0.00917625\eta^6 - 0.00430325\eta^7 + 0.0025966\eta^8 \\ & - 0.00144392\eta^9 + 0.000719194\eta^{10} - 0.000368404\eta^{11} + 0.000196706\eta^{12} -..\end{aligned}$$

6.4 Results and Discussion

Under the effect of a uniformly applied magnetic field normal to the surface, the heat exchange of nano particles and bioconvection in the unsteady fluid flow owing to gyrotactic microorganisms are investigated. In this work, exact and approximate solutions for all governing equations are generated utilizing DTM and Mathematica software and graphs are used to examine the impact of a wide variety of factors on fluid momentum, energy, concentration of nanoparticles, and motile microbes.

Velocity profile

Figures 6.4.1 – 6.4.4 depict the Casson fluid's velocity profile for a variety of parameter values. For increasing values of in Figure 6.4.1, the Casson nanofluid stream's velocity rises due to functional magnetic field normal to the sheet. Figure 6.4.2 shows the reduction in fluid velocity as the bioconvection Rayleigh number R_b rises. This is because of the buoyancy effect. Near the stretched sheet's edge, the Casson fluid's velocity falls. Figure 6.4.3 demonstrates how the fluid velocity decreases when the bioconvection ratio parameter is increased (N_r). The

concentration of nanoparticles near the sheet rises, causing this effect. The velocity of the Casson fluid decreases with rising Prandtl numbers, as seen in Figure 6.4.4. The impact of rising Prandtl numbers. As the Prandtl number rises, the density of nanoparticles rises, causing the coefficient of viscosity to rise and the liquid velocity to fall.

Temperature Profile

Figures 6.4.5- 6.4.8 show temperature profiles for various non-dimensional parameter values, and we discovered that a rise in temperature corresponds to increasing values of thermophoresis parameter, Brownian movement parameter, and buoyancy Rayleigh number, while a reduction in temperature corresponds to increasing values of slip parameter. Figure 6.4.5 shows how increasing the slip parameter causes a drop in the temperature profile. This is because increasing the slip parameter values for the liquid causes a decrease in pressure and temperature. Because a rise in Brownian movement parameter increases the collision frequency of the particles in the liquid, and therefore heat streams, Figure 6.4.6 demonstrates the augmentation of temperature profile for an increase in Brownian motion parameter. Figure 6.4.7 illustrates the effect of the thermophoresis parameter N_t . As the value of N_t rises, so does the temperature profile of the fluid. The reason for this is that the N_t values of nanoparticles vary. Figure 6.4.8 depicts the effect of the buoyancy Rayleigh number on temperature. As the buoyancy Rayleigh parameter increases, the temperature profile rises. The reason for this is that the rapidity of the liquid increases as microbes drag it, lowering the particle concentration in the fluid. As a result, the chance of random motion increases, resulting in an increase in temperature.

Concentration of nano particles and microorganisms:

Figures 6.4.9 to 6.4.12 show the concentration profiles of nanoparticles and microorganisms. Figure 6.4.9 shows that as the stretching parameter is increased, the concentration of nanoparticles falls. This is because the Brownian motion coefficient reduces as nano particles migrate away from the sheet. Figure 6.4.10 shows how the concentration of nanoparticles decreases as the thermophoresis parameter increases. The motive for this is because increasing the thermophoresis parameter causes nanoparticles to flow towards the cold, resulting in a drop in nanoparticle

concentration in the fluid. The relationship between nanoparticle concentration and the buoyancy ratio parameter is seen in Figure 6.4.11. With rising values of the buoyancy ratio constraint N_r , the density of nanoliquids also rises. As the buoyancy parameter increases, the fluid will exert an upward force that opposes the weight of the object in the fluid. Because the pressure at the bottom of a fluid is greater than at the top due to the weight of the overlaying fluid, the pressure deviation results in total ascendent force, and the nanofluids descend to the bottom. The rise in density of nanoparticles for increased magnetic field levels is seen in Figure 6.4.12. When a magnetic field is applied to nanoparticles, it causes magnetic dipoles to develop in the tendency of the magnetic field. The particles form chain link clusters in the direction of the functional magnetic field, increasing the nanoparticle density. The relationship among the Schmidt number and density of microbes is seen in Figure 6.4.13. As the Schmidt number increases, the density of the microbes drops. As the Schmidt number rises, the fluid's dynamic viscosity rises, while the density and mass diffusivity of the nanoparticles fall, lowering the microbes' concentration. The behaviour of the thermophoresis parameter on the density of microorganisms is depicted in Figure 6.4.14. As the thermophoresis parameter is increased, the concentration of bacteria falls. Because moving particles have varying capacity of temperature gradient, the thermophoresis parameter is most usually employed to analyze temperature influence on mobile particles. As the temperature of moving particles increases, the concentration of microorganisms decreases. The bioconvection constant is shown in Figure 6.4.15 as a function of the microbe concentration. Because bioconvection occurs when the density of mobile organisms falls below that of the fluid, we may see a reduction in the concentration of microorganisms as the bioconvection constant rises. The relationship between motile microorganisms and the non-dimensional Peclet number is seen in Figure 6.4.16. The density of microorganisms decreases as the Peclet number rises. The Peclet number aids in thinning the boundary layer.

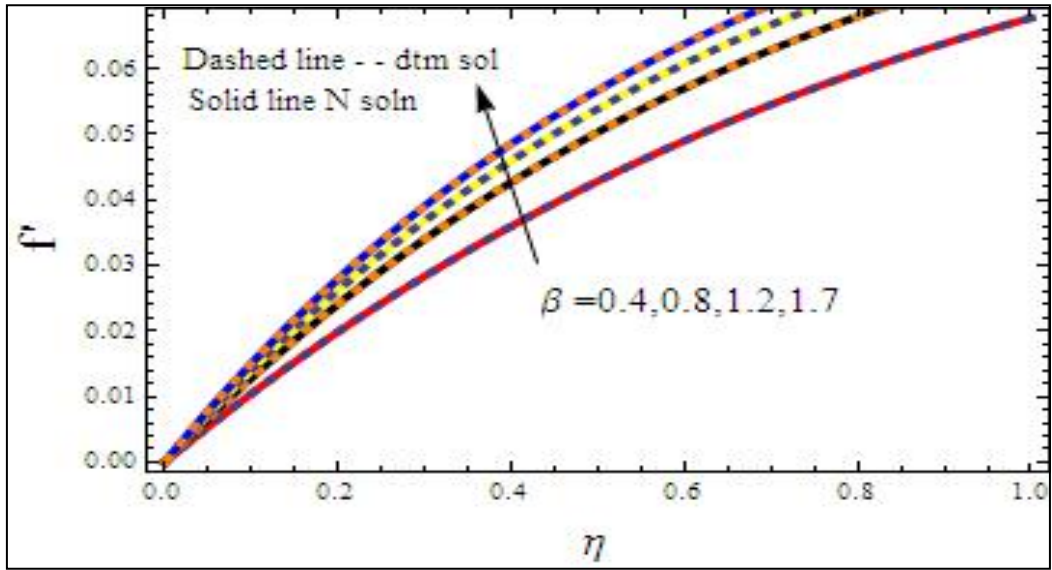


Figure 6.4.1 Velocity Profile of the liquids for $\beta= 0.5,0.6,0.7,0.8$.

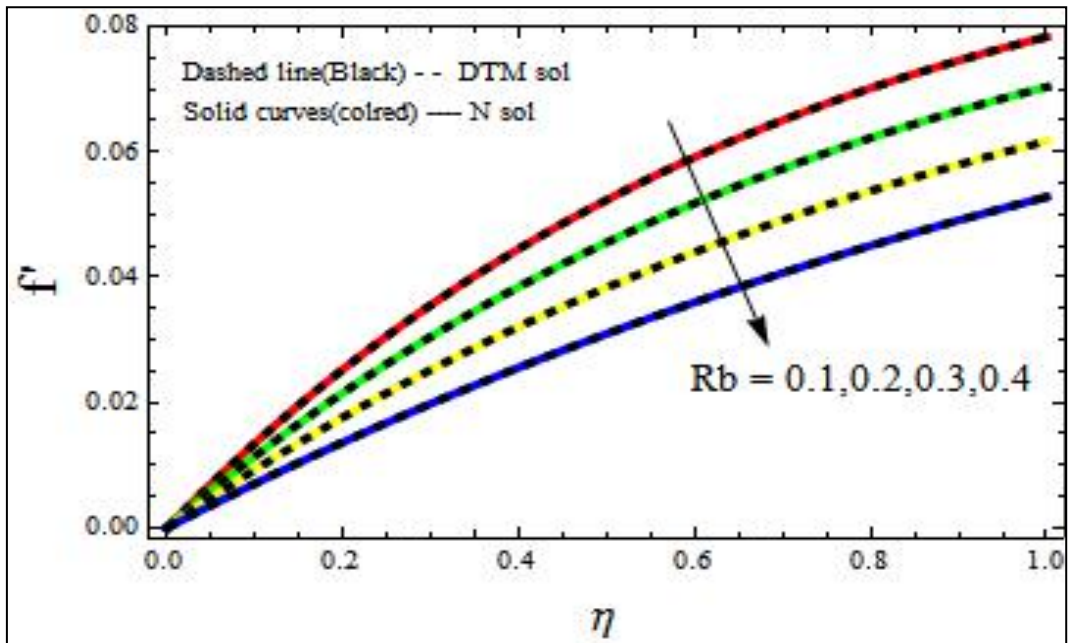


Figure 6.4.2 Velocity profile for variations of the parameter $R_b = 0.1,0.2,0.3,0.4$.

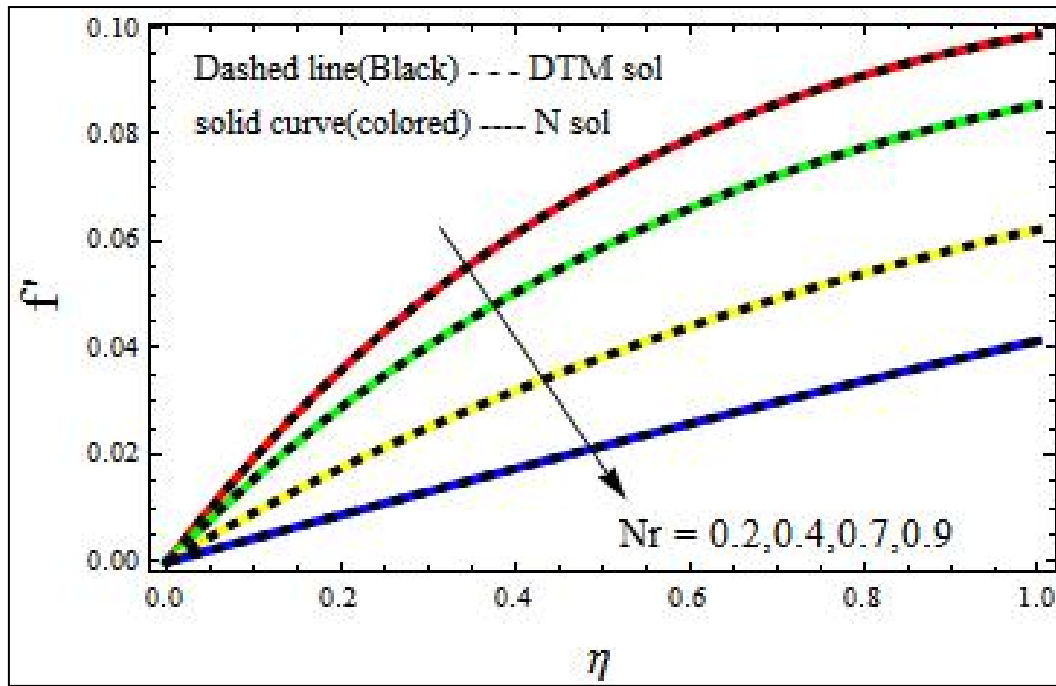


Figure 6.4.3 Velocity profile for variations of $N_r = 0.2, 0.4, 0.7, 0.9$.

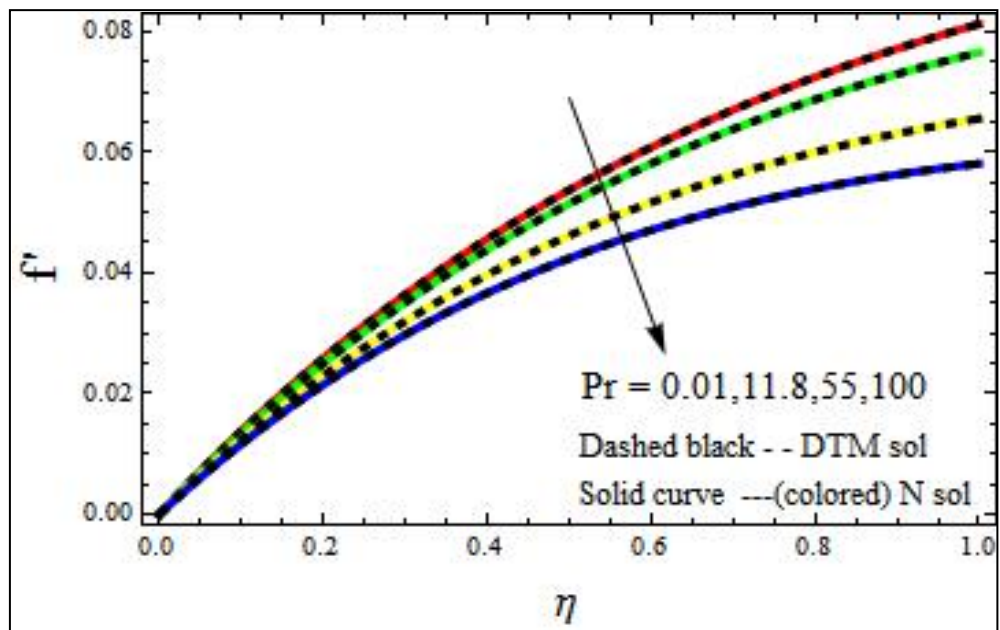


Figure 6.4.4 Velocity profile for the variations of $P_r = 0.01, 11.8, 55, 100$.

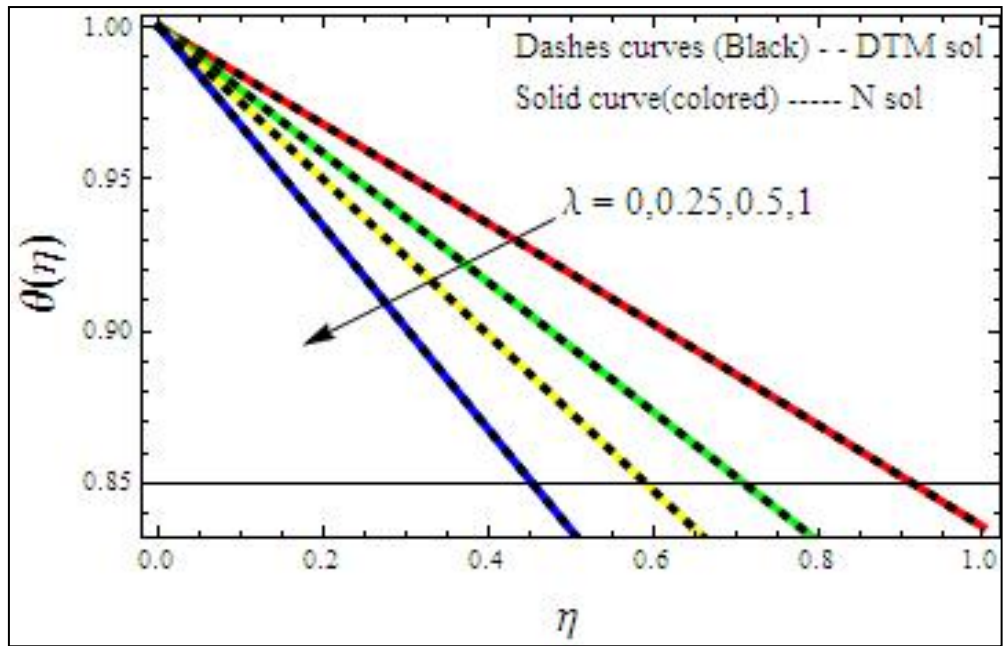


Figure 6.4.5 Energy profile for the variation of $\lambda=0,0.25,0.5,1$.

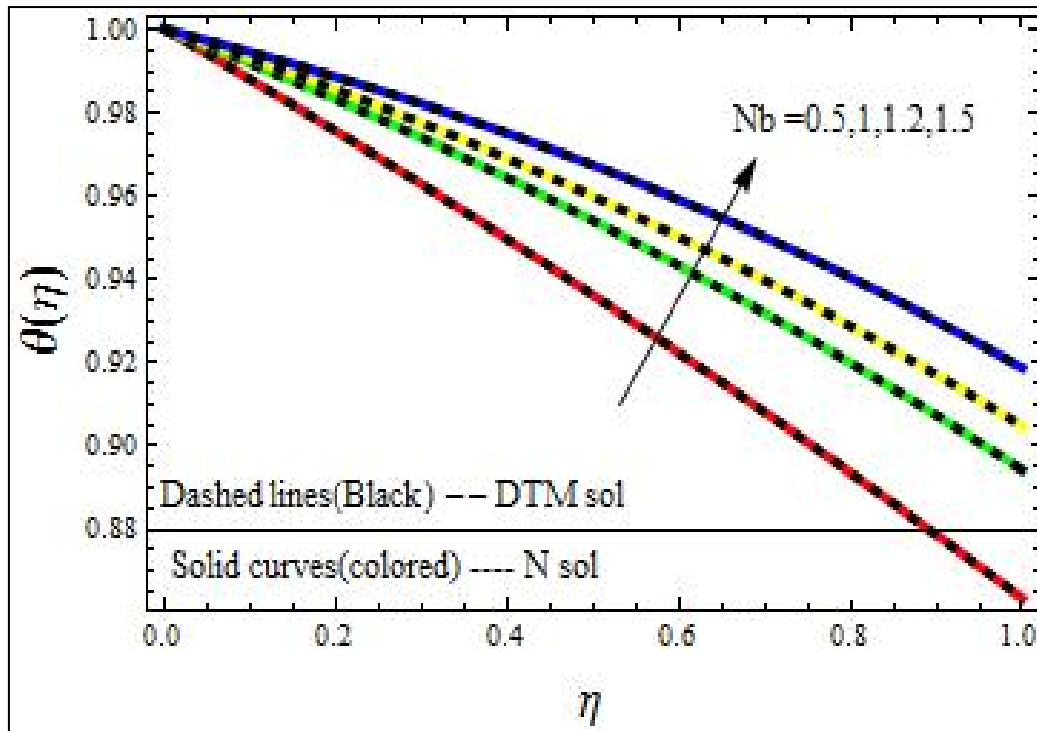


Figure 6.4.6 Energy profile for the variations of $N_b=0.5,1,1.2,1.5$.

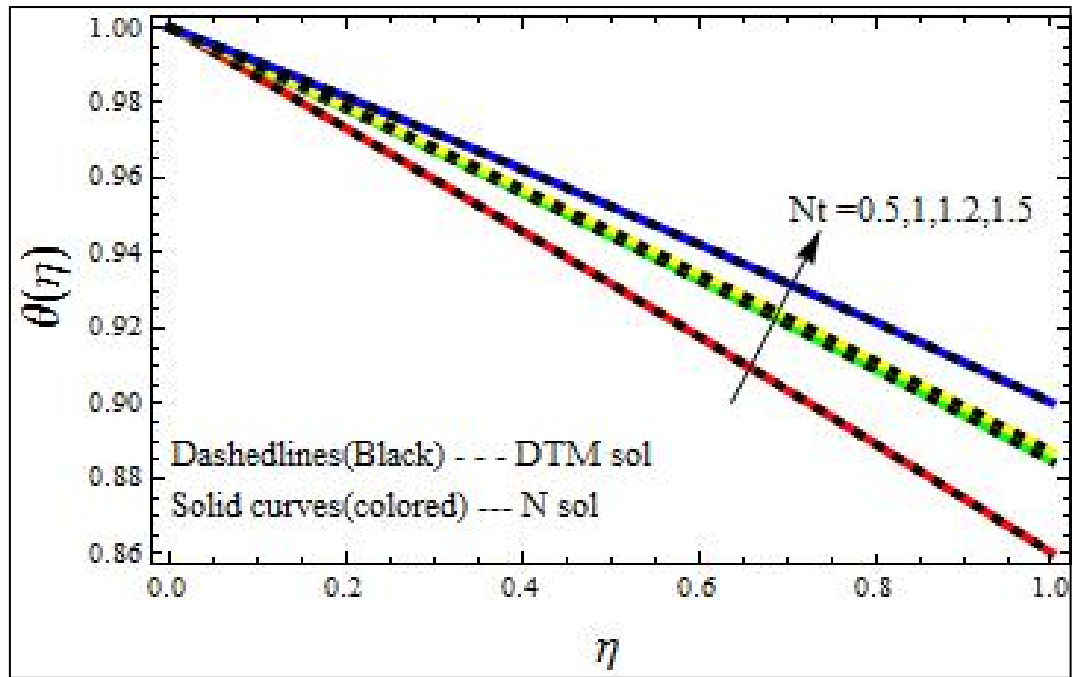


Figure 6.4.7 Energy profile for the variation of $N_t=0.5,1,1.2,1.5$.

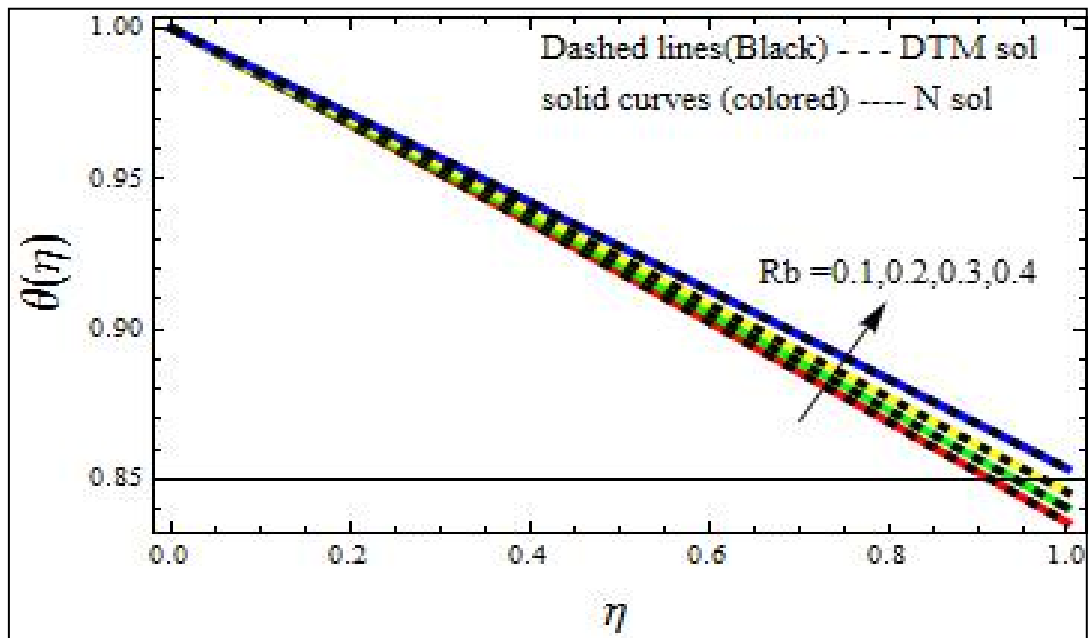


Figure 6.4.8 Energy profile for the variation of $R_b=0.1, 0.2, 0.3, 0.4$.

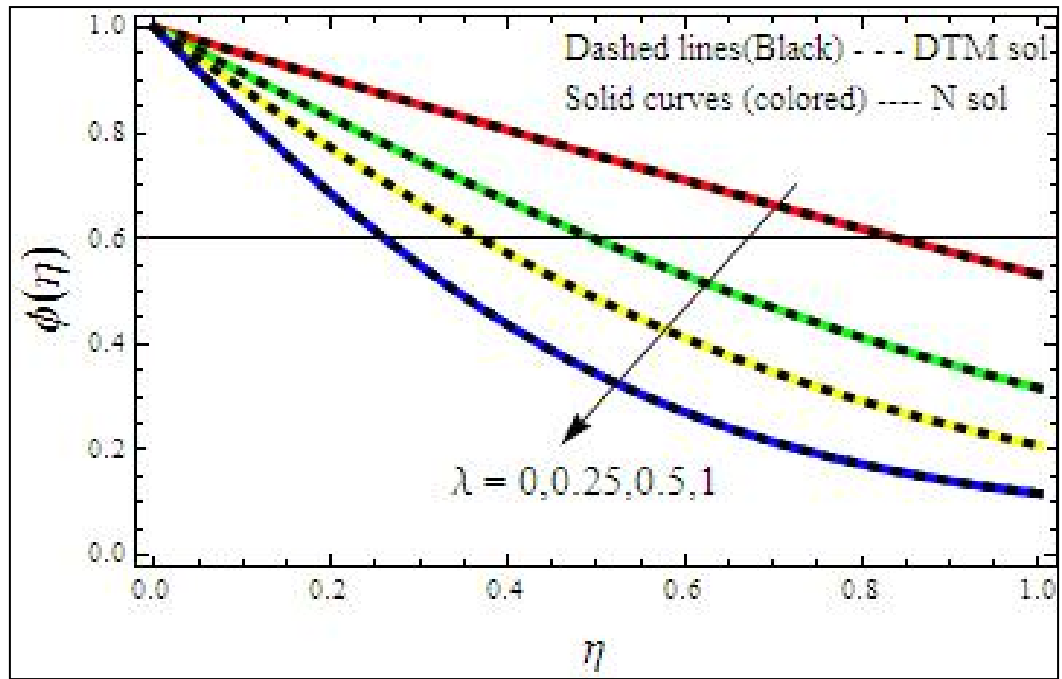


Figure 6.4.9. Concentration profile of the nanoparticles for the variations of $\lambda=0,0.25,0.5, 1$.

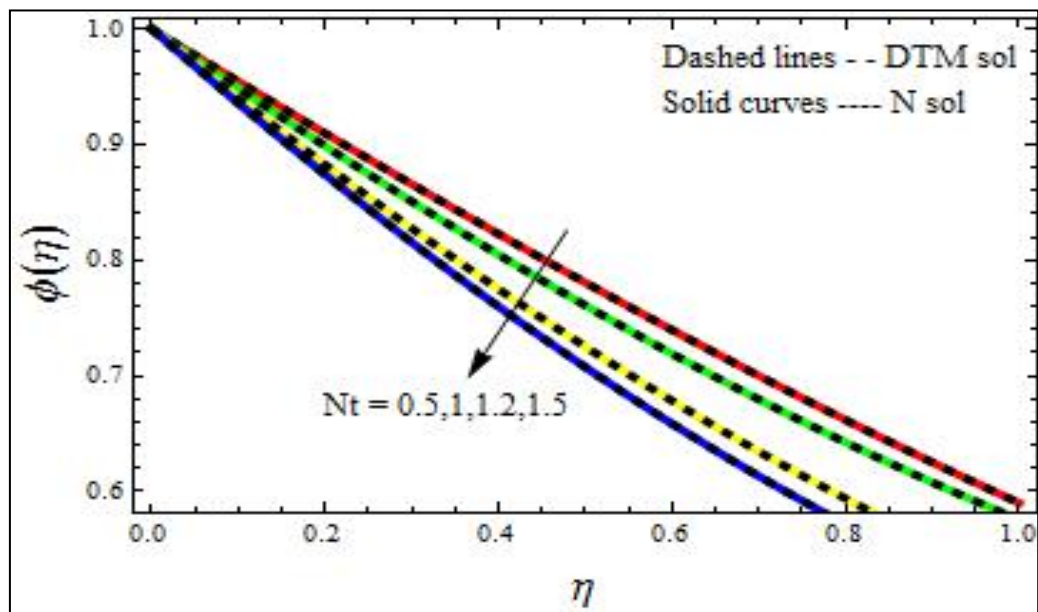


Figure 6.4.10. Concentration profile of the nanoparticles for the variations of $N_t = 0.5,1,1.2,1.5$.

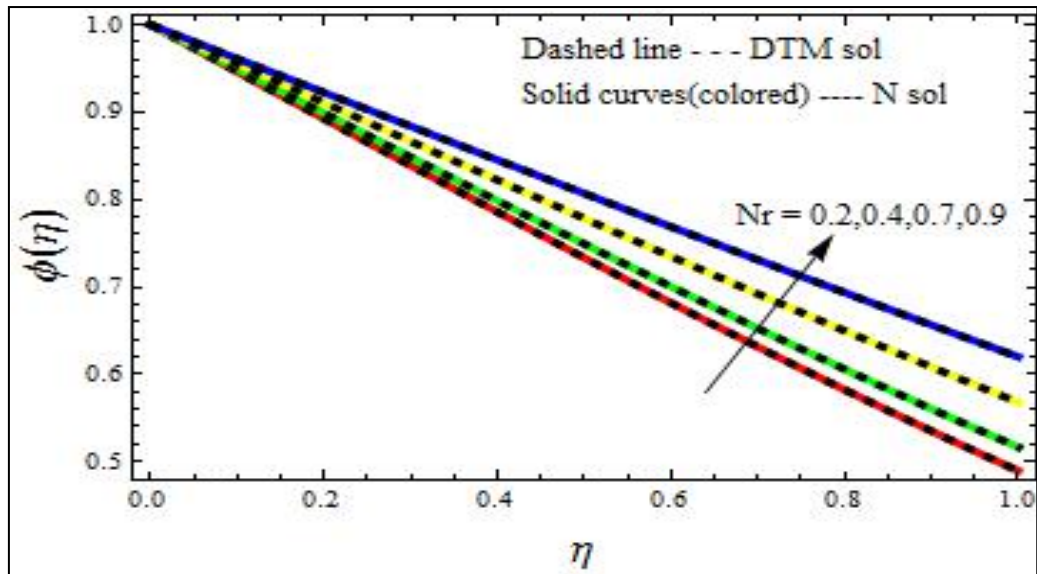


Figure 6.4.11 Concentration profile of the nanoparticles for the variations of $N_r = 0.2, 0.4, 0.7, 0.9$.

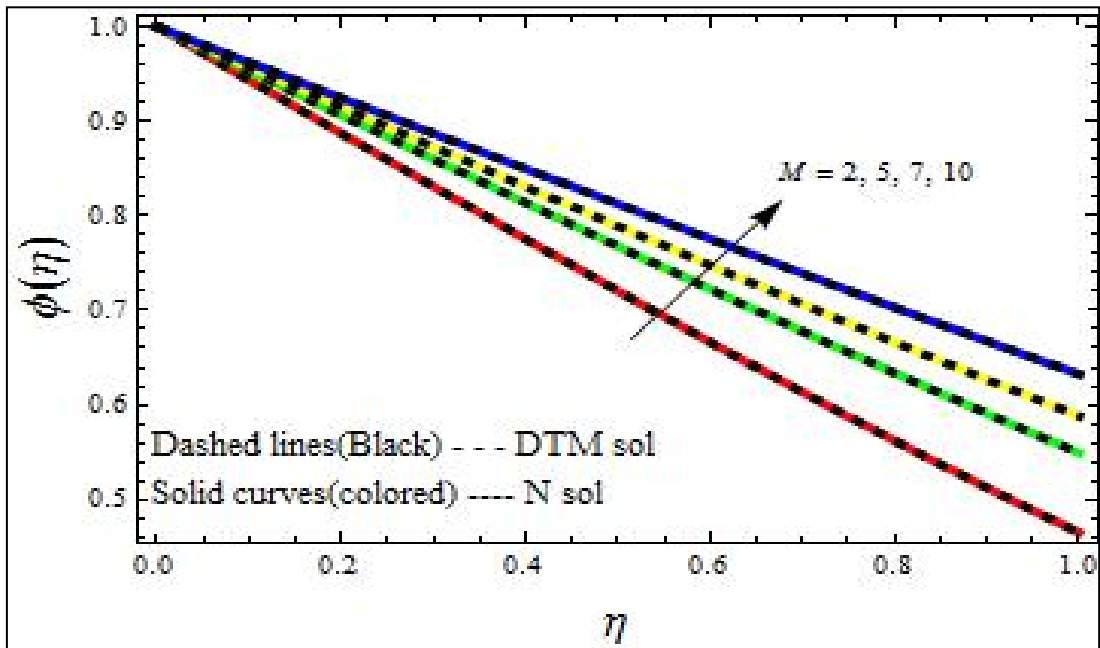


Figure 6.4.12 Concentration profile of the nanoparticles for the variations of $M = 2, 5, 7, 10$.

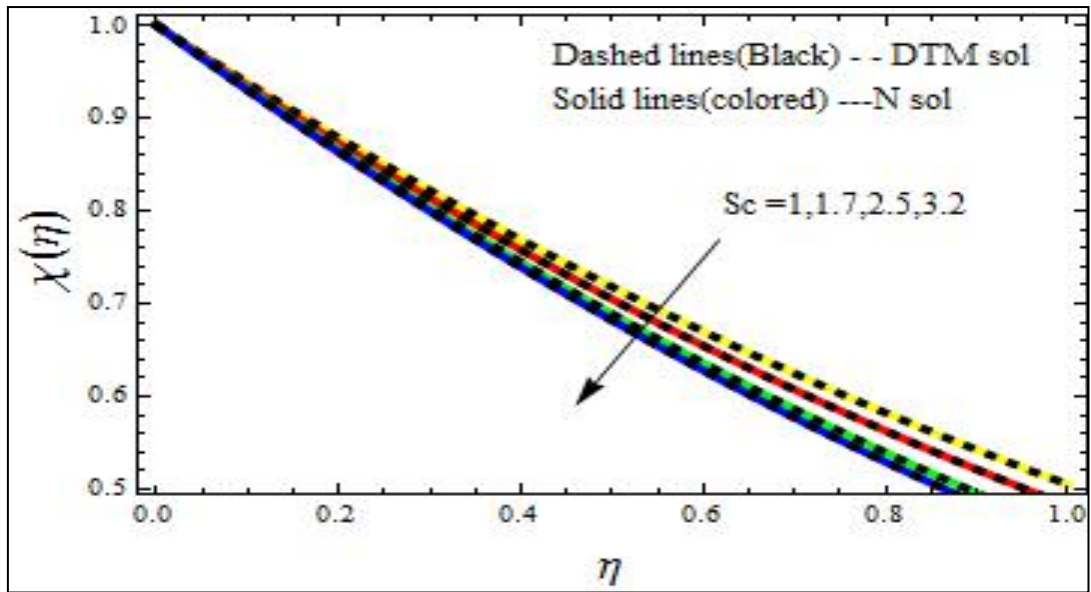


Figure 6.4.13 Concentration of microorganisms for the variations of $Sc = 1, 1.7, 2.5, 3.2$

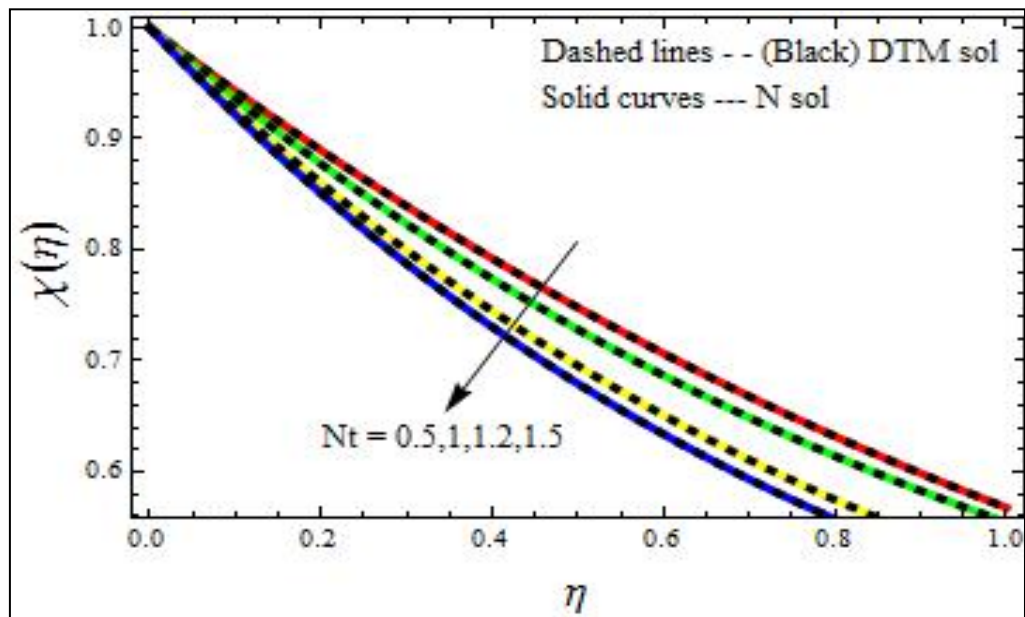


Figure 6.4.14 Density profile of microbes for the variations of $Nt = 0.5, 1, 1.2, 1.5$.

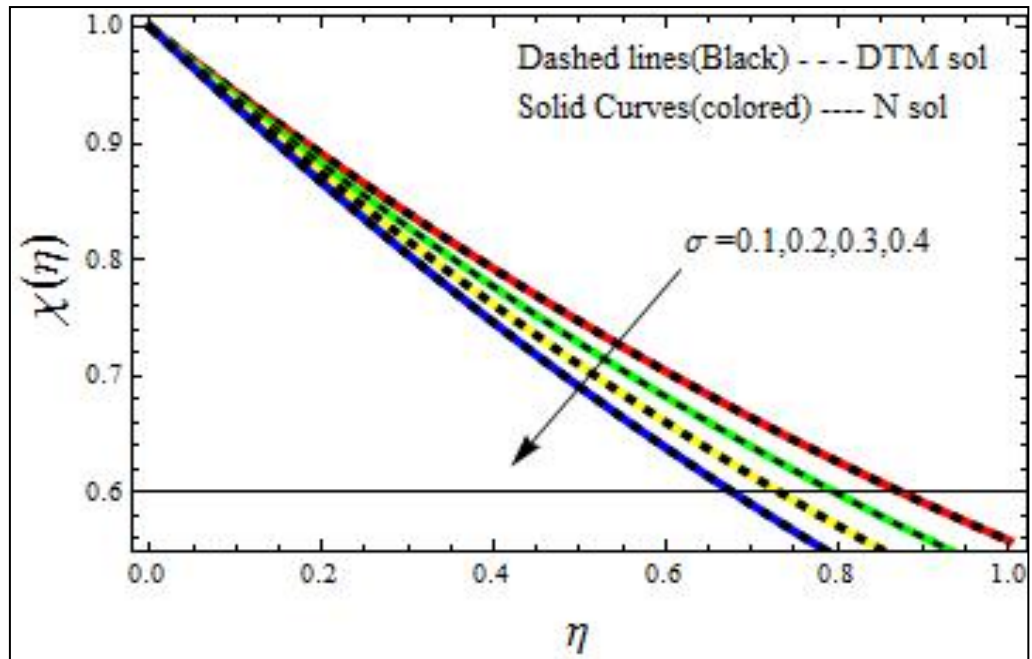


Figure 6.4.15 Concentration profile of microbes for the variations of $\sigma = 0.1, 0.2, 0.3, 0.4$

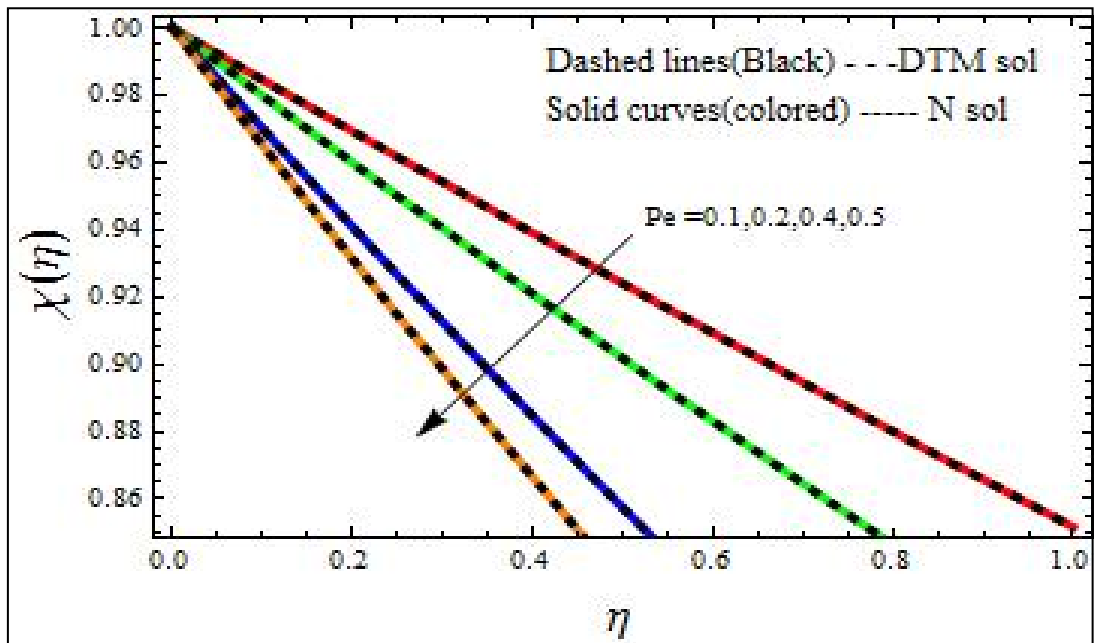


Figure 6.4.16 Density profile of microbes for the variations of $Pe = 0.1, 0.2, 0.4, 0.5$

6.5. Conclusion

The present research focuses on bioconvection in MHD boundary layer flow, energy transmission of nanofluids, and gyrotactic microbes across a linear stretched surface using semi-analytic and numerical methods. Via the Differential Transform technique, a Taylor's series solution is produced for the momentum, energy, nanofluid density, and microbes density equation, which is visually described using DTM solution and numerical solution. The answers are shown using graphs once non-dimensional parameters are modified. The velocity of the flow as well as the heat exchange is discussed in detail.

- The applied magnetic field normal to the stream causes the velocity of Casson fluid to rise versus Casson fluid parameter.
- The concentration of mobile microorganisms is reduced as the Schmidt number is increased.
- Because nanoparticles have different values of Brownian movement parameter (N_b) and thermophoresis parameter (N_t), the density of nanoliquids and heat conduction rises as N_b and N_t increase.
- Due to microorganism sensitivity and lowering of boundary layer thickness, the concentration of microorganisms decreases with increased magnitude of Peclet parameter.
- As the stretching parameter is increased, the friction near the sheet's surface decreases, and the temperature decreases.

CHAPTER 7

Casson Liquid Flow Comprising Microbes Across Porous Stretching Sheet With Viscous Dissipation

(The part of the chapter is published in springer journal)

7.1 INTRODUCTION

An analysis of bioconvection owing to Casson nanofluid and gyrotactic microbes across linear stretching surface through a porous media involving magnetic influence, and viscous dissipation is carried out in this chapter as a continuation of the previous work. Viscous dissipation is a term used in fluid dynamics to describe the elimination of changing velocity gradients caused by viscous strains. The transition of kinetic energy into internal energy of the fluid is a term used to describe this partially irreversible process. In geophysics, astrophysics, and many engineering and industrial operations, the magnetohydrodynamic boundary layer flow of an incompressible and electrically charged liquid occurs. The MHD heat and mass transmission in the boundary layer caused by a moving surface in a fluid has a wide range of applications in chemical engineering, electronics, meteorology, and metallurgy, among others. In the engineering and biotechnological industries, studies on the bioconvection flows produced by the mixed buoyancy impacts of nanoliquids and microbes under the sway of porous media have been important. Many Scholars have investigated the effect of various parameters on the heat exchange in the stream of non-Newtonian liquids. Partha et al. [119] investigated mixed convection flow and heat transfer from an exponentially expanding vertical surface in a quiescent liquid. They discovered that the temperature of the wall and the stretching velocity can have a distinct exponential form. In both helping and opposing flow scenarios, the effects of buoyancy and viscous dissipation on convective transport in the boundary layer region were investigated. Abel et al. [96] investigated viscoelastic fluid flow and heat transmission near a stretched sheet with varying viscosity. Makinde and Khan [162], Khan et al. [163], and Das et al. [48] evaluated the impact of bioconvection parameters on the dimensionless momentum, energy, density of nanoparticle, and motile microbes, as well as impact of various parameters on the molten stream. MHD

nanofluid bioconvection caused by gyrotactic microbes across a convectively heated extended surface, as well as a vertical sheet with Navier slip and chemical reaction in a pervious medium. Mahanta and Shaw [102] looked at three-dimensional Casson fluid flow near a stretching sheet in porous medium. Hossein Zadeh et al. [70] studied the impacts of viscous dissipation and magnetic field in the cross-fluid flow of gyrotactic microbes and nanoparticles across a horizontal cylinder on momentum, energy, and concentration profiles is carried out.

The current chapter examines the effect of viscous dissipation in bioconvection generated by nanofluid and gyrotactic microorganisms travelling through porous media above the stretched sheet in the MHD boundary region with Oberbeck-Boussinesq approximations. Brownian motion and thermophoresis were also studied to see how they influenced the nanofluid and heat transport. Under the influence of a magnetic field, a non-Newtonian fluid containing gyrotactic microorganisms is injected through porous media near the linear stretching surface.

7.2 MATHEMATICAL FORMULATION

Consider a non-Newtonian fluid with gyrotactic microorganisms that is permitted to flow through porous media along the x-axis above the linear stretching sheet. The magnetic field is applied evenly normal to the surface of the border zone, ignoring the influence of the induced magnetic field. Microorganisms are thought to be alive since the fluid is water-based, and nanoparticles have no influence on their activity. The bioconvection volatility caused by bacteria and nanoparticles is avoided by diluting the fluid. We may derive the following equations using these assumptions.

The governing equations are

$$\frac{\partial u}{\partial x} + \frac{\partial v}{\partial y} = 0, \quad (7.2.1)$$

$$u \frac{\partial u}{\partial x} + v \frac{\partial u}{\partial y} = \nu \left(1 + \frac{1}{\beta} \right) \frac{\partial^2 u}{\partial y^2} - \left(\frac{\sigma B_0^2}{\rho} + \frac{\vartheta}{K} \right) u + \left(\frac{1 - C_\infty}{\rho_f} \right) \rho_\infty g \alpha (T - T_\infty) - \left(\frac{\rho_p - \rho_\infty}{\rho_f} \right) g (C - C_\infty) - \left(\frac{\rho_m - \rho_f}{\rho_f} \right) g \gamma (N - N_\infty), \quad (7.2.2)$$

$$u \frac{\partial T}{\partial x} + v \frac{\partial T}{\partial y} = \left(\frac{K}{\rho c_p} \right) \frac{\partial^2 T}{\partial y^2} + \tau \left(D_B \frac{\partial C}{\partial y} \frac{\partial T}{\partial y} + \frac{D_T}{T_\infty} \left(\frac{\partial T}{\partial y} \right)^2 \right) + \left(\frac{\vartheta}{c_p} \right) \left(\frac{\partial u}{\partial y} \right)^2, \quad (7.2.3)$$

$$u \frac{\partial C}{\partial x} + v \frac{\partial C}{\partial y} = D_B \frac{\partial^2 C}{\partial y^2} + \left(\frac{D_T}{T_\infty} \right) \frac{\partial^2 T}{\partial y^2}, \quad (7.2.4)$$

$$u \frac{\partial N}{\partial x} + v \frac{\partial N}{\partial y} + \frac{bW_c}{c_w - c_\infty} \left(\frac{\partial}{\partial y} (NC_y) \right) = D_m \frac{\partial^2 N}{\partial y^2}, \quad (7.2.5)$$

where ρ is the Casson fluid density, γ average volume of microorganisms, D_B is Brownian diffusion coefficient, D_T is thermophoresis diffusion coefficient, and The following are the flow and heat flow boundary conditions:

$$\begin{aligned} v = 0, u = a_0 x, T = T_w, C = C_w, N = N_w \quad \text{as } y \rightarrow 0, \\ u \rightarrow 0, T \rightarrow T_\infty, C = C_\infty, n \rightarrow n_\infty \quad \text{as } y \rightarrow \infty, \end{aligned} \quad (7.2.6)$$

Where a_0 represents the rate of stretching. Incorporating the similarity transformation into the governing equations

$$\eta = \frac{y}{x} Ra_x^{1/4} f(\eta), \psi = m Ra_x^{1/4} f(\eta), \theta(\eta) = \frac{T - T_\infty}{T_w - T_\infty}, \phi(\eta) = \frac{C - C_\infty}{C_w - C_\infty},$$

$$\chi(\eta) = \frac{N - N_\infty}{N_w - N_\infty}, \quad Ra_x = \frac{(1 - C_\infty) \alpha g \Delta T_f}{m \nu} x^3,$$

The following coupled nonlinear ordinary differential equations were found.

$$(1 + 1/\beta) f_{\eta^3} - (1/2 \mathbf{P}_r) f_{\eta^2} + (3/4 \mathbf{P}_r) f f_{\eta^2} - (M + K_p) f_{\eta} + \theta - N_r \phi - R_b \chi = 0. \quad (7.2.7)$$

$$\theta_{\eta^2} + \left(\frac{3}{4} \right) f \theta_{\eta} + \mathbf{N}_b \theta_{\eta} \phi_{\eta} + \mathbf{N}_t \theta_{\eta}^2 + \mathbf{P}_r \mathbf{E}_c (f_{\eta^2})^2 = 0, \quad (7.2.8)$$

$$\phi_{\eta^2} + \left(\frac{3}{4} \right) Le f \phi_{\eta} + \left(\frac{\mathbf{N}_t}{\mathbf{N}_b} \right) \theta_{\eta^2} = 0. \quad (7.2.9)$$

$$\chi_{\eta^2} + (3/4) S_c f \chi_{\eta} - P_e \{ \phi_{\eta} \chi_{\eta} + \phi_{\eta^2} (\chi + \sigma) \} = 0, \quad (7.2.10)$$

The dimensionless boundary conditions that go with it are

$$\left. \begin{aligned} f(0) = 0, f_{\eta}(0) = \lambda, \theta(0) = 1, \phi(0) = 1, \chi(0) = 1 \quad \text{as } \eta \rightarrow 0 \\ f_{\eta}(\infty) = 0, \theta(\infty) = 0, \phi(\infty) = 0, \chi(\infty) = 0 \quad \text{as } \eta \rightarrow \infty \end{aligned} \right\}, \quad (7.2.11)$$

The dimensionless parameters used in (9–12) are defined as follows:

$$M = \frac{\sigma B_0^2 x^2}{\rho \nu Ra_x^{1/2}}, \mathbf{N}_r = \frac{(\rho_p - \rho_\infty) \Delta C_w}{\rho_f (1 - c_\infty) \alpha \Delta T_f}, \mathbf{R}_b = \frac{\gamma \Delta N_w \Delta \rho}{\rho_f \alpha (1 - C_\infty) \Delta T_w}, \mathbf{N}_t = \frac{\tau D_T (T_w - T_\infty)}{m T_\infty},$$

$$\mathbf{N}_b = \frac{\tau D_B (C_w - C_\infty)}{m}, Le = \frac{m}{D_B}, S_c = \frac{m}{D_m}, P_e = \frac{b W_c}{(C_w - C_\infty)}, \sigma = \frac{N_\infty}{(N_w - N_\infty)}, \lambda = \frac{a x^2}{m Ra_x^{1/2}}.$$

$$P_r = \nu/m, \kappa_p = \frac{1}{Ra_x^{1/2} Da} \quad E_c = \frac{m^2 Ra_x}{x^2 C_p D T_f}$$

Where κ_p is permeability constant, E_c is the Eckert number.

7.3 DTM SOLUTION

The equations (7.2.7) - (7.2.11) can be transformed in the following Differential forms:

$$\begin{aligned} \left(1 + \frac{1}{\beta}\right) (r+1)(r+2)(r+3)F[r+3] \\ = (M + \kappa_p)(r+1)F[r+1] - \theta[r] + N_r \phi[r] \\ + R_b \chi[r] + \frac{1}{2P_r} \sum_{m=0}^r (r-m+1) F[r-m+1](m+1)F[m+1] - \\ -(3/4 P_r) \sum_{m=0}^r F[r-m] (m+1)(m+2)F[m+2], \end{aligned}$$

$$\text{Where } F[0] = 0, F[1] = 0, F[2] = a_1, \quad (7.3.1)$$

$$\begin{aligned} (r+1)(r+2)\theta[r+2] = \left(-\frac{3}{4}\right) \sum_{m=0}^r F[r-m](m+1)\theta[m+1] - \\ - N_b \sum_{m=0}^r (r-m+1)\theta[r-m+1](m+1)\phi[m+1] - \\ - N_t \sum_{m=0}^r (r-m+1)\theta[r-m+1](m+1)\theta[m+1] - \\ - (P_r E_c) \sum_{m=0}^r (r-m+1)\theta[r-m+1](m+1)(m+2)\theta[m+2] \end{aligned}$$

$$\text{where } \theta[0] = 1, \theta[1] = a_2. \quad (7.3.2)$$

$$\begin{aligned} (r+1)(r+2)\phi[r+2] = (-3/4)Le \sum_{m=0}^r F[r-m](m+1)\phi[m+1] - \\ - \frac{N_t}{N_b} \sum_{m=0}^r (r+1)(r+2)\theta[r+2], \end{aligned}$$

$$\text{Where } \phi[0] = 1, \phi[1] = a_3, \quad (7.3.3)$$

$$\begin{aligned} (r+1)(r+2)\chi[r+2] = P_e \sum_{m=0}^r (r-m+1)\phi[r-m+1](m+1)\chi[m+1] + \\ + P_e \sum_{m=0}^r \chi[r-m](m+1)(m+2)\phi[m+2] + P_e \sigma (r+1)(r+2)\phi[r+2] - \\ - (3/4)S_c \sum_{m=0}^r F[r-m](m+1)\chi[m+1], \end{aligned}$$

$$\chi[0] = 1, \chi[1] = a_4, \quad (7.3.4)$$

$F[r]$, $\theta[r]$, $\phi[r]$ and $\chi[r]$ are the differential transforms of $f(\eta)$, $\theta(\eta)$, $\phi(\eta)$ and $\chi(\eta)$, while a_1, a_2, a_3 and a_4 are the assumed constants, which may be found using equations (6.3.1) - (6.3.4) and the boundary conditions. We get the following results for $r = 0, 1, 2, 3, \dots$

$$F[3] = \frac{a_1^2 P_r}{12\left(1+\frac{1}{\beta}\right)} + \frac{a_1\left(M-\frac{1}{Da\sqrt{Ra}}\right)}{6\left(1+\frac{1}{\beta}\right)} + \frac{-1+N_r+R_b}{6\left(1+\frac{1}{\beta}\right)},$$

$$\theta[2] = -\frac{1}{2}a_3a_4N_b - \frac{a_3^2N_t}{2} - \frac{1}{2}a_1^2E_cP_r,$$

$$\phi[2] = -\frac{N_t\left(-\frac{1}{2}a_3a_4N_b - \frac{a_3^2N_t}{2} - \frac{1}{2}a_1^2E_cP_r\right)}{N_b},$$

$$\chi[2] = \frac{a_4a_5P_e}{2} - \frac{N_tP_e\left(-\frac{1}{2}a_3a_4N_b - \frac{a_3^2N_t}{2} - \frac{1}{2}a_1^2E_cP_r\right)}{N_b} - \frac{N_tP_e\left(-\frac{1}{2}a_3a_4N_b - \frac{a_3^2N_t}{2} - \frac{1}{2}a_1^2E_cP_r\right)\sigma}{N_b},$$

we can find $F[4]$, $\theta[3]$, $\phi[3]$, $\chi[2]$, $\chi[3]$ and so on. Taking $P_r = 6.2$, $\beta = 1$, $M = 5$, $N_r = 0.5$, $R_b = 0.1$, $N_t = 0.1$, $N_b = 0.1$, $Le = 10$, $S_c = 0.1$, $P_e = 1$, $\sigma = 0.2$, $Ra = 0.5$, $Da = 0.5$ and solving for a_1, a_2, a_3, a_4 using the boundary conditions and the Pade approximation for $\lim_{\eta \rightarrow \infty} f'(\eta) = 0$, we obtain $a_1 = 0.130491$, $a_2 = 0.105687$, $a_3 = 4.05355$, $a_4 = 6.91778$, $a_5 = -0.579615$ and the Taylor's series solutions for the equations (7.2.7)-(7.2.10) are

$$f(\eta) = 0.130491\eta + 0.105687\eta^2 + 0.0254366\eta^3 + 0.00931264\eta^4 + 0.0315593\eta^5 - 0.00705885\eta^6 + 0.0000565214\eta^7 - 0.0010699\eta^8 - 0.000362508\eta^9 - 0.000426626\eta^{10} - 0.000221054\eta^{11} - \dots$$

$$\theta(\eta) = 1 + 4.05355\eta - 2.22364\eta^2 + 0.747091\eta^3 - 0.0810705\eta^4 + 0.0117574\eta^5 - 0.0306772\eta^6 + 0.00773456\eta^7 + 0.0069833\eta^8 - 0.00369728\eta^9 - 0.00112102\eta^{10} + 0.000891603\eta^{11} + \dots$$

$$\phi(\eta) = 1 + 6.91778\eta + 2.22364\eta^2 - 1.87547\eta^3 - 0.738584\eta^4 + 0.0213219\eta^5 + 0.231329\eta^6 + 0.0247125\eta^7 - 0.0279245\eta^8 + 0.0103749\eta^9 + 0.00405778\eta^{10} - 0.00242809\eta^{11} - \dots$$

$$\chi(\eta) = 1 - 0.579615\eta + 0.663541\eta^2 - 1.578781\eta^3 - 2.064390\eta^4 - 4.637221\eta^5 - 5.451773\eta^6 - 6.076239\eta^7 - 4.203908\eta^8 - 1.521497\eta^9 + 1.73707\eta^{10} + 3.626755\eta^{11} + \dots$$

7.4 RESULT AND DISCUSSION:

Bioconvection flow of Casson fluid nano particles and gyrotactic microorganisms across porous media under the effect of a uniformly applied magnetic field normal to the surface is discussed, as well as heat exchange analyses. For all of the governing equations, the answer is expressed in Taylor's series using DTM. Through graphs, it is aimed to investigate the influence of non-dimensional parameters on fluid velocity, temperature, nano particle concentration, and gyrotactic microorganisms.

Velocity profile

Figure 7.4.1-7.4.4 depicts the Casson fluid's velocity curve for a variety of parameter values. For increasing values of Casson fluid parameters, the velocity of the Casson fluid flow rises due to the applied magnetic field normal to the surface in Figure 7.4.1. The bioconvection effect of microorganisms and nanofluids, along with the separation of boundary layers generated by a magnetic field, generates growth in liquid speed. The rapidity of the molten increases with increasing values of the viscous dissipation parameter, as seen in Figure 7.4.2. The reason for this is that when the Eckert number increases, the fluid's viscosity improves, affecting the fluid's motion. Figure 7.4.3 demonstrates how the velocity decreases as the magnetic parameter increases. This is because the applied magnetic field is perpendicular to the fluid flow, resulting in an increase in the force required to fight the flow. Figure 7.4.4 shows the rise in velocity as the amount of Nb increases.

Temperature profile

Figures 7.4.5 to 7.4.8 show temperature profiles for various non-dimensional parameter values, and we discovered that the temperature rises with increasing Casson fluid parameter, viscous dissipation parameter, Brownian motion parameter, and thermophoresis parameter values. In Figure 7.4.5, increasing Casson fluid parameter values produces a rise in the temperature profile because the fluid velocity ascends with increasing Casson fluid parameter values. Figure 7.4.6 demonstrates how the

temperature profile improves when the viscous dissipation parameter is increased (E_c), Figures 7.4.7 and 7.4.8 depict the effects of N_b and N_t . Effects of N_b and N_t on fluid and heat flow with increasing N_b and N_t values, the temperature profile rises. The reason for this is that nanoparticles have varying N_b and N_t values.

Concentration of nanoparticles and microorganisms

Figures 7.4.9 to 7.4.13 show the concentration profiles of Casson nanoparticles and microorganisms. Figure 7.4.9 shows that when the value of Casson fluid parameters increases, the concentration of Casson nanofluid particles increases. The concentration of nanofluid particles drops when the Eckert number is raised, as seen in Figure 7.4.10. The concentration of nanofluid particles rises as the magnetic parameter value is increased, as seen in Figure 7.4.11. The relationship between nanofluid particle concentration and Brownian motion parameter is shown in Figure 7.4.12. The thermophoresis parameter and the concentration of microorganisms are shown in Figure 7.4.14. For rising levels of N_b , N_t the graph reveals a drop in nanofluid particle concentration and microorganism profiles. The profiles' results are attributable to the Brownian parameter's dependence on decreased thermal enhancement and concentration on temperature field. The concentration of nanoparticles reduces as the Lewis number increases, as seen in Figure 7.4.13. The reason for this is that when the Lewis number rises, heat in the fluid diffuses more quickly, causing the boundary layer to shrink and the concentration of nanoparticles to decrease. The concentration of microbes diminishes as the P_e values rise, as seen in Figure 7.4.15. The boundary layer viscosity reduces while the value of Peclet number rises. As a result, the density of microorganisms in the environment will decrease.

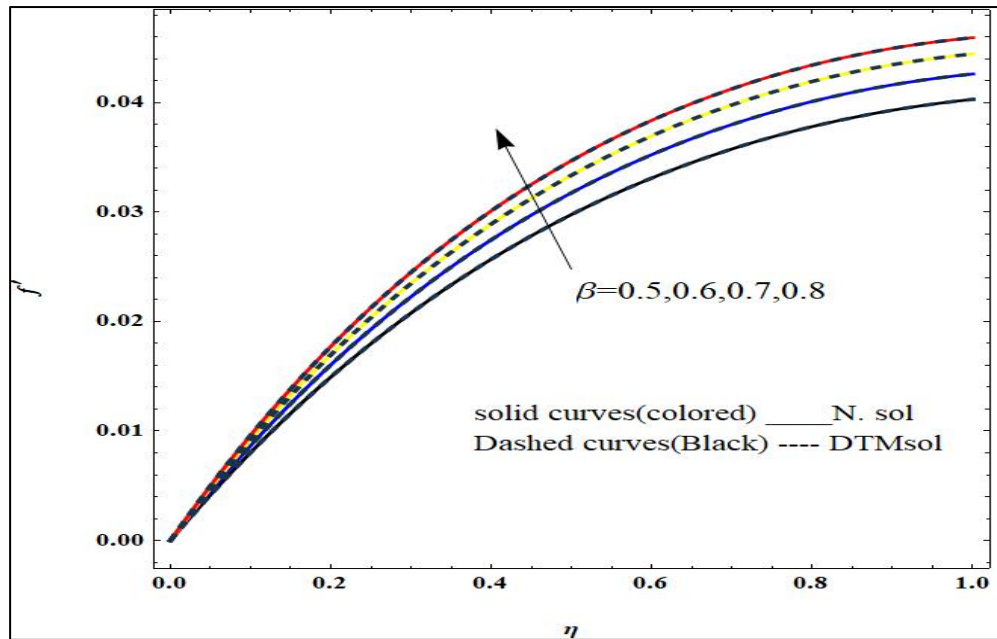


Figure 7.4.1 Velocity profile of the fluid for $\beta = 0.5, 0.6, 0.7, 0.8$

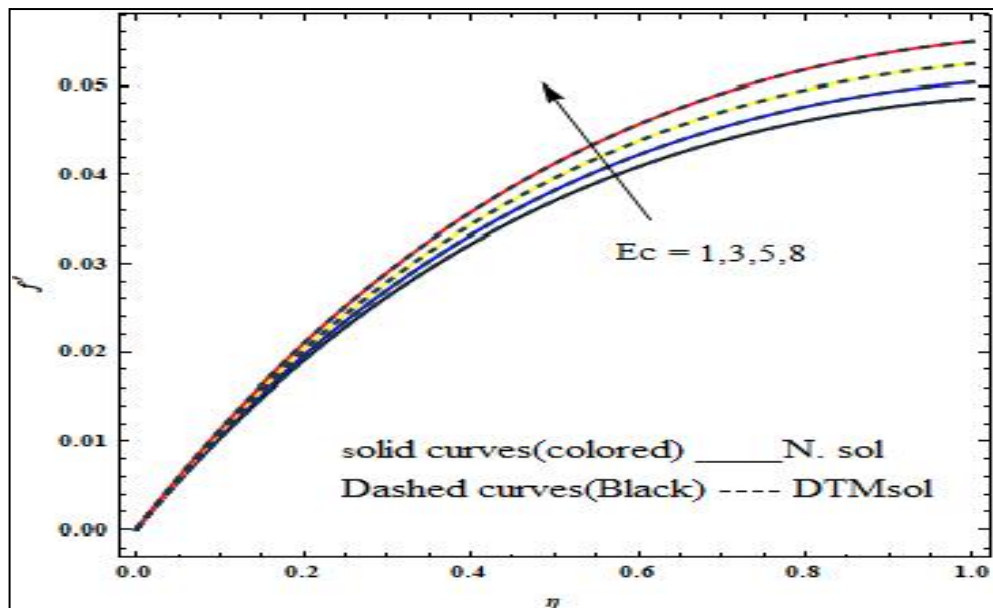


Figure 7.4.2 Velocity profile of the fluid for $E_c = 1, 3, 5, 8$.

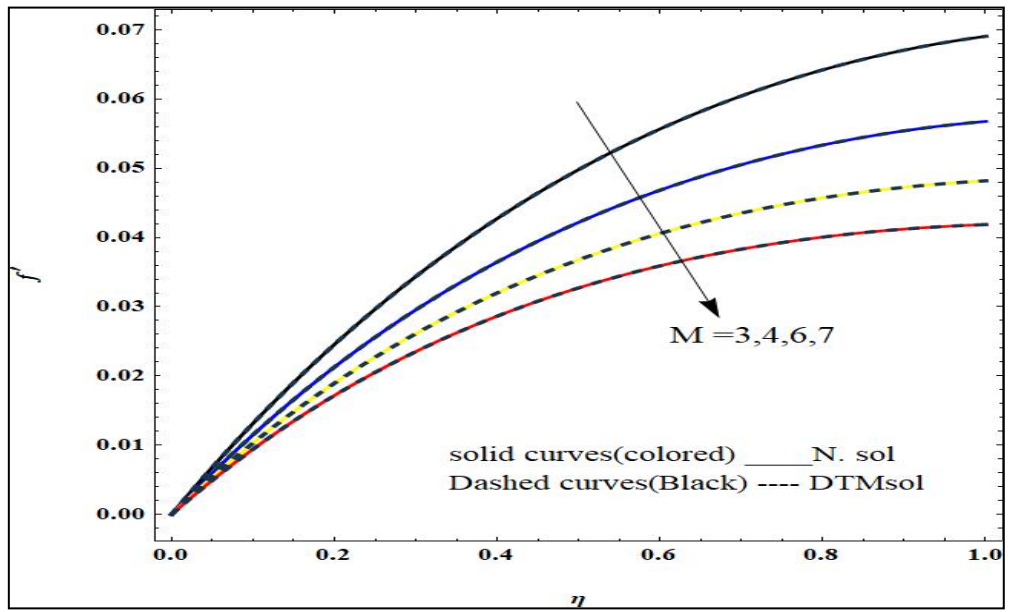


Figure 7.4.3 Velocity profile of the fluid for $M=3,4,6,7$

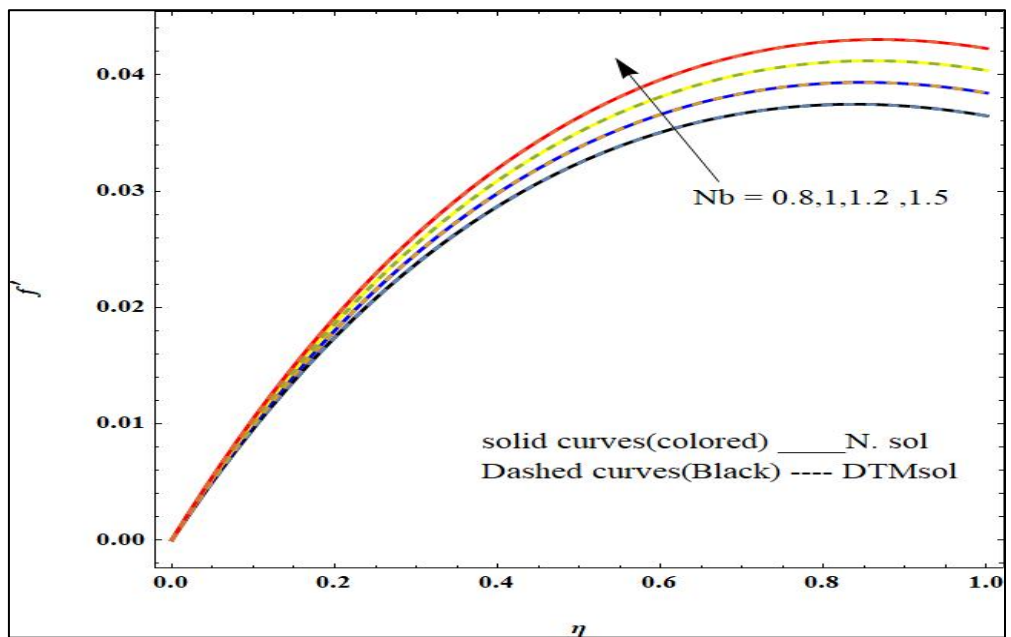


Figure 7.4.4 Velocity profile of the fluid for $N_b=0.8,1,1.2,1.5$

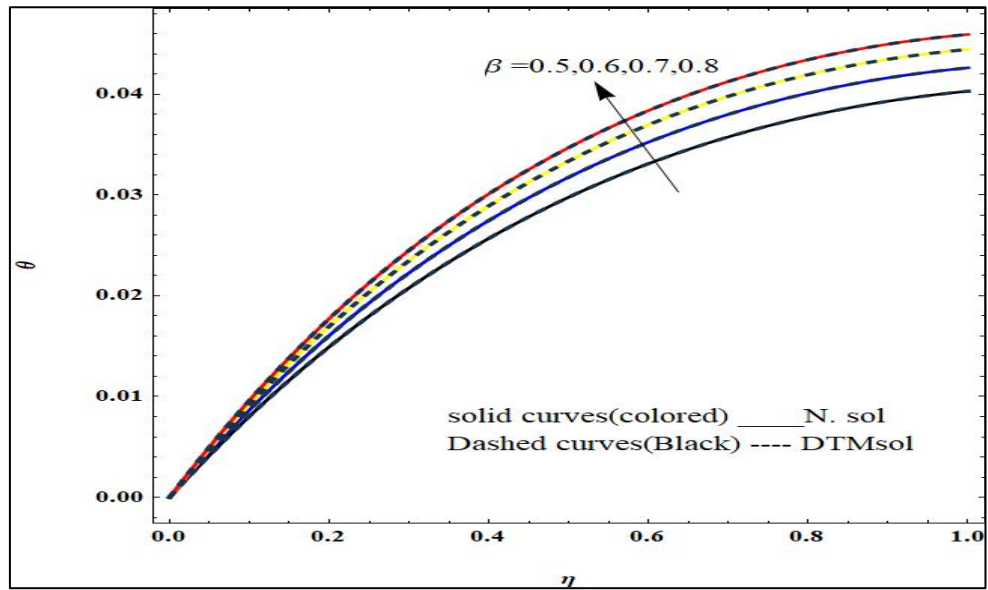


Figure 7.4.5 Temperature profile of the liquid for $\beta = 0.5, 0.6, 0.7, 0.8$

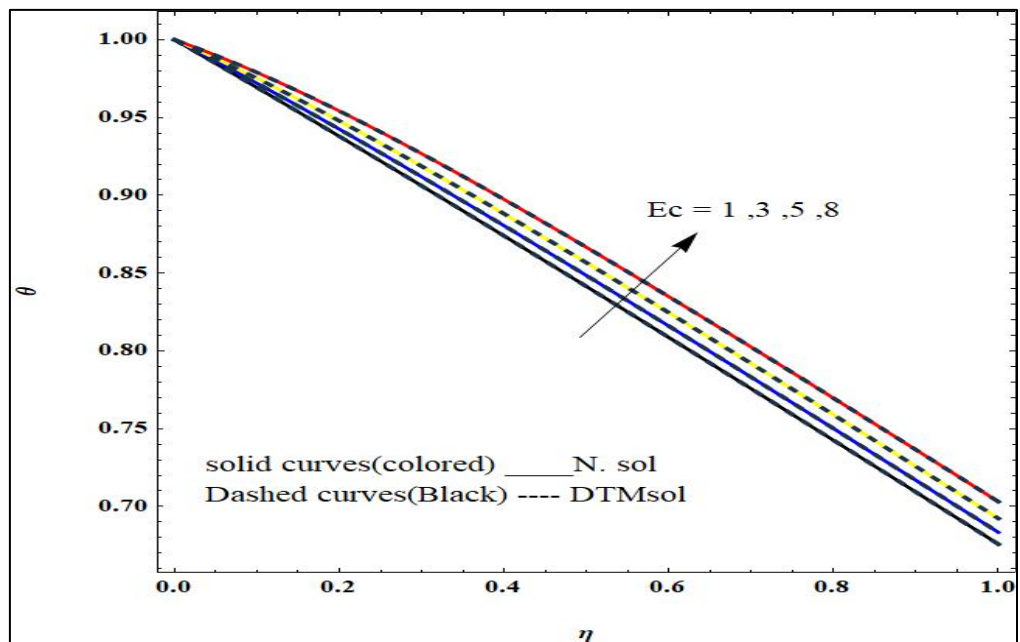


Figure 7.4.6 Temperature profile for $Ec = 1, 3, 5, 8$

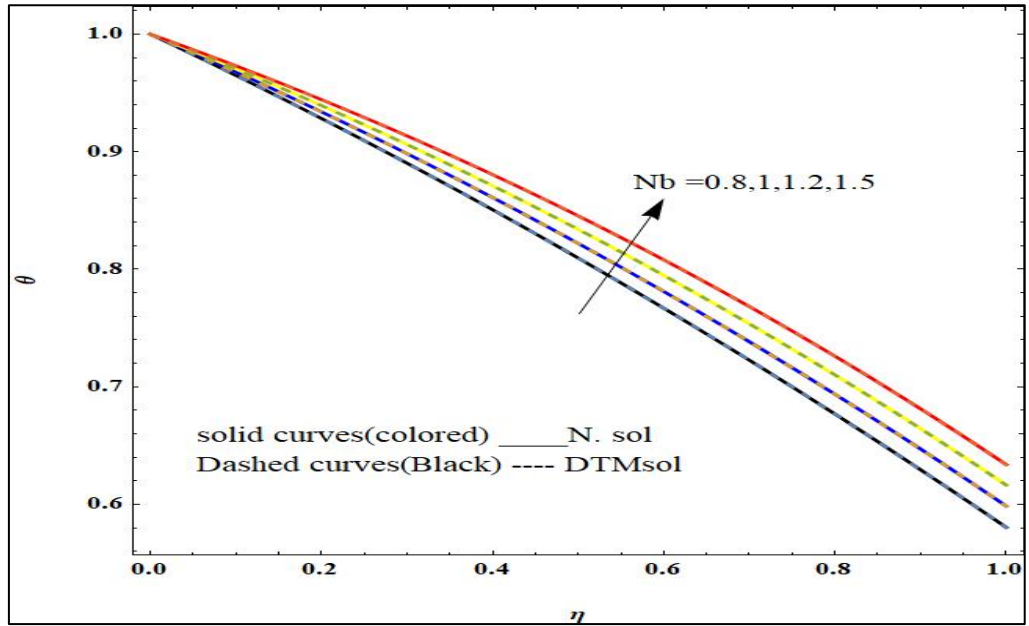


Figure 7.4.7 Temperature profile for $N_b=0.8,1,1.2,1.5$ and $N_t=0.1$

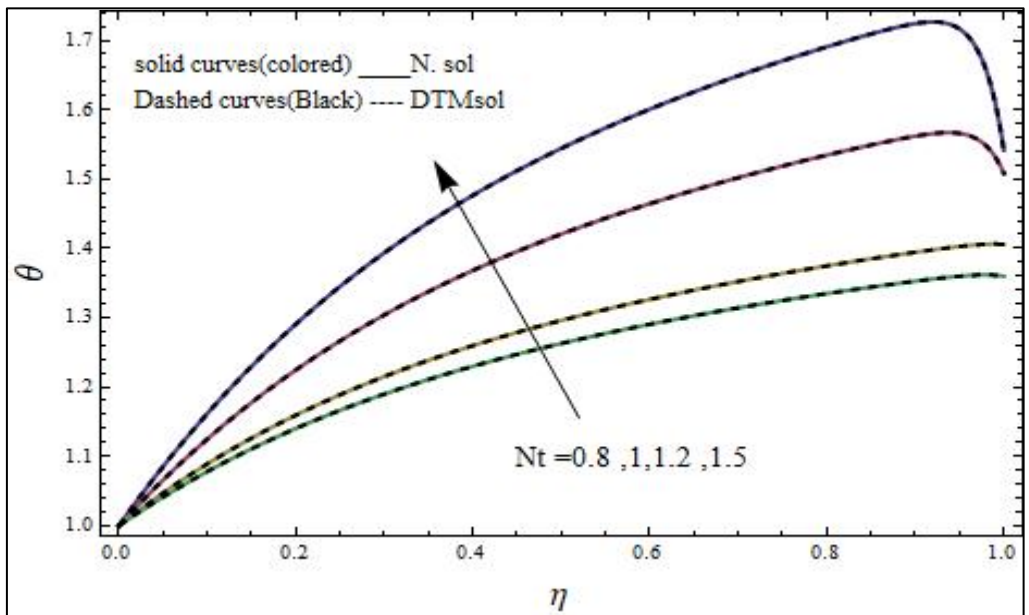


Figure 7.4.8 Temperature profile for $N_t=0.8,1,1.2,1.5$ and $N_b=0.1$

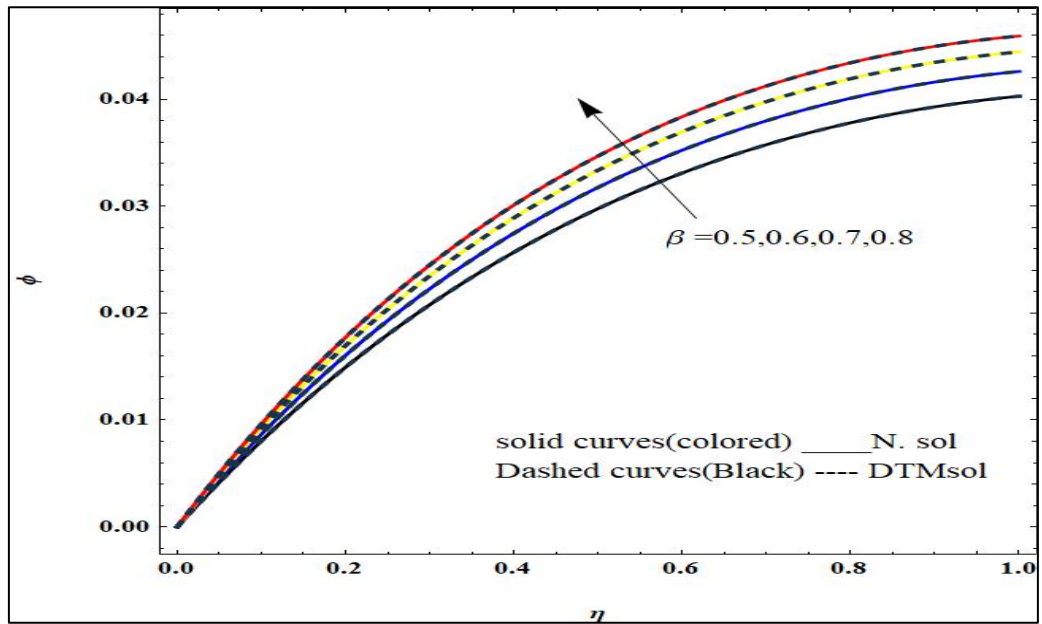


Figure 7.4.9 Concentration of nanoparticles for different values of Casson fluid parameter

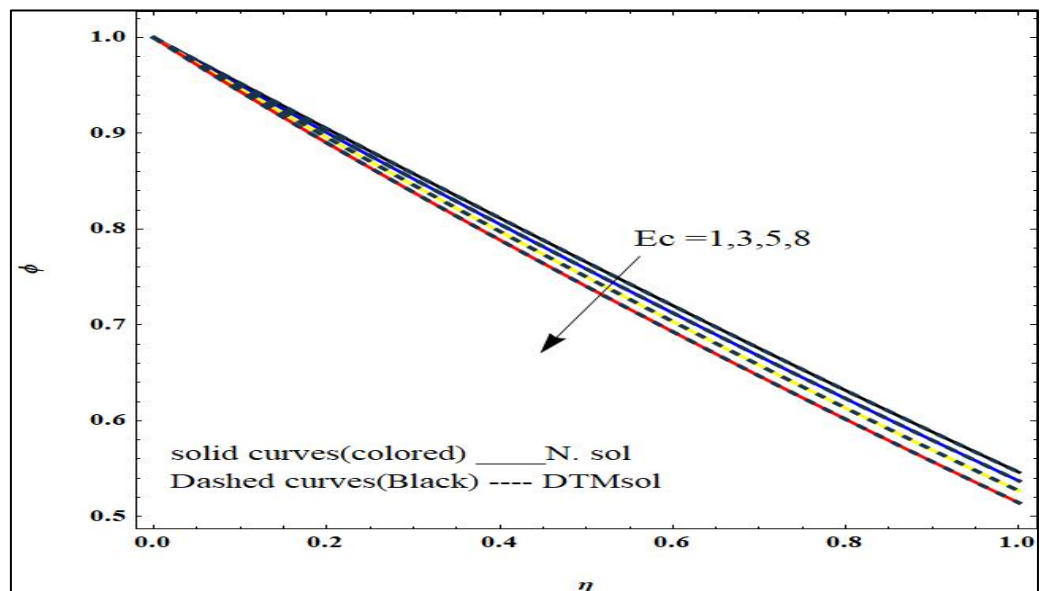


Figure 7.4.10 Concentration of nanoparticles for different values of viscous dissipation parameter.

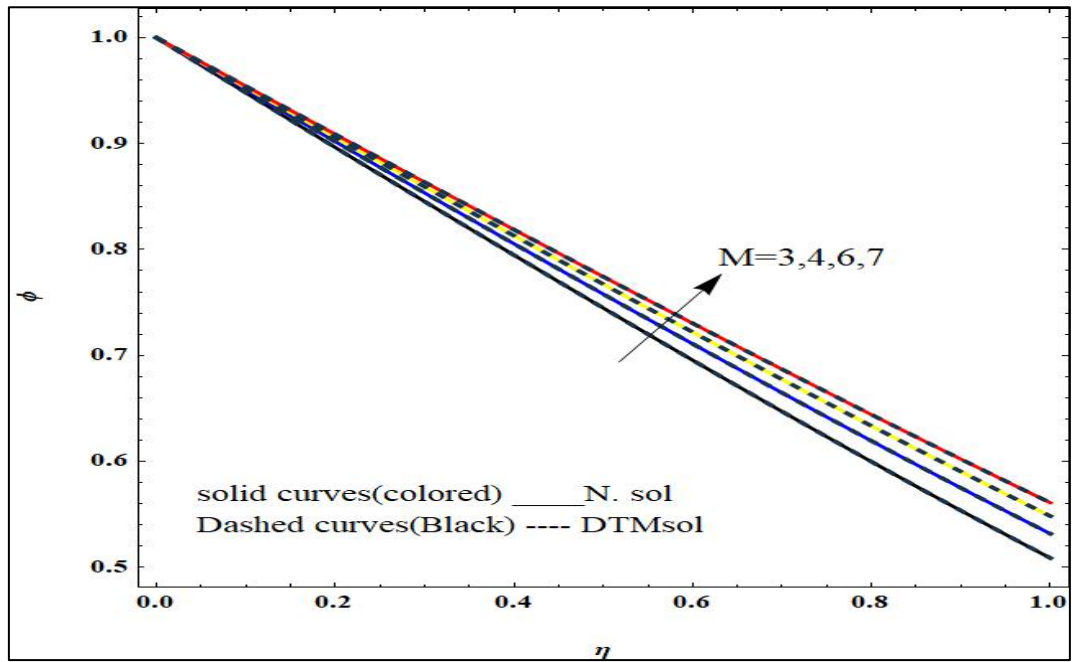


Figure 7.4.11 Concentration of Nano particles for $M=3,4,6,7$.

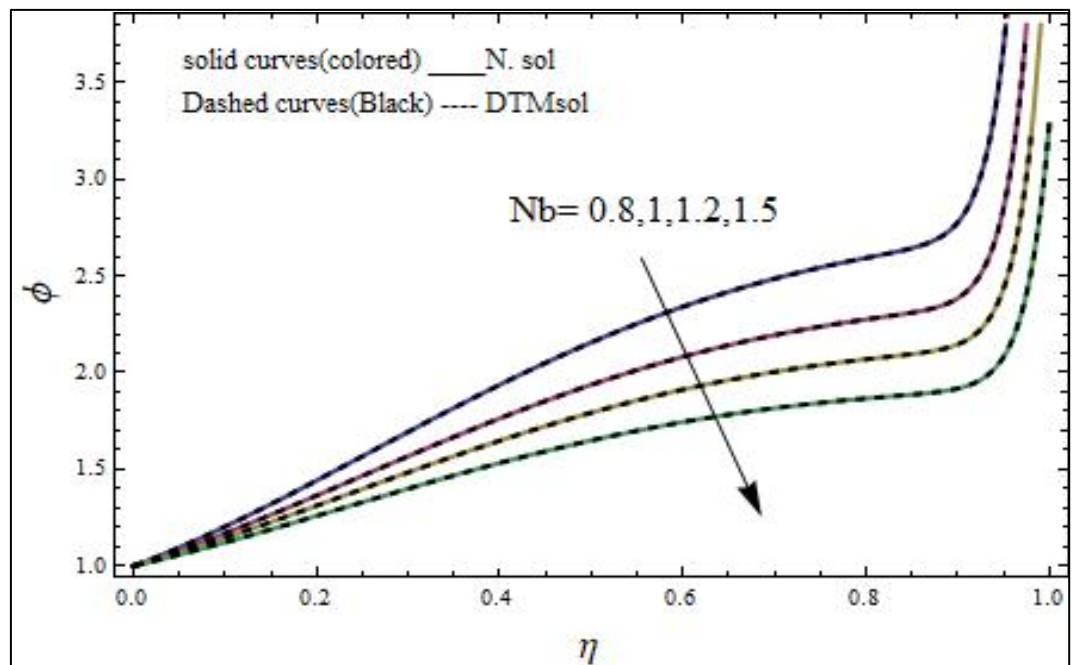


Figure 7.4.12 Concentration of nanofluid particles for $N_b=0.8,1,1.2,1.5$.

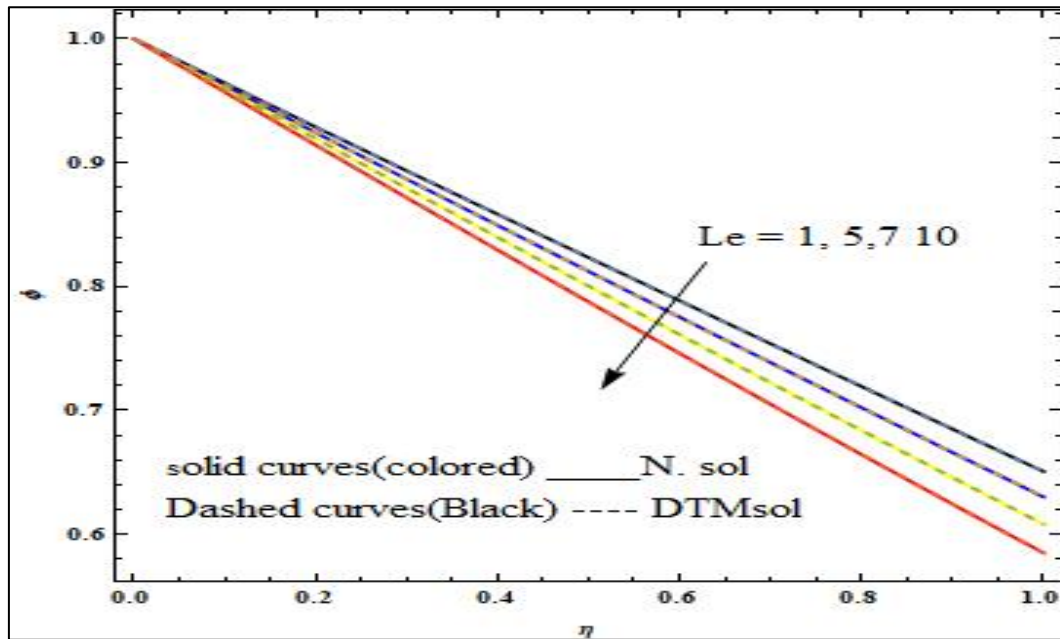


Figure 7.4.13 Concentration of nanofluid particles for $Le = 1, 5, 7, 10$

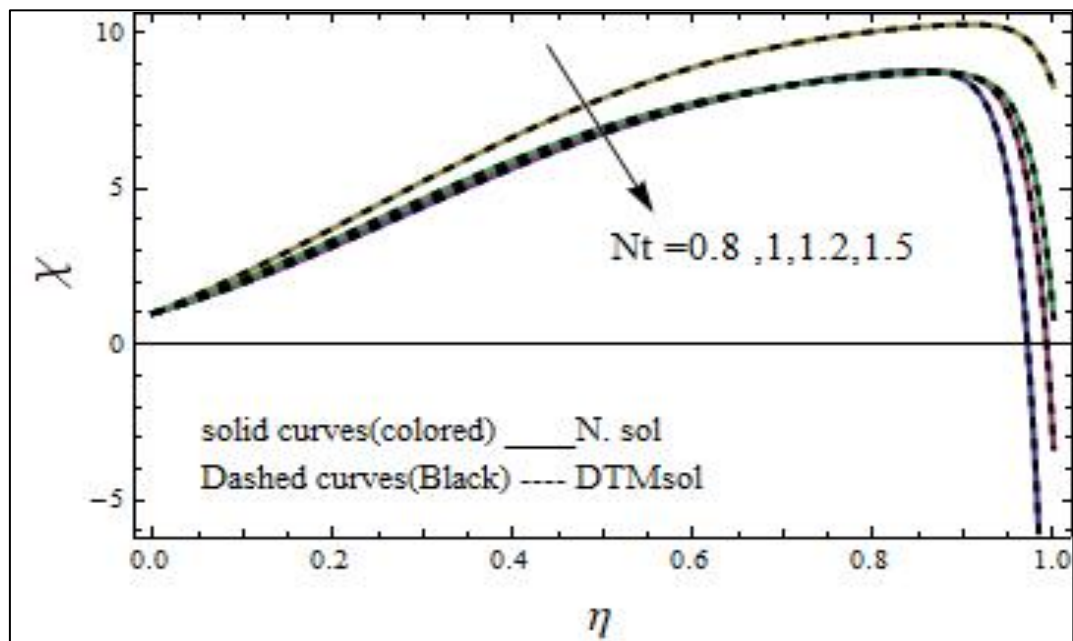


Figure 7.4.14 Concentration of microorganism for $N_t = 0.8, 1, 1.2, 1.5$ and $N_b = 0.1$

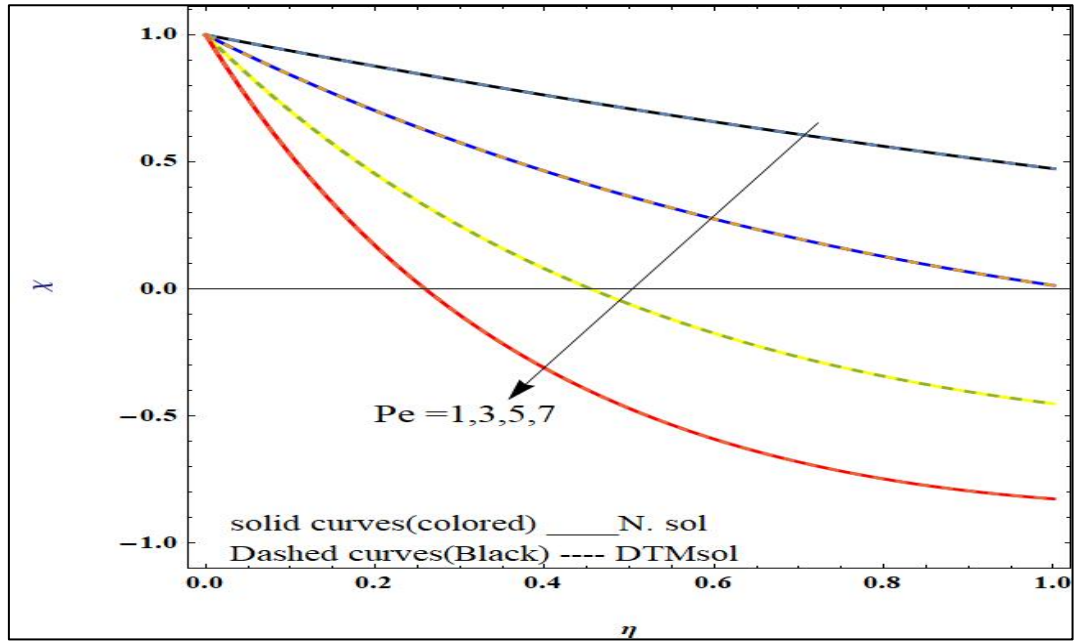


Figure 7.4.15 Concentration of microorganism for $P_e = 0.8, 1, 1.2, 1.5$

7.5 CONCLUSION

Our research focuses on the exact as well as the approximate solution of the governing equations of bioconvection of MHD boundary layer stream and heat transmission of Casson nanofluids and gyrotactic microorganisms via porous media across a linear stretching sheet. Using the Differential Transform technique, a Taylor's series solution for momentum, energy, nanofluid concentration equations, and gyrotactic microbe density equations is achieved and compared with numerical solutions through graphs. The velocity of the stream as well as the heat exchange are explained in detail.

- As the viscous dissipation parameter (E_c) is increased, the Casson fluid's velocity increases.
- Brownian movement, and thermophoresis constraint values in nanoparticles are different. As a result, the concentration of nanofluid and heat flow decreases as N_b and N_t values increase.
- As the Peclet number increases, the concentration of microorganisms drops due to the sensitivity of microorganisms and the weakening of the boundary layer thickness.
- As a result, for the ascending values of Lewis number, heat flow in the fluid gets diffused and hence there will be a fall in the concentration of nanoparticles near the thinned boundary layer region.

CHAPTER 8

Conclusion and Scope for Future Work

8.1 CONCLUSION

The objective of this research was intended to study, investigate and develop exact and numerical solutions for certain issues related to boundary layer theory in fluid dynamics, in particular the fluid flow in the presence of a magnetic field under various assumptions by considering the Casson fluid over the linear stretching sheet. Differential transformation method (DTM) and numerical method were used. Our method attacks non-linear problems in a manner as linear problems and overcomes the difficulty of linearization. DTM is reliable and powerful with promising results. The numerical code was adopted and implemented in Wolfram Mathematica. This study has been primarily concerned with analyzing flow and heat exchange phenomena in the Casson fluid near a stretching surface with or without viscous dissipation, and it has also been extended to the study of bioconvection in the fluid due to nanoparticles and microorganisms. Also, it offers extremely significant to the production of biotechnological goods as well as sheet extrusion.

Following are some of the important findings:

- The skin friction coefficient on the wall increases, while the temperature differential at the wall reduces as the Casson liquid parameter and Chandrasekhar number (Modified Magnetic parameter) expand. This is due to an induced magnetic field, which decreases the heat flow at the stream wall and slows the force applied to it. Furthermore, the Casson liquid parameter is more reactive under the influence of the magnetic domain. To reduce the thickness of the momentum boundary layer, Chandrasekhar number q is used. The results are consistent with Bhattacharya [80].
- The direction of heat transport can be determined by the magnitude of the temperature parameter λ_1 . We observed that increasing the radiation parameter, Brownian movement parameter, and thermophoresis parameter leads to greater temperatures, whereas decreasing the suction parameter and Prandtl

number leads to lower temperatures. The increase in temperature for the growth of the thermophoresis parameter (N_t). This is owing to the fact that each nano molecule has distinct thermophoresis parameter values, resulting in a decrease in the thickness of the thermal boundary layer at the wall, and hence an increase in temperature. The collision rate between nanoparticles increases as the value of (N_b) rises, contributing in the increase in heat generation. The findings of Chakraborty [156] and Nayak et al. [91] are supported by these findings.

- The concentration of nanoparticles falls when non-dimensional parameters such as the Lewis number (L_e), mass suction (s), and thermal radiation parameter (T_r) are changed. When L_e is raised, the concentration of nanoparticles volume falls. Nanoparticles with a low mass diffusivity have lower concentrations. These outcomes are in accord with the findings of Chakraborty [156], Shahid [149], Nayak et al. [91], Zadeh et al. [71],
- The density of microorganisms declines as the Schmidt number rises. The fluid's dynamic viscosity increases as the Schmidt number increases, while the density and mass diffusivity of the nanoparticles decrease, reducing the microbe concentration. The Casson liquids rapidity increases when the viscous dissipation parameter (E_c) is raised. As the P_e values increase, the concentration of microorganisms decreases. While the Peclet number increases, the boundary layer viscosity decreases. As a result, there will be fewer microbes in the environment. These findings are reliable with those of Nayak et.al [91] and Zadeh et.al [71].

8.2 Scope for future work

Addressing the inquiries brought up in this research has raised many new doubts, opening up extraordinary potential for future research that will have a substantial effect on the actual world. In the light of the limitations identified and the findings of the study, the following are recommended as future research work:

Our preliminary research indicates that the bioconvection study has a lot of potential. Bioconvection in non-Newtonian fluids containing various types of

microorganisms can be studied in the future using linear, Superlinear, nonlinear, and exponential stretching sheets with varied geometrical flow situations. It also aims to apply a variety of numerical or analytical approaches to handle nonlinear boundary value issues that arise.

BIBLIOGRAPHY

1. A Chakrabarti and A S Gupta, Hydromagnetic flow and heat transfer over a stretching sheet, 1979; Quarterly of Applied Mathematics.
2. A V Kuznetsov., 2011.Nanofluid bio-thermal convection: simultaneous effects of gyrotactic and oxytactic micro-organisms. Fluid dynamics research, volume 43, number 5. Res, 43 055505.
3. A. Aziz., W.A. Khan., I. Pop., 2012. Free convection boundary layer flow past a horizontal flat plate embedded in porous medium filled by nanofluid containing gyrotactic microorganisms. International Journal of Thermal Sciences, Volume 56, Pages 48-57, ISSN 1290-0729, <https://doi.org/10.1016/j.ijthermalsci.2012.01.011>
4. A.V. Kuznetsov, A.A. Avramenko., P. Geng., 2003. A similarity solution for a falling plume in bioconvection of oxytactic bacteria in a porous medium. Int., Comn., Heat Mass transfer, Vol. 30, No.1. pp 37-46. PII: S0735-1933(03)00005-8.
5. A.V. Kuznetsov, A.A. Avramenko., 2002. A 2d analysis of stability of bioconvection in a fluid saturated porous medium - estimation of the critical permeability value. Int., Comn., Heat Mass transfer, Vol. 29, No. 2. pp. 175-184.Elsevier Science Ltd.
6. A.V. Kuznetsov, A.A. Avramenko., 2004. Effects of small particles on the stability of bioconvection in a suspension of gyrotactic microorganisms in a layer of finite depth. Int., Comn., Heat Mass transfer, Vol. 31, No. 1. pp 1-10. PII: S0735-1933(03)00196-9.
7. A.V. Kuznetsov, A.A. Avramenko., 2004. Stability of a suspension of gyrotactic microorganisms in superimposed fluid and porous layers. Int., Comn., Heat Mass transfer, Vol. 31, No. 8. pp 1057-1066. PII: S0735-1933(04)00122-8.
8. A.V. Kuznetsov., 2010.The onset of nanofluid bioconvection in a suspension containing both nanoparticles and gyrotactic microorganisms. International Communications in Heat and Mass Transfer, Volume 37, Issue 10, Pages 1421-1425, ISSN 0735-1933, <https://doi.org/10.1016/j.icheatmasstransfer.2010.08.015>.

9. Aamir Ali., M. Sulaiman., S. Islam., Zahir Shah., Ebenezer Bonyah.,2018. Three-dimensional magnetohydrodynamic (MHD) flow of Maxwell nanofluid containing gyrotactic micro-organisms with heat source/sink. *AIP Advances* 8,085303, <https://doi.org/10.1063/1.5040540>.
10. Abderrahim Wakif .2020. A Novel Numerical Procedure for Simulating Steady MHD Convective Flows of Radiative Casson Fluids over a Horizontal Stretching Sheet with Irregular Geometry under the Combined Influence of Temperature-Dependent Viscosity and Thermal Conductivity. *Hindawi Mathematical Problems in Engineering* Volume 2020, Article ID 1675350, <https://doi.org/10.1155/2020/1675350>.
11. Abel.M. S. and Veena. P. H. 1998. Viscoelastic fluid flow and heat transfer in a porous medium over a stretching sheet, *Int. J. Non-Linear Mech.*, 33, 531.
12. Abel.M. S., JOSHI, A., Sonth. R. M., 2001. Heat Transfer in MHD viscoelastic fluid flow over a stretching surface, *ZAMM*, 10, 691.
13. Abramowitz. M. and Dover. Stegun. F., 1980. *Handbook of Mathematical Functions*, New York.
14. Afify A. A. 2004. MHD free convective flow and mass transfer over a stretching sheet with chemical reaction, *Heat Mass transfer*, 40, 495.
15. Amir Alizadeh-Pahlavan, Vahid Aliakbar, Farzad Vakili-Farahani, Kavyan Sadeghy.,2009. MHD flows of UCM fluids above porous stretching sheets using two- auxiliary-parameter homotopy analysis method. *Communication in nonlinear science and numerical simulation* 14, 473-488.
16. Andersson. H. I. 1992. MHD flow of a viscoelastic fluid past a stretching surface, *Acta Mech.*, 95, 227.
17. Andersson. H. I. 2002. Slip flow past a stretching surface, *Acta Mech.*,158, 121.

18. Andersson. H. I., 1995. An exact solution of the Navier-Stokes equations for MHDflow, *Acta Mech.*, 113, 241.
19. Andersson. H. I., Bech. K. H., Dandapat. B.S., 1992. Magnetohydrodynamic flow of a power-law fluid over a stretching sheet, *Int. J. Non-Linear Mech.*, 27, 929.
20. Andras Czirik., Imre M. Janosi., And John O. Kessler., 2000. Bioconvective dynamics: dependence on organism behaviour. *The Journal of Experimental Biology* 203, 3345–3354, Printed in Great Britain, The Company of Biologists Limited.
21. Andrews. L. C. 1992. *Special Functions of Mathematics for Engineers*, 2nd Ed., McGraw-Hill, New York.
22. Ariel. P. D. 1997. Generalized Gear's method for computing the flow of a viscoelastic liquid , *Comp. Meth. Appl. Mech. Engg.*, 142, 111.
23. Ariel. P. D. 2001. Axisymmetric flow of a second-grade fluid past a stretching sheet, *Int. J. Engg. Sci.*, 39, 529.
24. Bees, M.A. and Hill, N. (1999) Non-linear bioconvection in a deep suspension of gyrotactic swimming micro-organisms. *Journal of Mathematical Biology*, 38 (2). pp. 135-168. ISSN 0303-6812.
25. Bhatnagar. L., 1967. A lecture course on non-Newtonian fluids (constitutive equations), Indian Institute of Science, Bangalore, India.
26. Bhattacharyya, K., Hayat. T., Alsaedi. A., 2013. Analytic solution for magnetohydrodynamic boundary layer flow of Casson fluid over a stretching/shrinking sheet with wall mass transfer. *Chinese Physics B*, 22 (2), 024702. <http://dx.doi.org/10.1088/1674-1056/22/2/024702>.
27. (a) Blasius H. 1908. Grenzschichten in Flüssigkeiten mit kleiner Reibung, *ZAMP*, 56, 1
 (b) BOUSSINESQ, J. 1903. *Theorie analytique de la chaleur*.: Gathier-Villars, 2 Paris.

28. Bujurke N. M., Biradar. S. N. and Hiremath. S., 1987. Second order Fluid flow past a stretching sheet with heat transfer, ZAMP, 38, 653.
29. Buongiorno, J. (2006). "Convective Transport in Nanofluids." Journal of Heat Transfer, 128, 240 -250. <https://doi.org/10.1115/1.2150834>.
30. C.S.K. Raju, Mohammad Mainul Hoque, T. Sivasankar, 2017. Radiative flow of Casson fluid over a moving wedge filled with gyrotactic microorganisms. Advanced Powder Technology, Volume 28, Issue 2, Pages 575-583, ISSN 0921-8831, <https://doi.org/10.1016/j.appt.2016.10.026>.
31. Carragher. P. and Crane. L. J. 1982. Heat transfer on a continuous stretchingsheet, ZAMM, 62, 564.
32. Chakrabarti. A. and Gupta. A. S.1979. Hydromagnetic flow and heat transferover a stretching sheet, Q. Appl. Math., 37, 73.
33. Chang.W. D. 1989. The non-uniqueness of the flow of a visco-elastic fluid over a stretching sheet, Q. Appl. Math., 47, 365.
34. Char. M. I. 1994. Heat and mass in a hydromagnetic flow of the viscoelastic fluid over a stretching sheet, J. Math. Anal. Appl., 186, 674.
35. Char. M. I., and Chen. C. K., 1988. Temperature field in non-Newtonian flow over a stretching plate with variable heat flux, Int. J. Heat Mass Transfer, 31, 917.
36. Chen.C. H. 1998. Laminar mixed convection adjacent to vertical continuously stretching sheets, Heat Mass Transfer, 33, 471.
37. Chen.C. K., Char. M. I. and Cleaver J. W. 1990. Temperature field in a non-Newtonian flow over a stretching plate, J. Math. Anal. Appl., 151, 301.
38. Chiam. T. C., 1995. Hydromagnetic flow over a surface stretching with a power-lawvelocity, Int. J. Engg. Sci., 33, 429.

39. Chiam. T. C. 1997. Magnetohydrodynamic heat transfer over a non-Isothermal stretching sheet, *Acta Mech.*, 122, 169.
40. Childress, s., Lewandowsky, M., Spiegel, E.1975. Pattern formation in a suspension of swimming microorganisms: Equations and stability theory. *Journal of fluid mechanics*,69(3),591-613. Dio:10.1017/S0022112075001577.
41. Choi,S. U. S. , 1995, Enhancing Thermal Conductivity of Fluids With Nanoparticles, *Developments and Applications of Non-Newtonian Flows*, D. A. Siginer and H. P. Wang, eds., ASME, New York, FED-231/MD-66, pp.99–105.
42. Cortell. R., 2005. A note on magnetohydrodynamic flow of a power-law fluid over a stretching sheet, *Appl. Math. Comp.* 168, 557.
43. Crane. L. J. 1970. Flow past a stretching plate, *ZAMP*, 21, 645
44. D. Srinivasacharya., I. Sreenath.,2020. Bioconvection of Micropolar Fluid in an Annulus. *International Journal of Mathematical, Engineering and Management Sciences* Vol. 5, No. 2, 237-247, <https://doi.org/10.33889/IJMEMS.2020.5.2.019>
45. D.A. Nield., A V Kuznetsov., Cheng-Minkowycz., 2009. Problem for natural convective boundary Layer flow in porous medium saturated by a nanofluid. *Int. J. Heat mass Transfer*, 52, 5792-5795.
46. Dandapat. B. S. and Gupta. A. S. 1989. Flow and heat transfer in a viscoelastic fluid over a stretching sheet, *Int. J. Non-Linear Mech.*, 24, 215.
47. Dandapat. B. S., Holmedal. L. E. and Andersson. H. I., 1994. On the stability of MHD flow of a viscoelastic fluid past a stretching, *Arch. Mech.* 130, 143.
48. Das, K., Duari, P.R. & Kundu, P.K.,2015. Nanofluid bioconvection in presence of gyrotactic microorganisms and chemical reaction in a porous medium. *J Mech Sci Technol* 29, 4841–4849 . <https://doi.org/10.1007/s12206-015-1031-z>.

49. Datti P. S., Prasad K. V., Abel M. S. and Ambuja J. 2004. MHD viscoelastic fluid flow over a non-isothermal stretching sheet, *Int. J. Engg. Sci.*, 42, 935.
50. Dezhi Yang., Muhammad Yasir., Aamir Hamid., 2021. Thermal transport analysis in stagnation-point flow of Casson nanofluid over a shrinking surface with viscous dissipation. *Waves in Random and Complex Media*, DOI: 10.1080/17455030.2021.1972183.
51. Dutta. B. K. 1988. Heat transfer from a stretching sheet in a viscous flow over a stretching sheet with uniform heat flux, *ZAMM*, 68, 231.
52. Dutta. B. K. and Gupta. A. S. 1987. Cooling of a stretching sheet in a viscous flow, *Ind. Engg. Che. Res.*, 26, 333.
53. Ebraheem O. Alzahrani, Zahir Shah, Abdullah Dawar, Sharaf J. Malebary., 2019. Hydromagnetic mixed convective third grade nanomaterial containing gyrotactic microorganisms toward a horizontal stretched surface. *Alexandria Engineering Journal*, Volume 58, Issue 4, Pages 1421-1429, ISSN 1110-0168, <https://doi.org/10.1016/j.aej.2019.11.013>.
54. Eldabe. N. T., Elshehawey. E. F., Elbarbary. E. M. E., and Elgazery. N. S., 2005. Chebyshev finite difference method for MHD flow of a micropolar fluid past a stretching sheet with heat transfer, *Appl. Maths. Comp.*, 160, 437.
55. Erickson. L. E., Fan. L.T., and Fox. V. G. 1966. Heat and mass transfer on a moving continuous flat plate with suction or injection, *Ind. Engg. Chem. Fund.*, 5, 19.
56. F. G. Awad, P. Sibanda, M. Narayana and S. S. Motsa, 2011, Convection from a semi-finite plate in a fluid saturated porous medium with cross-diffusion and radiative heat transfer, *International Journal of the Physical Sciences* Vol. 6(21), pp. 4910-4923, DOI: 10.5897/IJPS11.295

57. Farshid Mirzaee, 2011 Differential Transform Method for Solving Linear and Nonlinear Systems of Ordinary Differential Equations, Applied Mathematical Sciences, 70(5): 3465-3472.
58. Fazal Haq, Seifedine Kadry, Yu-Ming Chu, Mair Khan, M. Ijaz Khan, 2020. Modeling and theoretical analysis of gyrotactic microorganisms in radiated nanomaterial Williamson fluid with activation energy. Journal of Materials Research and Technology, Volume 9, Issue 5, Pages 10468-10477, ISSN 2238-7854, <https://doi.org/10.1016/j.jmrt.2020.07.025>.
59. Fekry Mohamed Hady, A. Mahdy, Ramadan Abdalla Mohamed, Omima A. Abo Zaid, 2016. Effects of viscous dissipation on unsteady Mhd thermo bioconvection boundary layer flow of a nanofluid containing gyrotactic microorganisms along a stretching sheet. World Journal of Mechanics, Vol.6 No.12.
60. Fox. V. G., Erickson. L.E., and Fan. L.T. T., 1969. The laminar boundary on a moving continuous flat sheet immersed in a non-Newtonian fluid, AIChE J., 15, 327.
61. G. Mahanta, S. Shaw, 2015. 3D Casson fluid flow past a porous linearly stretching sheet with convective boundary condition, Alexandria Engineering Journal, Volume 54, Issue 3, Pages 653-659, ISSN 1110-0168, <https://doi.org/10.1016/j.aej.2015.04.014>.
62. Gangadhar, K., Bhargavi, D.N., Munagala, V.S.R., 2020. Steady boundary layer flow of Casson fluid over a nonlinear stretched sheet in presence of viscous dissipation using the spectral relaxation method. *Mathematical Modelling of Engineering Problems*, 7(3), 351-358. <https://doi.org/10.18280/mmep.070304>.
63. Grubka. L.J., Bobba. K.M. 1985. Heat transfer characteristics of a continuous stretching surface with variable temperature, ASME J. Heat Transfer, 107, 248
64. Gupta R.K., Sridhar T., 1985. Viscoelastic effects in non-Newtonian flows through porous media. *Rheological Acta*, 24 (2), pp. 148-151.

65. Gupta. P. S. and Gupta. A. S. 1977. Heat and mass transfer on a Stretching sheet with suction or blowing, *Can. J. Chem. Engg.*, 55, 744.
66. H. Xu, I. Pop.,2014. Mixed convection flow of a nanofluid over a stretching surface with uniform free stream in the presence of both nanoparticles and gyrotactic microorganisms, *International Journal of Heat and Mass Transfer*, Volume 75, Pages 610-623, ISSN 0017-9310, <https://doi.org/10.1016/j.ijheatmasstransfer.2014.03.086>.
67. Haritha, B., Umadevi, C., Dhange, M., 2020. Mathematical modeling of convective heat and mass transfer of a rotating nano-fluid bounded by stretching and stationary walls in a vertical conduit. *International Journal of Applied Mechanics and Engineering*, 25(4), 69-83.
68. Hatami M, Jing D. Differential transformation method for Newtonian and non-Newtonian nanofluids flow analysis: Compared to numerical solution. *Alexand Eng J.* 2016;55 (2):731–739. <http://dx.doi.org/10.1016/j.aej.2016.01.003>.
69. Hossein A, Milad H. An analytical technique for solving nonlinear heat transfer equations. *Appl Appl Math.* 2010;5 (10):1389–1399.
70. Hosseinzadeh Kh, Roghani S, Mogharrebi AR, Asadi A, Waqas M, Ganji DD. Investigation of cross fluid flow containing motile gyrotactic microorganisms and nanoparticles over a three-dimensional cylinder. *Alexand Eng J.* 2020;59:3297–3307. <http://dx.doi.org/10.1016/j.aej.2020.04.037>
71. Hosseinzadeh Kh, Sajad S, Mardani MR, Mahmoudi FY, Waqas M, Ganji DD. Investigation of nano-Bioconvective fluid motile microorganism and nanoparticle flow by considering MHD and thermal radiation. *Inf. Med. Unlocked.* 2020;21:100462. <http://dx.doi.org/10.1016/j.imu.2020.100462>.
72. J. K. Zhou, Differential Transform Method and its application for electrical circuit ,Hauzhang university Press,Wuhan,China,1986.
73. J.V. Ramana Reddy., K. Anantha Kumar., V. Sugunamma., N. Sandeep.,2018. Effect of cross diffusion on MHD non-Newtonian fluids flow past a stretching sheet with non-uniform heat source/sink: A comparative study, Alexandria

Engineering Journal, Volume 57, Issue 3, Pages 1829-1838, ISSN 1110-0168, <https://doi.org/10.1016/j.aej.2017.03.008>

74. K. Das, 2012. Slip effects on MHD mixed convection stagnation point flow of a micropolar fluid towards a shrinking vertical sheet, *Computers & Mathematics with Applications*, Volume 63, Issue 1, Pages 255-267, ISSN 0898-1221, <https://doi.org/10.1016/j.camwa.2011.11.018>.
75. Kameswaran, P., Narayana, M., Sibanda, P. *et al.* 2012 .On radiation effects on hydromagnetic Newtonian liquid flow due to an exponential stretching sheet. *Bound Value Probl* , 105 (2012). <https://doi.org/10.1186/1687-2770-2012-105>.
76. Karahalios. G. T. 1992. A note on a time-dependent flow from a stretching planesurface, *Int. J. Non-Linear Mech.*, 27, 293.
77. Kelly. D., Vajravelu. K. and Andrews. L 1999. Analysis of heat and mass transfer of a viscoelastic, electrically conducting fluid past a continuous stretching Sheet. *Nonlinear Analysis*, 36, 767.
78. Khalil Ur Rehman, Aneeqa Ashfaq Malik, M. Tahir, M.Y. Malik, 2018. Undersized description on motile gyrotactic micro-organisms individualities in MHD stratified water-based Newtonian nanofluid, *Results in Physics*, Volume 8, Pages 981-987, ISSN 2211-3797, <https://doi.org/10.1016/j.rinp.2018.01.028>.
79. Khidir, A.A., Narayana, M., Sibanda, P. *et al.* 2015. Natural convection from a vertical plate immersed in a power-law fluid saturated non-Darcy porous medium with viscous dissipation and Soret effects. *Afr. Mat.* **26**, 1495–1518. <https://doi.org/10.1007/s13370-014-0301-8>.
80. Krishnendu Bhattacharya, M.S. Uddin., G.C. Layek., 2016. Exact solution for thermal boundary layer in Casson fluid over permeable shrinking sheet with variable wall temperature and thermal radiation. *Alexandria Engineering journal* , 55, 1703-1712.
81. Kumaran. and Ramanaiyah. G. 1996. A note on the flow over a stretching sheet, *Acta Mech.*, 119, 229.

82. Kumari. M. and Nath. G. 1999. Flow and heat transfer in a stagnation-point flow over a stretching sheet with a magnetic field, *Mech. Res. Comm.*, 26, 469.
83. Kumari. M., Takhar. H. S., and Nath. G., 1990. MHD flow and heat transfer over a stretching surface with prescribed wall temperature or heat flux, *Warme und Stoffübertragung*, 25, 331.
84. Liao S. J. 2003. On the analytic solution of magnetohydrodynamic flows of non-Newtonian fluids over a stretching sheet, *J. Fluid Mech.*, 488, 189.
85. Liao. S. J., 2003. On the analytic solution of magnetohydrodynamic flows of non-Newtonian fluids over a stretching sheet, *J. Fluid Mech.*, 488, 189.
86. Liao. S. J., 2005. A new branch of solutions of boundary-layer over an impermeable stretched plate, *Int. J. Heat Mass Transfer*, 48, 2529.
87. Liao. S. J., and POP, I. 2004. Explicit analytic solution for similarity boundary layer equations, *Int. J. Heat Mass Transfer*, 47, 75.
88. Liu. I.C., 2005. A note on heat and mass transfer for a hydromagnetic flow over a stretching sheet, *Int. Comm. Heat Mass Transfer*, 32, 1075.
89. M. A. Bees and N. A. Hill, 1998. Linear bioconvection in a suspension of randomly swimming, gyrotactic micro-organisms. *American Institute of Physics*. VOLUME 10, NUMBER 8, S1070- 6631-98!02808-6.
90. M. A. Bees and N. A. Hill, 1997. Wavelengths of bioconvection patterns, *The Journal of Experimental Biology* 200, 1515–1526, Printed in Great Britain, The Company of Biologists Limited.
91. M. K. Nayak, J. Prakash, D. Tripathi, V. S. Pandey, S. Shaw, O. D. Makinde, 2019. 3D Bioconvective multiple slip flow of chemically reactive Casson nanofluid with gyrotactic micro-organisms. <https://doi.org/10.1002/htj.21603>.
92. M. Subhas Abel., N. Mahesha., Jagadish Tawade., 2009. Heat transfer in a liquid film over an unsteady stretching surface with viscous dissipation in presence of

- external magnetic field. *Applied Mathematical Modelling*, Volume 33, Issue 8, Pages 3430-3441, ISSN 0307-904X, <https://doi.org/10.1016/j.apm.2008.11.021>.
93. M. Veera Krishna, N. Ameer Ahammad, Ali J. Chamkha., 2021. Radiative MHD flow of Casson hybrid nanofluid over an infinite exponentially accelerated vertical porous surface. *Case Studies in Thermal Engineering*, Volume 27, 101229, ISSN 2214-157X, <https://doi.org/10.1016/j.csite.2021.101229>.
94. M.A. Talha., M. Osman gani., M. Ferdows., 2018. Numerical solution of steady magnetohydrodynamic boundary layer flow due to gyrotactic microorganism for Williamson nanofluid over stretched surface in the presence of exponential internal heat generation. *World academy of science and Engineering technology, International journal of Mathematical and computational Sciences*, volume 12, No.2
95. M.J. Uddin, Yasser Alginahi, O. Anwar Bég, M.N. Kabir, 2016. Numerical solutions for gyrotactic bioconvection in nanofluid-saturated porous media with Stefan blowing and multiple slip effects, *Computers & Mathematics with Applications*, Volume 72, Issue 10, Pages 2562-2581, ISSN 0898-1221, <https://doi.org/10.1016/j.camwa.2016.09.018>.
96. M.S. Abel, P.G. Siddheshwar, Mahantesh M. Nandeppanavar., 2007. Heat transfer in a viscoelastic boundary layer flow over a stretching sheet with viscous dissipation and non-uniform heat source. *Int. J. Heat Mass Transfer*, 50(2007), 960-966.
97. Magyari. E. and Keller. B., 2000. Exact analytic solution for free convection boundary layers on a heated vertical plate with lateral mass flux embedded in a saturated porous medium, *Heat Mass Transfer*, 36, 109.
98. Magyari. E. and Keller. B., 2001. The wall jet an limiting case of a boundary-layer flow induced by a permeable stretching surface, *ZAMP*, 52, 696.

99. Magyari. E. and Keller.B. 1999. Heat and mass transfer in the boundary layers on an exponentially stretching continuous surface, *J. Phys. D: Appl. Phys.*,32, 577.
100. Magyari. E., Pop. I., Keller. B. 2003. New analytical solutions of a well-known boundary value problem in fluid mechanics, *Fluid Dyn. Res.*, 33,313.
101. Magyari. E., Pop. I., Keller. B., 2002. The missing similarity boundary-layerflow over a moving plane surface, *ZAMP*, 53,782.
102. Mahanta, G., Shaw, S., 2015. 3D Casson fluid flow past a porous linearly stretching sheet with convective boundary condition. *Alexandria Engineering Journal*, 54(3), 653-659. <https://doi.org/10.1016/j.aej.2015.04.014>.
103. Mahapatra. T. R. and Gupta. A. S. 2003. Stagnation-point flow towards a stretching surface, *Can. Chem. Engg. J*, 81, 258.
104. Mahapatra. T.R. and Gupta. A. S. 2001. Magnetohydrodynamic stagnation-pointflow towards a stretching sheet, *Acta Mech.*, 152, 191.
105. Massoudi. M and Maneschy C. E. 2004. Numerical solution to the flow of a second-grade fluid over a stretching sheet using the method of quasi-linearization, *Appl. Math. Comp.*, 149, 165.
106. Mathew M. Hopkinsi and LiSA J. Fauci J., A Computational Model of The Collective Fluid Dynamics Of Motile Microorganisms, *Fluid Mech.* 2002. vol. 455, pp. 149–174. Cambridge University Press.
107. Md. Shakhaoath Khan, Md. Mahmud Alam, M. Ferdows, 2013.Effects of Magnetic Field on Radiative Flow of a Nanofluid Past a Stretching Sheet, *Procedia Engineering*, Volume56, Pages316-322, ISSN1877-7058, <https://doi.org/10.1016/j.proeng.2013.03.125> .
108. Mogharrebi, Amirreza & Ganji, Ali & Hosseinzadeh, Khashayar & Roghani, Soroush Asadi, Armin & Fazlollahtabar, Amin.2021. Investigation of magnetohydrodynamic nanofluid flow contain motile oxytactic microorganisms

over rotating cone. International Journal of Numerical Methods for Heat & Fluid Flow. ahead-of-print. 10.1108/HFF-08-2020-0493.

109. Muhammad Ramzan, Jae Dong Chung, Naeem Ullah, 2017. Radiative magnetohydrodynamic nanofluid flow due to gyrotactic microorganisms with chemical reaction and non-linear thermal radiation. International Journal of Mechanical Sciences, Volume 130, Pages 31-40,ISSN 0020-7403, <https://doi.org/10.1016/j.ijmecsci.2017.06.009>.
110. N A Hill and T J Pedley.,2005. Bioconvection. The Japan Society of Fluid Mechanics and IOP Publishing Ltd., Fluid Dynamics Research, Volume 37, Res. 37 1.
111. N. S. Akbar, Z. H. Khan: Magnetic field analysis in a suspension of gyrotactic microorganisms and nano particles over a stretching surface, Journal of Magnetism and Magnetic materials, 410 (2016), 72–80.
112. N. Saeed Khan, T. Gul, M. Altaf Khan, E. Bonyah, S. Islam: -Mixed convection in gravity-driven thin film non-Newtonian nanofluids flow with gyrotactic microorganisms, Adv. Powder Tech., 7 (2017), 4033–4049.
113. Noor Saeed Khan.,2018. Bioconvection in Second Grade Nanofluid Flow Containing Nanoparticles and Gyrotactic Microorganisms. *Braz J Phys* **48**, 227–241. <https://doi.org/10.1007/s13538-018-0567-7> .
114. O A Croze., E E Ashraf and M A Bees.,2010. Sheared bioconvection in a horizontal tube. *Phys. Biol.* 7, 046001 (12pp) doi:10.1088/1478-3975/7/4/04600.
115. P Keblinski, S.R Phillpot, S.U.S Choi, J.A Eastman,2002. Mechanisms of heat flow in suspensions of nano-sized particles (nanofluids), International Journal of Heat and Mass Transfer,Volume 45, Issue 4,Pages 855-863, ISSN 0017-9310,[https://doi.org/10.1016/S0017-9310\(01\)00175-2](https://doi.org/10.1016/S0017-9310(01)00175-2).
116. P. G. Siddheshwar, U.S. Mahabaleshwar, Effects of radiation and heat source on MHD flow of a viscoelastic liquid and heat transfer over a stretching sheet, International Journal of Nonlinear Mechanics, 2005, Volume 40, 807-820. UNITED STATES OF AMERICA.

117. P. N. V. Kumar, U. S. Mahabaleshwar , P. H. Sakanaka³, and G. Lorenzini. 2018. An MHD Effect on a Newtonian Fluid Flow Due to a Super linear Stretching Sheet. ISSN 1810- 2328, Journal of Engineering Thermo physics, Vol. 27, No. 4, pp. 501–506.
118. Pal, D., Mondal, S.K. 2018. Influence of Chemical Reaction and Nonlinear Thermal Radiation on Bioconvection of Nanofluid Containing Gyrotactic Microorganisms with Magnetic Field. *BioNanoSci.* 8, 1065–1080. <https://doi.org/10.1007/s12668-018-0555-y>
119. Partha. M. K., Murthy. P., Rajasekhar. G. P. 2004. Effect of viscous dissipation on the mixed convection heat transfer from an exponentially stretching surface, *Heat Mass Transfer*, 41, 360.
120. Patra A, Saha Ray S. Multistep differential transform method for the numerical solution of classical neutron point kinetic equation. *Comput Math Model.* 2013;24:604–615.
121. Pavlov. K. B. 1974. Magnetohydrodynamic flow of an incompressible viscous fluid caused by deformation of a plane surface, *Magnitnaya Gidrodinamika*, 4, 146.
122. Pedley, T. & Kessler, J., (1992). Hydrodynamic phenomenon in suspensions of swimming microorganisms. *Annual Review of Fluid Mechanics* 24, 313–358.
123. Pedley, T. Hill, N. & Kessler, J. (1988). The growth of bioconvection patterns in a uniform Suspension of gyrotactic microorganisms. *Journal of Fluid Mechanics* 195, 223-237.
124. Pedley. T. J., Hill. N. A., Kessler. J. O. 1988. The growth of bioconvection patterns in a uniform suspension of gyrotactic micro-organisms. *J. Fluid Mech.* 195: 223-37.
125. Platt J. R, 1961, “Bioconvection Patterns in Cultures of Free-Swimming Organisms,” *Science*, 133, 1766, <https://doi.org/10.1126/science.133.3466.1766>.

126. Rahila Naz, Mughira Noor, Zahir Shah, Muhammad Sohail, Poom Kumam, Phatiphat Thounthong, 2020. Entropy generation optimization in MHD pseudoplastic fluid comprising motile microorganisms with stratification effect. Alexandria Engineering Journal, Volume 59, Issue 1, Pages 485-496, ISSN 1110-0168, <https://doi.org/10.1016/j.aej.2020.01.018>.
127. Rajagopal. K. R., and Gupta. A. S. 1984. Exact solution for the flow of a non-Newtonian fluid past an infinite porous plate, *Meccanica*, 19, 158.
128. Rajagopal. K. R., Gupta. A. S., and Wineman. A. S., 1980. On a boundary layer theory for non-Newtonian fluids, *Lett. Appl. Engg. Sci.*, 18, 875.
129. Rajagopal. R., Na. T. Y., and Gupta. A. S., 1987. A non-similar boundary layer on a stretching sheet in a non-Newtonian fluid with uniform free stream, *J. Math. Phys. Sci.*, 21, 189.
130. Rajagopal. K. R., Na. T. Y., and Gupta. A. S. 1984. Flow of a viscoelastic fluid over a stretching sheet, *Rheol. Acta*, 23, 213.
131. Ramaiah, D., & Gangadhar, K., 2017. Effect of joule heating on mixed convection flow of Casson nanofluid over a non-linear permeable stretching sheet with heat generation or absorption.
132. Rollins. D. and Vajravelu. K. 1991. Heat transfer in a fluid over a continuous stretching surface, *Acta Mech.*, 89, 167.
133. Rudraiah, N., Kaloni, P.N. & Radhadevi, P.V., 1989. Oscillatory convection in a Viscoelastic fluid through a porous layer heated from below. *Rheol Acta* 28, 48–53. <https://doi.org/10.1007/BF01354768>.
134. S. GHORAI AND N. A. HILL, 2000. Wavelengths of Gyrotactic Plumes in Bioconvection. *Bulletin of Mathematical Biology* 62, 429–450, doi:10.1006/bulm.1999.0160.
135. S. Manjunatha, B. J. Giresha and C. S. Bagewadi. 2012. Effect of thermal radiation on boundary layer flow and heat transfer of dusty fluid over an unsteady

- stretching sheet. *International Journal of Engineering, Science and Technology* Vol. 4, No. 4, pp. 36-48.
136. S. Nadeem., Rizwan Ul Haq., C. Lee., 2012.MHD flow of a Casson fluid over an exponentially shrinking sheet, *Scientia Iranica*, Volume 19, Issue 6, Pages 1550-1553, ISSN1026-3098. <https://doi.org/10.1016/j.scient.2012.10.021>.
137. S. Pramanik, 2014. Casson fluid flow and heat transfer past an exponentially porous stretching surface in presence of thermal radiation. *Ain Shams Engineering journal* 5,205-212.
138. S.Sepasgozar, M.Faraji, P.Valipour, 2017.Application of differential transformation method (DTM) for heat and mass transfer in a porous channel, 6(1): 41-48.
139. Sadia Siddiq, Gul-e-Hina, Naheed Begum, S. Saleem, M.A. Hossain, Rama Subba Reddy Gorla, 2016. Numerical solutions of nanofluid bioconvection due to gyrotactic microorganisms along a vertical wavy cone. *International Journal of Heat and Mass Transfer*, Volume 101, Pages 608-613, ISSN 0017-9310, <https://doi.org/10.1016/j.ijheatmasstransfer.2016.05.076>.
140. Sakiadis. B. C. 1961. Boundary-layer behavior on continuous solid surfaces I: The boundary layer on a equations for two dimensional and axisymmetric flow, *AICHE J*, 7, 26.
141. Sakiadis. B. C. 1961. Boundary-layer behavior on continuous solid surfaces II: Theboundary layer on a continuous flat surface, *AICHE J*, 7, 221.
142. Sakiadis. B. C. 1961. Boundary-layer behavior on continuous solid surfaces III: The boundary layer on a continuous cylindrical surface, *AICHE J*, 7, 467.
143. Sam. L. P. and Rao. B. N. 1992. Heat transfer in the flow of viscoelastic fluid Over a stretching sheet, *Acta Mech.*, 93, 53.

144. Sam. L. P. and Rao. B. N. 1993. Reinvestigation of the uniqueness of the flow of a viscoelastic fluid over a stretching sheet, *Q. Appl. Math.*, 51, 401.
145. Samina Zuhra., Noor Saeed Khan., Muhammad Alam., Saeed Islam., Aurangzeb Khan.2020. Buoyancy effects on nanoliquids film flow through a porous medium with gyrotactic microorganisms and cubic autocatalysis chemical reaction. *Advances in Mechanical Engineering*, Vol.12(1),1–17 . DOI: 10.1177/1687814019897510 journals.sagepub.com/home/ade.
146. Sankad, G., Dhange, M., 2017. Effect of chemical reactions on the dispersion of a solute in peristaltic motion of Newtonian fluid with wall properties. *Malaysian Journal of Mathematical Sciences*, 11(3), 347-363.
147. Sarpakaya. T. 1961. Flow of non-Newtonian fluids in magnetic field, *AIChE J.*, 7,324.
148. Seddeek. M.A. 2001. Effect of Hall and ion-slip currents on magneto-micropolar fluid and heat transfer over a non-isothermal stretching sheet with suction and blowing, *Proc. Roy. Soc. Lond. A*, 457, 3039.
149. Shahid A, Zhou Z, Bhatti MM, Tripathi D. Magneto hydrodynamics nanofluid flow containing gyrotactic microorganisms propagating over a stretching surface by successive Taylor series linearization method. *Microgravity Sci Technol*. 2018;30(4):445–455.
150. Siddappa. B. and Abel. M. S. 1985. Non-Newtonian flow past a stretching plate, *ZAMP*, 36, 890.
151. Siddappa. B., and Abel. M. S., 1986. Viscoelastic boundary layer flow past a stretching plate with suction and heat transfer, *Rheol. Acta*, 23, 815.
152. Soewono. E., Vajravelu. K. and Mahapatra. N. 1992. Existence of solutions of a nonlinear boundary value problem, arising in flow and heat transfer over a stretching sheet, *Nonlinear Analysis, Theory, Methods and Applications*, 18, 93.

153. Spiegel, E. A. and Veronis, G. 1960. On the Boussinesq approximation for a compressible fluid, *Astrophys. J.* 131, 34.
154. Stephen U. S. Choi and Jeffrey A. Eastman. 1995. Enhancing thermal conductivity of fluids with nanoparticles. *Proceedings of the ASME International Mechanical Engineering Congress and Exposition.* 66.
155. Swati Mukhopadhyaya., Krishnendu Bhattacharyya., and Tasawar Hayat., 2013. Exact solutions for the flow of Casson fluid over a stretching surface with transpiration and heat transfer effects. *Chin. Phys. B* Vol. 22, No. 11, 114701. DOI: 10.1088/1674-1056/22/11/114701.
156. Takhar. H. S., Chamkha. A. J., and NATH, G. 2000. Flow and mass transfer on a stretching sheet with a magnetic field and chemically species, *Int. J. Engg. Sci.*, 38, 1303.
157. Tanmoy Chakraborty, Kalidas Das, Prabir Kumar Kundu, 2018. Framing the impact of external magnetic field on bioconvection of a nanofluid flow containing gyrotactic microorganisms with convective boundary conditions, *Alexandria Engineering Journal*, Volume 57, Issue 1, Pages 61-71, ISSN 1110-0168, <https://doi.org/10.1016/j.aej.2016.11.011>.
158. Tausif S.K., Das K., Kundu P.K. 2016. Multiple slip effects on bioconvection of nanofluid flow containing gyrotactic microorganisms and nanoparticles. *J Mol Liq*, 220 (2016), pp. 518-526.
159. Vajravelu K. and Hadjinicolaou. A. 1997. Convective heat transfer in a electrically conducting fluid at a stretching surface with uniform free stream, *Int. J. Engg. Sci.*, 35, 1237.
160. Vajravelu. K., and Nayfeh. J., 1993. Convective heat transfer at a stretching sheet, *Acta Mech.*, 96, 47.
161. Vedat SE. Application of differential transformation method to linear sixth-order boundary value problems. *Appl Math Sci.* 2007;1(2):51–58.

162. W.A. Khan, O.D. Makinde, 2014. MHD nanofluid bioconvection due to gyrotactic microorganisms over a convectively heat stretching sheet, *International Journal of Thermal Sciences*, Volume 81, Pages 118-124, ISSN 1290-0729, <https://doi.org/10.1016/j.ijthermalsci.2014.03.009>.
163. W.A. Khan, O.D. Makinde, Z.H. Khan, 2014. MHD boundary layer flow of a nanofluid containing gyrotactic microorganisms past a vertical plate with Navier slip, *International Journal of Heat and Mass Transfer*, Volume 74, Pages 285-291, ISSN 0017-9310, <https://doi.org/10.1016/j.ijheatmasstransfer.2014.03.026>.
164. Wang. C. Y., 2002. Flow due to a stretching boundary with partial slip - an exact solution of the Navier- Stokes equations, *Chem. Engg. Sci.*, 57, 3745.
165. Winifred Nduku Mutuku, Oluwole Daniel Makinde, 2014. Hydromagnetic bioconvection of nanofluid over a permeable vertical plate due to gyrotactic microorganisms, *Computers & Fluids*, Volume 95, Pages 88-97, ISSN 0045-7930, <https://doi.org/10.1016/j.compfluid.2014.02.026>.
166. Xu. H. 2005. An explicit analytic solution for convective heat transfer in an electrically conducting fluid at a stretching surface with uniform free stream, *Int. J. Engg. Sci.*, 43, 859.
167. Yu-Ming Chu, M. Israr Ur Rehman, M. Ijaz Khan, S. Nadeem, Seifedine Kadry, Zahra Abdelmalek, Nadeem Abbas., 2020. Transportation of heat and mass transport in hydromagnetic stagnation point flow of Carreau nanomaterial: Dual simulations through Runge-Kutta Fehlberg technique, *International Communications in Heat and Mass Transfer*, Volume 118, 104858, ISSN 0735-1933, <https://doi.org/10.1016/j.icheatmasstransfer.2020.104858>.
168. Z. Alloui., T.H. Nguyen., E. Bilgen., 2005. Bioconvection of gravitactic microorganisms in a vertical Cylinder. *International Communications in Heat and Mass Transfer*, Volume 32, Issue 6, Pages 739-747, ISSN 0735-1933, <https://doi.org/10.1016/j.icheatmasstransfer.2004.10.005>.
169. Z. Mehmood., Z. Iqbal: Interaction of induced magnetic field and stagnation point flow on bioconvection nanofluids submerged in gyrotactic microorganisms, *Journal of Molecular Liquids*, 224 (2016), 1083–1091.

LIST OF PAPERS

Published/Communicated

List of published papers

1. Sankad, G.C., Ishwar Maharudrappa, “**Boundary Layer Flow and Heat Transfer of Casson Fluid Over a Porous Linear Stretching Sheet with Variable Wall Temperature and Radiation**” .*Proceedings of NHTFF 2018*. In book: Numerical Heat Transfer and Fluid Flow. DOI: [10.1007/978-981-13-1903-7_20](https://doi.org/10.1007/978-981-13-1903-7_20).
2. Sankad G C., Ishwar Maharudrappa., Mallinath Dhange “**Bioconvection in Casson fluid flow with gyrotactic microorganisms and heat transfer over a linear stretching sheet in presence of magnetic field**”. *Advances in Mathematics: Scientific journal* 10(1):155-169, January 2021.
3. Sankad, G.C., Ishwar Maharudrappa.,”**MHD Boundary Layer Flow of Casson Fluid with Gyrotactic Microorganisms over Porous Linear Stretching Sheet and Heat Transfer Analysis with Viscous Dissipation**”. *In book: Recent Trends in Mathematical Modelling and High-Performance Computing January 2021* DOI: [10.1007/978-3-030-68281-1_4](https://doi.org/10.1007/978-3-030-68281-1_4).
4. Sankad G. C., Ishwar Maharudrappa., Mallinath Dhange., “**Varying wall temperature and thermal radiation effects on MHD boundary layer liquid flow containing gyrotactic microorganisms**”. *Partial Differential Equations in Applied Mathematics*, 4 (2021)10009, Elsevier Publications. DOI:[10.1016/j.padiff.2021.100092](https://doi.org/10.1016/j.padiff.2021.100092).

List of papers communicated

1. Sankad. G.C., Ishwar Maharudrappa., Mallinath Dhange., “**Casson fluid flow due to stretching sheet with magnetic effect and variable thermal conductivity**”. *International journal of Applied Mechanics and Engineering*. sept.2021.